



33 **ABSTRACT**

34

35 To date, there is no analytical approach available that allows the full identification and  
36 characterization of highly complex disinfection by-product (DBP) mixtures. This study  
37 aimed at investigating the chemodiversity of drinking water halogenated DBPs using  
38 diverse analytical tools: measurement of adsorbable organic halogen (AOX) and mass  
39 spectrometry (MS)-based target and non-target analytical workflows. Water was  
40 sampled before and after chemical disinfection (chlorine or chloramine) at four drinking  
41 water treatment plants in Sweden. The target analysis had the highest sensitivity,  
42 although it could only partially explain the AOX formed in the disinfected waters. Non-  
43 target Fourier transform ion cyclotron resonance (FT-ICR) MS analysis indicated that  
44 only up to 19 Cl and/or Br-CHO formulae were common to all disinfected waters.  
45 Unexpectedly, a high diversity of halogenated DBPs (presumed halogenated  
46 polyphenolic and highly unsaturated compounds) was found in chloraminated surface  
47 water, comparable to that found in chlorinated surface water. Overall, up to 86 DBPs  
48 (including isobaric species) were tentatively identified using liquid chromatography  
49 (LC)-Orbitrap MS. Although further work is needed to confirm their identity and assess  
50 their relevance in terms of toxicity, they can be used to design suspect lists to improve  
51 the characterization of disinfected water halogenated mixtures.

52

53

54 **KEYWORDS:** chlorination; chloramination; non-target analysis; identification  
55 workflow; haloacids

56

## 57 INTRODUCTION

58 Water disinfection is essential to protect public health from waterborne infectious  
59 diseases. Although disinfection can be achieved through physical and chemical  
60 methods, adding chemical disinfectants like chlorine or chloramine to the final product  
61 is common, as they are cheap, easy to handle, effective, and, most importantly, they  
62 provide residual disinfection that prevents pathogen regrowth in the distribution system  
63 network. Chemical disinfectants are strong oxidants that react with building blocks or  
64 alter the metabolism of pathogenic organisms, eventually killing them as the ultimate  
65 consequence [1]. However, oxidative reactions are not specific to the substrate and thus,  
66 all organic and inorganic constituents of water may be involved. As a result, a wide  
67 range of disinfection by-products (DBPs) will be unintentionally formed during the  
68 process [2].

69 The scientific community and the drinking water sector has been concerned about the  
70 formation of DBPs and their effects since the first discovery of DBPs in chlorinated  
71 water in two independent studies conducted in parallel in the mid-1970s [3, 4]. Research  
72 in this field has pointed out that many DBPs are highly cytotoxic and genotoxic to  
73 mammalian cells [5], and a few of the tested DBPs even have all the toxicological  
74 characteristics to be classified as carcinogens to human (regulated trihalomethanes  
75 (THMs), formaldehyde, acetaldehyde, mutagen X (MX) and N-nitrosodimethylamine  
76 (NDMA)) [6]. Indeed, long-term exposure to THMs has been associated in  
77 epidemiological studies to an increased incidence of bladder cancer [7] and may also  
78 have reproductive and developmental effects (mainly related to growth retardation) [7,  
79 8]. *In vitro* toxicological studies have provided evidence on the different toxic potency  
80 of individual DBPs depending on their chemical structure. While nitrogen-containing  
81 DBPs are generally more toxic than only carbon-based DBPs [9], and halophenolic

82 DBPs are generally more toxic than haloaliphatic DBPs [10], the toxicity of halogenated  
83 DBPs is also related to the halogen present in their structure, and increases in the order  
84 chloro-DBPs<<<bromo-DBPs<iodo-DBPs [9].

85 The chemical composition of the DBP mixtures and their formation from dissolved  
86 natural organic matter (NOM) are strongly dependent on the disinfectant used and the  
87 disinfection conditions (dose, contact time, water pH and temperature, etc.) and the  
88 source water characteristics (type and amount of NOM, inorganic ions such as bromide,  
89 iodide, ammonia, etc.) [11-14].

90 Due to the high chemodiversity of NOM (DBP precursors) and DBP mixtures, their  
91 comprehensive understanding and monitoring become a challenge [15, 16].  
92 Furthermore, their full characterization is not possible with a single analytical  
93 technique. Pan et al. [17] have recently reviewed the approaches used for NOM  
94 characterization in drinking water sources. As for DBP mixtures, only regulated DBPs  
95 are systematically monitored, and the analytical methods employed for their isolation  
96 and concentration and analysis are only capable of identifying and characterizing a  
97 specific fraction of the material formed during disinfection processes [18]. Most of the  
98 DBPs known to date (nearly 700 [19]), especially those that are usually quantified in  
99 disinfected water, belong to the semi- to the highly-volatile fraction of the adsorbable  
100 organic halogenated material (AOX) formed during disinfection of water and are  
101 amenable to liquid-liquid extraction (LLE) and gas chromatography (GC)-mass  
102 spectrometry (MS) analysis [20]. However, the non-volatile fraction, for which major  
103 constituents and characteristics are largely unknown, may be toxicologically more  
104 relevant than the volatile portion [21]. Solid-phase extraction (SPE) approaches and  
105 liquid chromatography interfaced with MS (LC-MS) techniques are being applied  
106 during the last few years to characterize the unknown AOX fraction [19, 22].

107 Recently, high-resolution mass spectrometry (HRMS) techniques have become more  
108 popular using non-target workflows to unveil previously unknown DBPs [23-42] and  
109 also to discover DBP precursors [43, 44]. However, the results of these studies are  
110 based on the use of one analytical technique only, i.e., GC-HRMS [23, 25], Fourier  
111 transform ion cyclotron resonance (FT-ICR) MS [26-34] or LC-HRMS [35-42], and  
112 hence, the characterization of the DBP mixture is limited to one fraction. The majority  
113 of the LC-MS-based studies conducted to date in this field focus on discovering the  
114 DBPs generated by selected emerging organic contaminants during disinfection  
115 processes usually in pure water, using time-trends of features of interest [36-39] or  
116 developing specific suspect lists [35]. There are only a few studies on purely LC-MS-  
117 based non-target workflows to unveil unknown DBPs in real mixtures [40-42], and they  
118 focused on the identification of specific groups of compounds such as amino-  
119 compounds [41], halogenated carboxylic acids [40], peptide-DBPs [42], or chlorine-  
120 [45], bromine- [46] or iodine-containing DBPs [47] through the so-called product ion  
121 scan approach [22].

122 In this context, this study aimed at expanding the knowledge of real DBP mixtures  
123 produced by chlorine and chloramine-based disinfection processes at full-scale drinking  
124 water treatment plants (DWTPs) by applying different complementary analytical tools  
125 for DBP characterization. Target and non-target approaches were combined. GC-MS in  
126 combination with various extraction procedures offered a broad (~50) screening for  
127 known DBPs in the volatile fraction and HRMS tools, *viz.*, FT-ICR MS and LC-  
128 Orbitrap MS, and non-target data treatment workflows unveiled the composition and  
129 chemodiversity of DBPs in the non-volatile fraction. Furthermore, the results from the  
130 aforementioned HRMS tools were compared with each other.

131

## 132 MATERIALS AND METHODS

### 133 *Chemicals*

134 In total 47 DBPs were included in the target analysis including 8 THMs, 4  
135 trihalogenated haloacetaldehydes (THALs), 8 haloacetonitriles (HANs), 13  
136 haloacetamides (HACMs), and 14 haloacids (HAAs). The list has been provided in  
137 Table 1.

138 Ultrapure water (resistivity of 18.2 M $\Omega$ ·cm at 25 °C; TOC  $\leq$  5 ppb) used to prepare  
139 analytical methods blanks and to rinse sampling bottles and labware during the cleaning  
140 process was obtained using a Milli-Q Advantage system and aQ-POD dispenser  
141 equipped with a Millipack® Express 40 filter (Asymmetric PolyEtherSulfone (PES)  
142 membrane, 0.22  $\mu$ m) for particles and bacteria removal, connected in series with a LC-  
143 Pack® Point-of-use Polisher cartridge (C18 reverse-phase silica) for trace organics  
144 removal (Merck Millipore).

145 All reagents and solvents used were of high purity and mostly supplied either by VWR  
146 International (Spånga, Sweden) or Merck KgaA (Darmstadt, Germany).

147 L(+)-ascorbic acid and sodium thiosulfate pentahydrate used to quench chlorine in  
148 water were Normapur® grade and supplied by VWR. Anhydrous sodium sulfate used to  
149 increase the ionic strength of the water to improve LLE efficiency and to dry the  
150 extracts was also Normapur® grade (VWR). ISOLUTE® Na<sub>2</sub>SO<sub>4</sub> drying cartridges  
151 used to dry extracts for HACMs and HAAs analysis were obtained from Biotage,  
152 Sweden.

153 As for the acids used, ACS reagent grade formic acid (98-100%) (Emsure®), nitric acid  
154 70%, and hydrochloric acid 30% (Suprapure®) were provided by Merck, whereas  
155 sulfuric acid 96% was supplied by VWR.

156 **Table 1.** Target DBPs, and corresponding acronyms, CAS numbers, purity and  
 157 provider of the analytical standard, molecular formula, and mass.

DBP class	Analyte	Acronym	Molecular formula	Mass (Da)*	CAS Number	Supplier (purity, %)
Trihalo-methanes (THMs)	Dibromochloromethane	DBCM	Br <sub>2</sub> ClCH	206	124-48-1	Sigma (>99)
	Bromoform	TBM	Br <sub>3</sub> CH	250	75-25-2	Sigma (>99)
	Dichloro-iodomethane	DCIM	Cl <sub>2</sub> ICH	210	594-04-7	CanSyn (>95)
	Chloro-bromo-iodomethane	BCIM	BrClICH	254	34970-00-8	CanSyn (>95)
	Dibromo-iodomethane	DBIM	Br <sub>2</sub> ICH	298	593-94-2	CanSyn (90-95)
	Chloro-diiodomethane	CDIM	ClI <sub>2</sub> CH	302	638-73-3	CanSyn (90-95)
	Bromo-diiodomethane	BDIM	BrI <sub>2</sub> CH	346	557-95-9	CanSyn (90-95)
	Iodoform	TIM	I <sub>3</sub> CH	394	75-47-8	Sigma (99)
Trihalo-acetaldehydes (THALs)	Chloral	TCAL	Cl <sub>3</sub> C <sub>2</sub> HO	146	75-87-6	Sigma (>98)
	Bromodichloroacetaldehyde	BDCAL	BrCl <sub>2</sub> C <sub>2</sub> HO	190	34619-29-9	CanSyn (90-95)
	Dibromochloroacetaldehyde	DBCAL	Br <sub>2</sub> ClC <sub>2</sub> HO	234	64316-11-6	CanSyn (90-95)
	Bromal	TBAL	Br <sub>3</sub> C <sub>2</sub> HO	278	115-17-3	Sigma (>97)
Halo-acetonitriles (HANs)	Chloroacetonitrile	CAN	C <sub>2</sub> H <sub>2</sub> ClN	75	107-14-2	Sigma (>99)
	Bromoacetonitrile	BAN	C <sub>2</sub> H <sub>2</sub> BrN	119	590-17-0	Sigma (>97)
	Iodoacetonitrile	IAN	C <sub>2</sub> H <sub>2</sub> IN	167	624-75-9	Sigma (>98)
	Dichloroacetonitrile	DCAN	C <sub>2</sub> HCl <sub>2</sub> N	109	3018-12-0	Sigma (>98)
	Dibromoacetonitrile	DBAN	C <sub>2</sub> HBr <sub>2</sub> N	197	3252-43-5	Sigma (>90)
	Bromodichloroacetonitrile	BDCAN	C <sub>2</sub> BrCl <sub>2</sub> N	187	60523-73-1	CanSyn (>85)
	Dibromochloroacetonitrile	DBCAN	C <sub>2</sub> Br <sub>2</sub> ClN	231	144772-39-4	CanSyn (>85)
	Tribromoacetonitrile	TBAN	C <sub>2</sub> Br <sub>3</sub> N	275	<b>75519-19-6</b>	CanSyn (90-95)
Halo-acetamides (HACMs)	Chloroacetamide	CACM	ClC <sub>2</sub> H <sub>4</sub> ON	93	79-07-2	Sigma (>98)
	Bromoacetamide	BACM	BrC <sub>2</sub> H <sub>4</sub> ON	137	683-57-8	Sigma (>98)
	Iodoacetamide	IACM	IC <sub>2</sub> H <sub>4</sub> ON	185	144-48-9	Sigma (>98)
	Bromochloroacetamide	BCACM	BrClC <sub>2</sub> H <sub>3</sub> ON	171	62872-24-8	CanSyn (>99)
	Dichloroacetamide	DCACM	Cl <sub>2</sub> C <sub>2</sub> H <sub>3</sub> ON	127	683-72-7	Sigma (>99)
	Dibromoacetamide	DBACM	Br <sub>2</sub> C <sub>2</sub> H <sub>3</sub> ON	215	598-70-9	CanSyn (>99)
	Chloroiodoacetamide	CIACM	ClIC <sub>2</sub> H <sub>3</sub> ON	219	62872-35-9	CanSyn (>99)
	Bromoiodoacetamide	BIACM	BrIC <sub>2</sub> H <sub>3</sub> ON	263	62872-36-0	CanSyn (>85)
	Diiodoacetamide	DIACM	I <sub>2</sub> C <sub>2</sub> H <sub>3</sub> ON	311	5875-23-0	CanSyn (>99)
	Trichloroacetamide	TCACM	Cl <sub>3</sub> C <sub>2</sub> H <sub>2</sub> ON	161	594-65-0	Sigma (>99)
	Bromodichloroacetamide	BDCACM	BrCl <sub>2</sub> C <sub>2</sub> H <sub>2</sub> ON	205	98137-00-9	CanSyn (>99)
	Dibromochloroacetamide	DBCACM	ClBr <sub>2</sub> C <sub>2</sub> H <sub>2</sub> ON	249	855878-13-6	CanSyn (>99)
	Tribromoacetamide	TBACM	Br <sub>3</sub> C <sub>2</sub> H <sub>2</sub> ON	293	594-47-8	CanSyn (>99)
	Haloacids (HAAs)	Chloroacetic acid	CAA	ClC <sub>2</sub> H <sub>3</sub> O <sub>2</sub>	94	79-11-8
Bromoacetic acid		BAA	BrC <sub>2</sub> H <sub>3</sub> O <sub>2</sub>	138	79-08-3	Sigma (>99)
Iodoacetic acid		IAA	IC <sub>2</sub> H <sub>3</sub> O <sub>2</sub>	186	64-69-7	Sigma (98)
Chlorobromoacetic acid		BCAA	BrClC <sub>2</sub> H <sub>2</sub> O <sub>2</sub>	172	5589-96-8	Sigma (>99)
Dichloroacetic acid		DCAA	Cl <sub>2</sub> C <sub>2</sub> H <sub>2</sub> O <sub>2</sub>	128	79-53-6	Sigma (>99)
Dibromoacetic acid		DBAA	Br <sub>2</sub> C <sub>2</sub> H <sub>2</sub> O <sub>2</sub>	216	631-64-1	Sigma (>99)
Chloroiodoacetic acid		CIAA	ClIC <sub>2</sub> H <sub>2</sub> O <sub>2</sub>	220	53715-09-6	CanSyn (>90)
Bromoiodoacetic acid		BIAA	BrIC <sub>2</sub> H <sub>2</sub> O <sub>2</sub>	264	71815-43-5	CanSyn (>85)
Diiodoacetic acid		DIAA	I <sub>2</sub> C <sub>2</sub> H <sub>2</sub> O <sub>2</sub>	312	598-89-00	CanSyn (>90)
Trichloroacetic acid		TCAA	Cl <sub>3</sub> C <sub>2</sub> HO <sub>2</sub>	162	76-03-9	Sigma (>99)
Bromodichloroacetic acid		BDCAA	BrCl <sub>2</sub> C <sub>2</sub> HO <sub>2</sub>	206	71133-14-7	Sigma (>99)
Dibromochloroacetic acid		DBCAA	Br <sub>2</sub> ClC <sub>2</sub> HO <sub>2</sub>	250	5278-95-5	Sigma (>99)
Tribromoacetic acid		TBAA	Br <sub>3</sub> C <sub>2</sub> HO <sub>2</sub>	294	75-96-7	Sigma (>99)
Dalapon (2,2-dichloropropanoic acid)		DCPA	Cl <sub>2</sub> C <sub>3</sub> H <sub>4</sub> O <sub>2</sub>	142	75-99-0	Sigma (>99)

158 \*Nominal monoisotopic mass (Da).

159

160 The solvents used for sample extraction and liquid chromatography analysis were: Ethyl  
161 acetate (EtAc) for pesticide residue analysis, HPLC-grade water (Chromasolv<sup>TM</sup>), and  
162 HPLC-grade methanol (MeOH) (LiChrosolv®) and methyl *tert*-butyl ether (MTBE)  
163 (SupraSolv®) were provided by Merck.

164 All reagents used in the production of diazomethane (derivatization agent) were  
165 supplied by Sigma Aldrich (Merck): diazald® (99%), Aldrich® diazomethane-generator  
166 with System 45<sup>TM</sup> compatible connection, diethylene glycol monoethyl ether (carbitol  
167 <sup>TM</sup>) (99%) and ACS-grade potassium hydroxide.

168

### 169 ***Sample collection***

170 Water samples were collected at four different DWTPs in Sweden in October 2018. A  
171 volume of 24 L was grab sampled before (IN) and after (OUT) the final chemical  
172 disinfection process in each plant using stainless steel POP-cans (12 L, Sharpville  
173 container/NSF Component<sup>®</sup>). Additional water volumes were collected in 100 mL and  
174 500 mL polyethylene (PE) bottles for general physical-chemical characterization and  
175 AOX measurements. To preserve AOX, sodium thiosulphate was added at a  
176 concentration of 5 mg/L and the water pH was lowered below 2 with concentrated nitric  
177 acid, following previous studies [48] and EN ISO 9562:2004I recommendations [49].  
178 After collection, samples were transported under cool conditions and stored at 4°C in  
179 the dark until extraction, which took place the next day. Chlorine of water collected in  
180 POP-cans was not quenched to prevent potential interferences in the analysis or  
181 contamination. Furthermore, this allows mimicking the DBP mixtures to which  
182 consumers are exposed to since ~24 hours is the time that the finished water is in  
183 contact with the residual disinfectant before reaching the majority of the households in  
184 Sweden.



185 Once in the lab, ascorbic acid (2.5 mg/L), (freshly prepared in Milli-Q-grade water) was  
 186 used to remove free chlorine in sample aliquots used for target analysis, as it was  
 187 reported to be the safest chlorine quenching agent for the analysis of the targeted DBPs  
 188 [50].

189 The selection of DWTPs was based on the type of the source water treated (i.e., surface  
 190 water, or groundwater, and bromide content), and the chemical disinfectant applied (i.e.,  
 191 chlorine or chloramine). Thus, different DBP mixtures were expected to be formed. In  
 192 all plants except in DWTP1, additional disinfection through UV radiation was  
 193 conducted, in all cases before the chemical disinfection (Table2). However, the sample  
 194 collection was designed and performed to examine only the effects of chemical  
 195 disinfection. The investigated DWTPs have different treatment capacities, with daily  
 196 treated water volumes in the range of 10,000 - 200,000 m<sup>3</sup> (for details see Tables 2 and  
 197 3, and Figure 1).

198

199 **Table 2.** Characteristics of the water in the four DWTPs sampled

CODE	Type of source water	Disinfection treatment <sup>a</sup>	TOC (mg/L) <sup>b</sup>	SUVA (L/mg-M) <sup>b</sup>	T (°C) <sup>b</sup>	pH <sup>b</sup>	Br <sup>-</sup> (mg/L) <sup>b</sup>	Residual total Cl <sub>2</sub> (mg Cl <sub>2</sub> /L) <sup>c</sup>
DWTP1	Artificial groundwater (infiltrated river water)	NaOCl	3.7	1.998	10	8.3	0.11	0.50
DWTP2	Surface water (lake)	(UV +) NH <sub>2</sub> Cl	4.8	1.536	10	7.7	0.064	0.34
DWTP3	Groundwater	(UV +) NH <sub>2</sub> Cl	2.5	1.958	12	8.6	0.21	0.24
DWTP4	Surface water (river)	(UV +) NaOCl	4.0	1.399	11	8.6	0.052	0.13

200 <sup>a</sup> IN samples were collected after UV disinfection and OUT samples after chemical disinfection;  
 201 <sup>b</sup> measured in the sample collected before disinfection; <sup>c</sup> measured in the sample collected after  
 202 disinfection

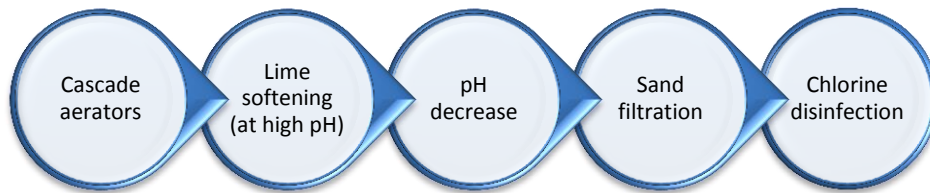
203

204

205

**DWTP1 (46,000 m<sup>3</sup>/day)**

Artificial groundwater (surface water infiltrated into the subsoil)



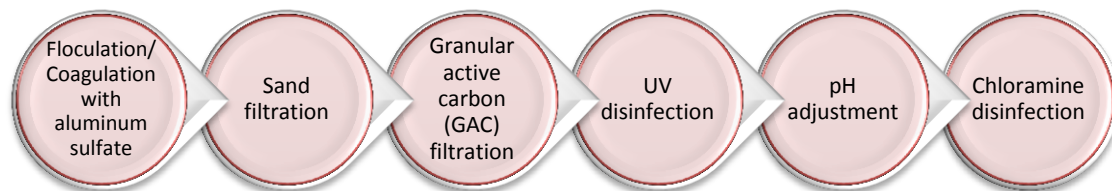
206

207

208

**DWTP2 (200,000 m<sup>3</sup>/day)**

Surface water



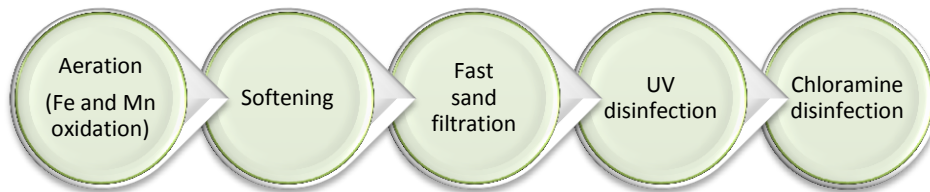
209

210

211

**DWTP3 (26,000 m<sup>3</sup>/day)**

Groundwater



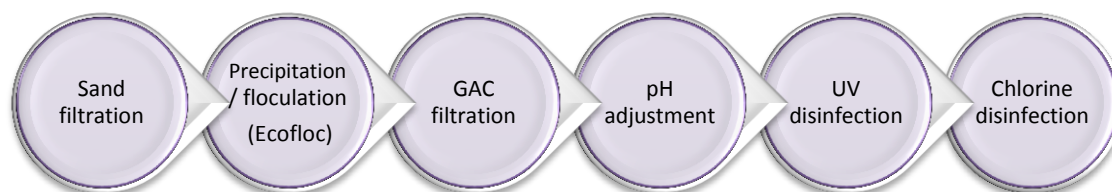
212

213

214

**DWTP4 (10,000 m<sup>3</sup>/day)**

Surface water



215

216

217

218

**Figure 1.** Scheme of the water treatment trains implemented in the DWTPs investigated.

219

220

221 **Table 3.** Additional physical-chemical characterization of water samples.

222

SAMPLE CODE*	A <sub>254</sub> (Abs/m)	Cl <sup>-</sup> (mg/L)	S-SO <sub>4</sub> <sup>-</sup> (mg/L)	F <sup>-</sup> (mg/L)	I-IO <sub>3</sub> <sup>-</sup> (mg/L)	N-NH <sub>4</sub> <sup>+</sup> (mg/L)	N-NO <sub>2</sub> <sup>-</sup> (mg N/L)	N-NO <sub>3</sub> <sup>-</sup> (mg N/L)	Na <sup>+</sup> (mg/L)	K <sup>+</sup> (mg/L)	Mg <sup>2+</sup> (mg/L)	Ca <sup>2+</sup> (mg/L)
<i>LOQs</i>	-	0.03	0.02	0.01	0.03	0.01	0.004	0.02	0.01	0.01	0.01	0.5
DWTP1 IN	7.3	35	11	0.77	5.6	<LOQ	<LOQ	1.9	16	5.0	10	32
DWTP1 OUT	6.6	35	11	0.77	5.6	<LOQ	<LOQ	1.9	16	5.1	10	33
DWTP2 IN	7.3	15	15.	0.15	1.1	<LOQ	<LOQ	0.04	13	2.7	4.7	24
DWTP2 OUT	6.9	15	15.	0.16	1.1	0.06	0.01	0.04	13	2.7	4.7	31
DWTP3 IN	4.9	55	5.2	0.29	2.1	<LOQ	<LOQ	1.1	36	2.9	15	15
DWTP3 OUT	4.8	556	5.2	0.29	2.1	0.02	0.06	1.1	36	2.9	15	15
DWTP4 IN	5.6	18	3.2	0.19	1.4	<LOQ	<LOQ	0.02	13	1.7	2.5	17
DWTP4 OUT	4.8	19	3.1	0.19	1.3	<LOQ	<LOQ	0.03	16	1.7	2.5	18

223

224 \*IN samples were collected after UV disinfection and before chemical disinfection; OUT samples were collected after chemical disinfection.

225 Iodide (I<sup>-</sup>), and phosphate (P-PO<sub>4</sub><sup>-3</sup>), chlorite (ClO<sub>2</sub><sup>-</sup>) and chlorate (ClO<sub>3</sub><sup>-</sup>) were below the limit of quantification (<LOQ) in all samples (LOQ of I<sup>-</sup>: 0.025226 mg/L, LOQ of P-PO<sub>4</sub><sup>-3</sup>: 0.003 mg/L, LOQ of ClO<sub>2</sub><sup>-</sup>: 0.005 mg/L and LOQ of ClO<sub>3</sub><sup>-</sup>: 0.011 mg/L.

227

228 *Sample extraction for target analysis*

229 LLE was used for the target analysis of 47 DBPs. The LLE approaches used to  
230 extract targeted DBPs from water samples were based on the US Environmental  
231 Protection Agency (USEPA) method for the analysis of DBPs in drinking water  
232 (Hodgeson and Cohen 1990). All samples were extracted in duplicate.

233 Ascorbic acid (2.5 mg/L) freshly prepared in Milli-Q-grade water was used to  
234 quench residual free chlorine (<0.5 mg/L) in the samples and preserve the target DBPs.

235 For extraction of THMs, THALs, and THANs, 100 mL of water was acidified to  
236 pH<0.5 with 5 mL of concentrated H<sub>2</sub>SO<sub>4</sub> and then 30 g of dried granular Na<sub>2</sub>SO<sub>4</sub> was  
237 added to increase the ionic strength of the water and favor the partition of the analytes  
238 into the extracting solvent (MTBE). After dissolution, the internal standard (IS) (100 µL  
239 x 1 µg/mL of 1,2-dibromopropane (Sigma Aldrich) in MTBE) was added and mixed in  
240 the solution. Finally, the extracting solvent (2.5 mL of MTBE) was added. Samples  
241 were agitated with a mechanical shaker at 500 rpm for 30 min. After settling for 5 min,  
242 the MTBE, laying on the top of the sample, was collected and dried using a Na<sub>2</sub>SO<sub>4</sub>  
243 column, and stored in a 2-mL vial at -20°C in the dark until GC-MS analysis.

244 To extract HAAs, a similar procedure was followed, using 50 mL and  
245 proportional amounts of H<sub>2</sub>SO<sub>4</sub> (2.5 mL) and Na<sub>2</sub>SO<sub>4</sub> (15 g). After dissolution, the  
246 internal standard (IS) (100 µL x 1 µg/mL of 2,3-dibromopropanoic acid (Sigma  
247 Aldrich) in MTBE). Then, 5 mL of the extracting solvent (MTBE) was added and the  
248 sample was vigorously manually shaken for 2 min. After settling for 5 min, the MTBE,  
249 laying on the top of the sample, was collected and transferred to 20 mL vial. The  
250 extraction step with 5 mL of MTBE was repeated twice, and finally, the combined  
251 MTBE extract was dried using ISOLUTE® Na<sub>2</sub>SO<sub>4</sub> drying cartridges (Biotage,

252 Sweden) and concentrated under N<sub>2</sub> to a volume of 0.4 mL in a graduated test tube. The  
253 HAA extract (0.4 mL) was derivatized for one hour at room temperature with 0.2 mL of  
254 freshly prepared diazomethane. During the derivatization process, the methyl esters of  
255 HAAs were formed. These compounds are more volatile than HAAs and thus, amenable  
256 to GC-MS analysis. Diazomethane was produced in small (~3 mL) amounts from  
257 diazald using a diazomethane generator (Sigma Aldrich, Merck), following the  
258 manufacturer indications. After derivatization, the extract was transferred to a 2-mL vial  
259 with 300 µL insert for GC-MS analysis.

260 The extraction of HACMs was conducted following the same steps as  
261 aforementioned for the extraction of HAAs. However, three main differences in the  
262 extraction protocol have to be highlighted: i) the water pH was lowered only to 5 with  
263 diluted H<sub>2</sub>SO<sub>4</sub> to avoid HACMs degradation, ii) the use of <sup>13</sup>C-bromoacetamide  
264 dissolved in EtAc as IS, and iii) the use of EtAc as extracting solvent. The combined  
265 extract of EtAc obtained after three extraction cycles was dried using ISOLUTE®  
266 Na<sub>2</sub>SO<sub>4</sub> drying cartridges and concentrated under N<sub>2</sub> to a volume of 0.2 mL in a  
267 graduated test tube. Finally, the concentrated extract was transferred to a 2-mL vial with  
268 300 µL insert for GC-MS analysis.

269

### 270 *Sample extraction for non- target analysis*

271 For non-target analysis, the water samples were concentrated in triplicate using an  
272 automated SPE-DEX 4790 system (Horizon Technology Inc, Lake Forest, CA). The  
273 extraction approach used was based on previous works conducted for NOM  
274 characterization [26, 51]. Briefly, 5 L of water was acidified to pH 2.5 with 3 M  
275 hydrogen chloride (HCl) and then passed through an Atlantic hydrophilic-lipophilic  
276 balance (HLB)-H disk (Horizon Technology) previously conditioned with LC-grade

277 methanol (MeOH) (2 x 30 s soak) and acidified LC-grade water (pH=2.5) (2 x 30 s  
278 soak). After sample load, the disk was washed using 0.1% formic acid aqueous solution  
279 (2 x 10 s soak followed by 10 s N<sub>2</sub> dry) to remove chloride and other ions that may  
280 potentially interfere in the FT-ICR MS analysis (e.g., adduct formation). The disk was  
281 eluted with MeOH (2 x 90 s soak followed by 30 s N<sub>2</sub> flow). One-third (~10 mL) of the  
282 final extract (~160-fold concentrated water) was weighted and stored at -20°C in the  
283 dark until FT-ICR MS analysis. This portion of the extract was further diluted with  
284 MeOH to a DOC concentration of ~20 µg/mL to prevent the negative effects of ion  
285 overload or space charging within the ICR cell. The other portion of the final extract  
286 (~20 mL) was reserved for LC-Orbitrap MS analysis. After evaporating its MeOH  
287 fraction, the aqueous extract was further processed using SPE with an Oasis HLB (200  
288 mg) cartridge, using the same conditioning and elution solvents as for SPE-DEX  
289 extraction, to remove excess water (~36 %) and pre-concentrate to a final volume of  
290 200 µL (ultimately a ~16,500-fold concentrated water sample). This extraction protocol  
291 did not allow capturing volatile-DBPs. Although a recovery study was not performed in  
292 this work, a previous study has reported a fairly good capacity of Oasis HLB sorbent to  
293 retain adsorbable organic chlorine and adsorbable organic bromine under acidic pH  
294 [21].

295

### 296 ***Physical-chemical characterization***

297 Major ions were measured in all samples collected using ion chromatography coupled  
298 either to UV detection (230 nm, for iodide and iodate) or conductivity detection (for the  
299 remaining ions). Iodide and iodate were measured with an in house validated procedure,  
300 whereas the analysis of major ions was performed following ISO 10304-1:2007 [52]  
301 and ISO 14911:1998 [53].

302 Total organic carbon (TOC) content was measured in triplicate in non-disinfected water  
303 samples as the non-purgeable organic carbon (NPOC) fraction using a TOC-V<sub>CPH/CPN</sub>  
304 (Shimadzu, Japan) and the high-temperature combustion method (Standard method  
305 5310B) [54]. Samples were first acidified to pH 2 with HCl to convert inorganic carbon  
306 species (e.g., carbonates) to CO<sub>2</sub> that is removed by volatilization after sparging with  
307 synthetic air. Note that some volatile organic compounds are likely to be (partially) lost  
308 during this process. Finally, the sample was injected onto a heated column where  
309 organic compounds are oxidized to CO<sub>2</sub> and the evolved CO<sub>2</sub> is measured with a non-  
310 dispersive infrared gas detector.

311 Specific ultraviolet absorbance (SUVA) of non-disinfected waters was calculated after  
312 triplicate measurements of their UV absorbance at 254 nm with a UV-VIS  
313 spectrophotometer Lambda 365 (Perkin Elmer) following standard method 5910 [55].  
314 Data acquisition was managed with the UV Winlab software 6.4.0.971 (Perkin Elmer).

315 Temperature and pH of the water and residual free chlorine in disinfected water samples  
316 were obtained from on-line probes installed at the DWTPs.

317

### 318 ***Target analysis of halogenated DBPs***

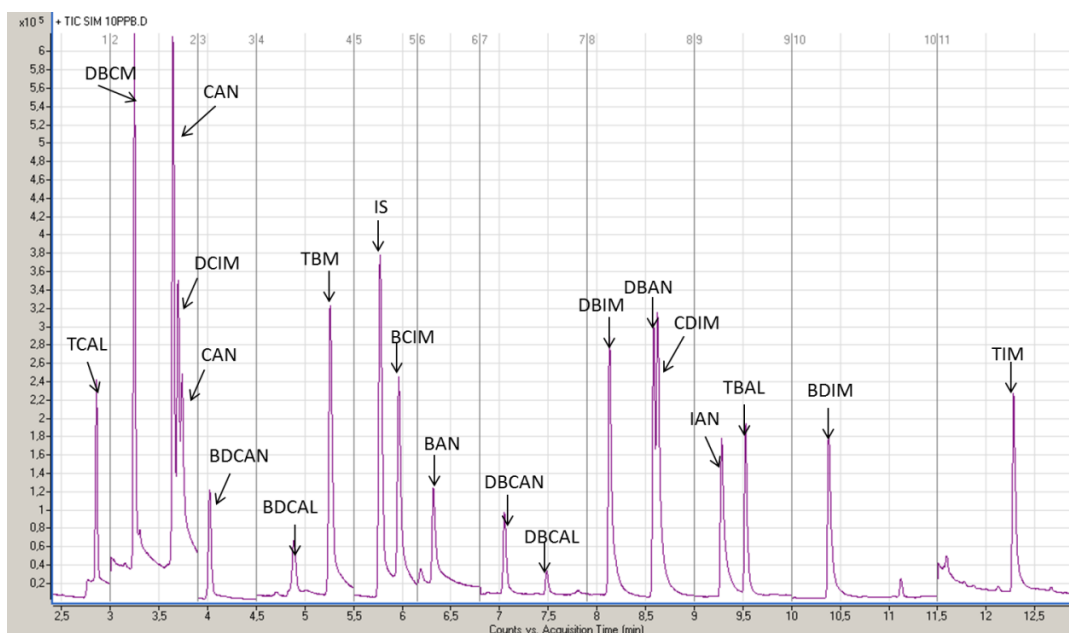
#### 319 *GC-EI-MS analysis of THMs, THALs, HANs, and HACMs*

320 The target analysis of the selected THMs (all except TCM and BDCM), THALs, HANs,  
321 and HACMs was conducted with GC-electron ionization (EI)-MS using a 7890B GC  
322 connected in series with a 5977A MSD (Agilent Technologies). One  $\mu$ L of the extract  
323 was injected in splitless mode using a 7693 automated autosampler equipped with a  
324 multimode inlet (split flow=50 mL/min, splitless time=1.5 min). The temperature of the  
325 injector was maintained at 200°C for 0.1 s and rapidly increased to 300 °C (600°C/min).

326 GC separation was achieved with a capillary GC column Rtx-200 MS (30 m x 0.25 mm  
327 x 0.25  $\mu\text{m}$ ) (Restek, Teknokroma, Barcelona), 1.2 mL/min of constant Helium flow, and  
328 a temperature gradient. For the analysis of THMs, THALs, and HANs the temperature  
329 gradient started at 30°C (held for 5 min), and ramped at a rate of 9°C/min to 165 °C, and  
330 then at a rate of 20 °C/min to 300°C (held for 5 min). In the case of HACMs, the  
331 temperature gradient started at 50°C (held for 3 min) and then, ramped at a rate of  
332 9°C/min to 165°C and a rate of 25°C/min to 285 °C (held for 10 min). During both  
333 analytical runs, the temperatures of the GC-MS transfer line, and the MS source were  
334 set to 280 °C and 200 °C, respectively.

335 The analyzer was operated in selected ion monitoring (SIM) mode. A minimum  
336 of four ions was registered per analyte (see Table 4). Figures 2 and 3 show the total ion  
337 chromatogram obtained after analysis of calibration standard solutions at a  
338 concentration of 10  $\mu\text{g/mL}$ . Mass acquisition and data analysis were performed using  
339 Mass Hunter B.07.00 software (Agilent Technologies).

340

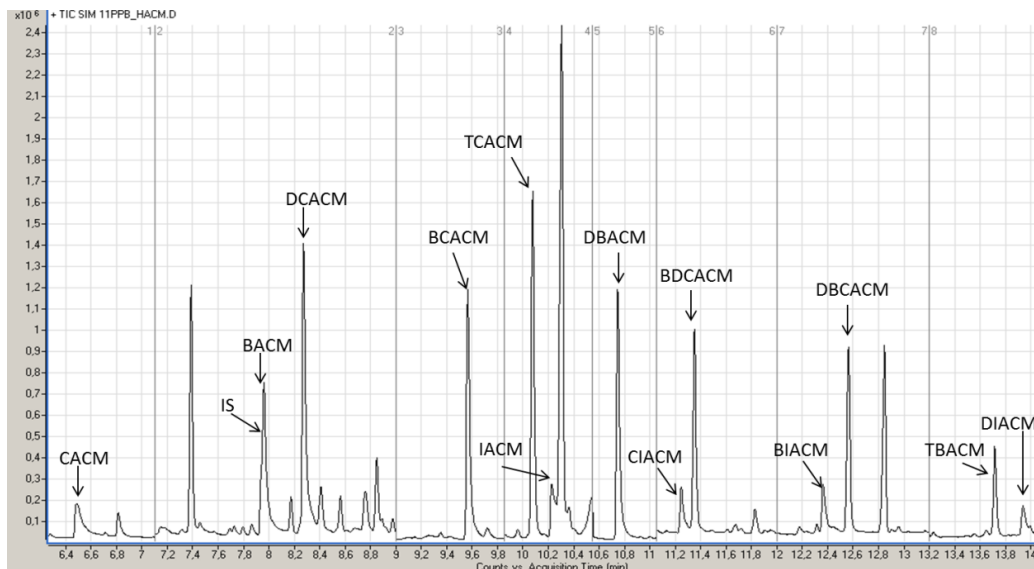


341

342 **Figure 2.** Total ion chromatogram (TIC) obtained after GC-EI-MS analysis of MilliQ  
343 water fortified with the target THMs, THALs, and HANs at a concentration of 10  $\mu\text{g/L}$ .



344 The THMs chloroform (TCM) and dichlorobromomethane (DCBM) were not  
345 captured with the analytical conditions used as they eluted in the solvent peak front and  
346 therefore, they had to be excluded from the analysis.



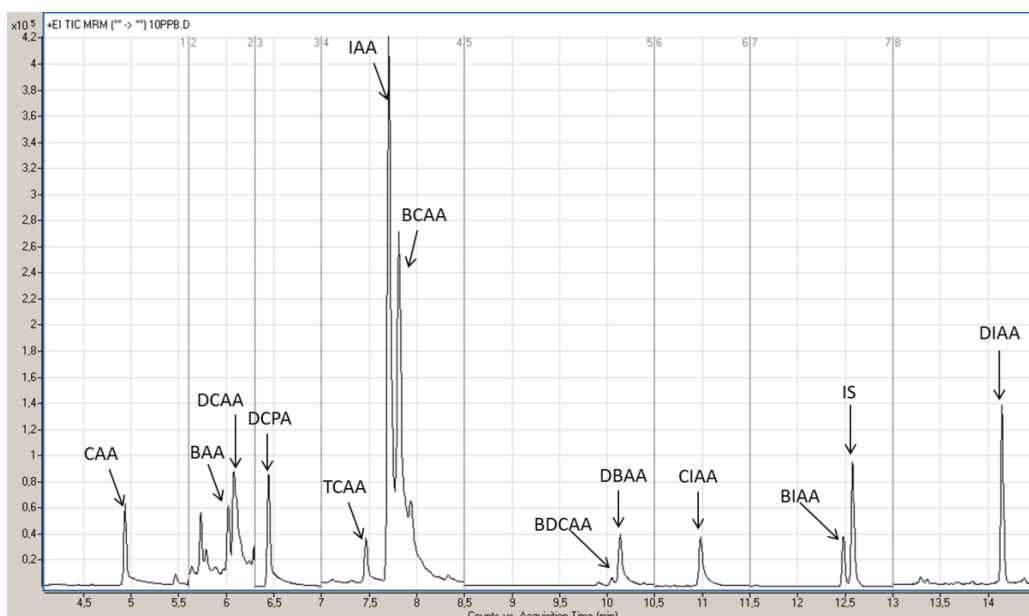
347  
348 **Figure 3.** Total ion chromatogram (TIC) obtained after GC-EI-MS analysis of MilliQ  
349 water fortified with the target HACMs at a concentration of 10 µg/L.  
350

351  
352 GC-EI-MS/MS analysis of HAAs.

353 Analytical determination of methyl esters of HAAs was performed using a 7890B GC  
354 connected in series to a 7000C triple quadrupole (Agilent Technologies). Ionization was  
355 carried out in the electron ionization mode. One µL of the derivatized extract was  
356 injected in splitless mode using a7638B automated injector (split flow=50 mL/min,  
357 splitless time=1.5 min). GC separation of the analytes was achieved using a capillary  
358 GC column Rtx-200 MS (30 m x 0.25 mm x 0.25 µm) (Restek, Teknokroma,  
359 Barcelona), 1.2 mL/min constant flow of Helium and a temperature gradient (40 °C held  
360 for 2 min, then increased at 10 °C/min to 65 °C and held for 2 min, and further increased  
361 at 10 °C/min to 110°C and at 20°C/min to 285 °C and held for 15 min. The temperatures

362 of the injector, the GC/MS transfer line, and the MS source were set to 250 °C, 280 °C,  
363 and 200 °C, respectively.

364 The analyzer was operated in selected reaction monitoring (SRM) mode, using nitrogen  
365 (1.5 mL/min) as the collision gas. A minimum of two SRM transitions was acquired per  
366 analyte (see Table 4). Figure 4 shows the total ion chromatogram obtained after the  
367 analysis of a standard calibration solution at a concentration of 10 µg/mL. Mass  
368 acquisition was performed using MSD ChemStation and data analysis was done with  
369 Mass Hunter B.08 (Agilent Technologies).



370  
371 **Figure 4.** Total ion chromatogram (TIC) obtained after GC-EI-MS/MS analysis of  
372 MilliQ water fortified with the target HAAs at a concentration of 10 µg/L.  
373

#### 374 Performance of target methods

375 The performance of the targeted methods was evaluated in terms of linearity,  
376 sensitivity, and accuracy (analyte recovery) and method repeatability. The results are  
377 summarized in Table 4. Quantification was performed by the internal standard method.  
378 For this, calibration curves were constructed by plotting the ratio of the analyte and the  
379 internal standard peak areas obtained in the different standard calibration solutions

380 (Milli Q water fortified at different concentration levels with the mixture of the target  
381 DBPs). A minimum of five calibration data points (exceptionally four in the case of few  
382 DBPs) in the range 0.1-50  $\mu\text{g/L}$  in the case of THMs, THALs, and HANs, and 0.05-50  
383  $\mu\text{g/L}$  in the case of HACMs, and HAAs were used to construct these calibration curves.  
384 Quantitation of each analyte in the investigated samples was done according to the  
385 least-squares linear regression model obtained after the linear fitting of its calibration  
386 curve. The linearity range observed for each analyte and the coefficient of determination  
387 obtained for the corresponding model are summarized in Table 4.

388 Method sensitivity was estimated from the analyte signal observed at the lowest  
389 calibration solutions. Method reporting limits corresponded with the analyte  
390 concentration that provided a signal-to-noise ratio of 10, and concentrations below the  
391 MRL with an S/N ratio of 3 were provided as detected but could not be quantified.

392 Analyte absolute recoveries and method repeatability were evaluated through a  
393 recovery study. For this, LC-grade waters were fortified with the target DBPs at 0.5  
394  $\mu\text{g/L}$  ( $n=4$ ) or higher concentration in the case of regulated THMs, DBCM, and TBM,  
395 and the trihalo-HANs BDCAN, DBCAN and TBAN, (1  $\mu\text{g/L}$ ,  $n=3$ ) or those DBPs with  
396  $\text{MRL} \geq 2.5 \mu\text{g/L}$  (DIACM, DBCACM, BDCAA, DBCAA, and TBAA) (5  $\mu\text{g/L}$ ,  $n=4$ )  
397 and extracted following the analytical protocols described. To calculate analyte absolute  
398 recoveries and repeatability the peak areas obtained in fortified water samples and  
399 standard solutions at equivalent concentrations were compared. The lowest recoveries  
400 were found for HACMs, which affects the sensitivity of the method for these  
401 compounds. However, analyte losses during the extraction were automatically corrected  
402 in the quantification process because calibration solutions were prepared by fortifying  
403 LC-grade water at different concentrations and processing these solutions as if they  
404 were samples.

405 **Table 4.** Retention time and ions/SRM transitions monitored for GC-MS analysis of  
 406 the target DBPs. The quantification ion/SRM transition is highlighted in bold.

Class	Analyte	SIM or SRM (m/z)	t <sub>R</sub>	Linearity**		Recovery* % (RSD)	
				Range(µg/L)	R <sup>2</sup>		
THMs	DBCM	<b>129</b> ,127,131	3.24	0.1-25	0.9979	108 (11)	
	TBM	<b>173</b> ,171,252	5.27	0.1-5	0.9978	124 (13)	
	DCIM	<b>83</b> ,127,175	3.73	0.1-10	0.9951	76 (19)	
	BCIM	<b>127</b> ,129,175	5.96	0.1-25	0.9959	79 (15)	
	DBIM	<b>173</b> ,171,127	8.10	0.1-5	0.9917	90 (19)	
	CDIM	<b>175</b> ,177,127	8.60	0.1-5	0.9959	70 (19)	
	BDIM	<b>219</b> ,127,140	10.38	0.25-5	0.9971	39 (15)	
	TIM	<b>267</b> ,394,127	12.30	0.1-5	0.9964	76 (17)	
THALs	TCAL	<b>82</b> ,84,111	2.77	0.25-2.5	0.9992	62 (10)	
	BDCAL	83, <b>111</b> ,128	4.81	0.25-2.5	0.9993	68 (23)	
	DBCAL	127, <b>129</b> ,157	7.49	0.25-2.5	0.9963	55 (21)	
	TBAL	<b>173</b> ,175,252	9.52	0.1-2.5	0.9935	70 (21)	
HANs	CAN	<b>75</b> ,77,48	3.74	0.25-10	0.9913	41 (21)	
	BAN	<b>119</b> ,121,79	6.34	0.1-2.5	0.9903	54 (15)	
	IAN	<b>167</b> ,127,139	9.28	0.1-2.5	0.9915	54 (24)	
	DCAN	74, <b>82</b> ,76	3.65	0.1-10	0.9971	96 (17)	
	DBAN	118, <b>120</b> ,199	8.60	0.1-2.5	0.9926	90 (27)	
	BDCAN	108, <b>110</b> ,154	4.02	1-10	0.9924	82 (17)	
	DBCAN	<b>154</b> ,152,79	7.06	0.25-5	0.9905	84 (10)	
	TBAN	<b>198</b> ,200,117	9.54	0.25-5	0.9921	78 (28)	
HACMs	CACM	44,49, <b>93</b>	6.56	0.5-10	0.9941	12 (9)	
	BACM	44, <b>137</b> ,139	8.00	0.5-10	0.9965	17 (3)	
	IACM	58,127, <b>185</b>	10.24	0.5-25	0.9934	23 (8)	
	BCACM	44, <b>173</b> ,93	9.50	0.25-10	0.9971	67 (8)	
	DCACM	<b>44</b> ,85,129	8.30	0.1-10	0.9919	60 (6)	
	DBACM	44,217, <b>174</b>	10.76	0.1-10	0.9868	68 (9)	
	CIACM	44, <b>219</b> ,176	11.27	0.5-25	0.9911	32 (14)	
	BIACM	138,220, <b>263</b>	12.38	0.25-10	0.9916	47 (8)	
	DIACM	127, <b>184</b> ,311	13.97	2.5-50	0.9921	23 (7)	
	TCACM	<b>44</b> ,82,98	10.01	0.05-5	0.9944	77 (7)	
	BDCACM	<b>44</b> ,126,82	11.34	0.1-10	0.9939	42 (13)	
	DBCACM	<b>44</b> ,207,251	12.57	2.5-10	0.9641	18 (5)	
	TBACM	44, <b>172</b> ,295	13.73	0.5-25	0.9923	39 (10)	
HAAs	CAA	<b>77&gt;49</b> , 79>51, 108>76	4.93	0.25-25	0.9910	59 (10)	
	BAA	<b>121&gt;93</b> , 123>95	6.07	0.25-25	0.9971	68 (9)	
	IAA	<b>200&gt;73</b> , 169>141	7.80	0.05-25	0.9971	73 (9)	
	BCAA	<b>127&gt;92</b> , 129>94	7.94	1-50	0.9952	89 (13)	
	DCAA	<b>83&gt;47</b> , 85>47, 111>83	6.11	0.5-25	0.9981	86 (9)	
	DBAA	<b>171&gt;92</b> , 173>94	10.13	0.1-25	0.9949	84 (11)	
	CIAA	<b>234&gt;79</b> , 175>48, 234>107	10.98	0.5-25	0.9952	60 (19)	
	BIAA	<b>280&gt;125</b> , 278>123, 221>94	12.47	0.1-2.5	0.9983	68 (21)	
	DIAA	<b>326&gt;171</b> , 326>199	14.14	0.05-2.5	0.9969	51 (25)	
	TCAA	<b>117&gt;82</b> , 119>84	7.46	0.1-25	0.9971	84 (17)	
	BDCAA	<b>161&gt;82</b> , 163>82	10.05	2.5-25	0.9913	65 (32)	
		DBCAA	<b>187&gt;159</b> , 209>128, 207>128	12.13	-	-	NR
		TBAA	<b>251&gt;172</b> , 253>172	13.76	-	-	NR
	DCPA	<b>97&gt;61</b> , 278<123, 187<105	6.44	0.05-5	-	68 (19)	

407 \*Average absolute recoveries observed at 0.5 µg/L (n=4) and relative standard deviation (RSD). In the  
 408 case of regulated THMs, DBCM, and TBM, and the trihalo-HANs BDCAN, DBCAN, and TBAN,  
 409 recoveries were investigated at 1 µg/L (n=3). For those analytes with MRL≥2.5 µg/L (DIACM,  
 410 DBCACM, BDCAA, DBCAA, and TBAA, average absolute recoveries were studied at a concentration  
 411 level of 5 µg/L (n=4). NR: Analyte not properly recovered (RSD>100 and absolute recovery <30).  
 412 \*\*A minimum of 5 calibration points (exceptionally four) in the range 0.1-50 µg/L in the case of THMs,  
 413 THALs, and HANs, and 0.05-50 µg/L in the case of HACMs, and HAAs were used to construct  
 414 calibration curves.

415 ***AOX analysis***

416 AOX was determined to assess the bulk of halogenated compounds present in the water.  
417 AOX analyses were conducted in all samples in triplicate, according to ISO standard  
418 9562:2004 [49]. Briefly, 100 mL of water was transferred to an Erlenmeyer flask,  
419 followed by pH adjustment to ~pH 2 using concentrated HNO<sub>3</sub> and the addition of 5 mL  
420 acidic nitrate solution (0.02 M HNO<sub>3</sub>, 0.2 M KNO<sub>3</sub>) and 50 mg ( $\pm$ 3 mg) activated  
421 carbon. The flask was shaken for 60 min at 180 rpm. The samples were then filtered to  
422 retain the activated carbon with the adsorbed organic compounds (polycarbonate  
423 material, 0.4  $\mu$ m) (GE Healthcare Life Sciences, Uppsala, Sweden). Remaining halides  
424 were washed out from the filter using sequentially 2x10 mL of an acid nitrate solution  
425 (1 mM HNO<sub>3</sub>, 10 mM KNO<sub>3</sub>) and 2x10 mL of acidified Milli-Q water (pH 2, after  
426 addition of concentrated HNO<sub>3</sub>). The adsorbed organic compounds were combusted at  
427 1000 °C in O<sub>2</sub> atmosphere and the halides (HX) released in the process were determined  
428 by on-line microcoulometric titration (ECS 3000, Thermo Fisher Scientific).

429

430 ***Non-target FT-ICR MS analysis of halogenated DBPs***

431 Non-target analysis of halogenated DBPs in SPE-DEX extracts was performed using a  
432 Bruker SolariX 12 Tesla FT-ICR MS and an APPOLO II ionization source, operating in  
433 negative electrospray ionization (ESI(-)) mode. The analysis was performed with a  
434 spray current of -3.6 kV and a flow rate of 2  $\mu$ L min<sup>-1</sup>. A source heater temperature of  
435 200°C was maintained to ensure rapid desolvation in the ionized droplets. The spectra  
436 were acquired with a time-domain of 4 megawords, and 300 scans were accumulated for  
437 each mass spectrum over the mass range  $m/z$  147.4 to 1000. Injection lines were washed  
438 with a mixture of MeOH:water (8:2, v/v) between each sample, and MeOH solvents  
439 were run to control cross-contamination and carry-over.

440 The non-target approach used is suitable to investigate non-volatile, medium to low  
441 polarity, and oxygen-containing compounds, e.g., molecules with carboxyl and/or  
442 hydroxyl moieties (amenable to ESI(-)).

443 For data processing, unique molecular formulae were assigned to  $m/z$  ions present in the  
444 mass spectra using in-house software, developed at the Helmholtz Center for  
445 Environmental Health, Munich (Germany). Element constraints for the molecular  
446 formulae assignments were  $^{12}\text{C}$ : 0–100,  $^1\text{H}$ : 0– $\infty$ ,  $^{16}\text{O}$ : 0–80,  $^{14}\text{N}$ : 0–3,  $^{32}\text{S}$ : 0–2,  $^{35}\text{Cl}$ : 0–  
447 5 and  $^{79}\text{Br}$ : 0–5. As a first data filter, only molecular formulas with a total ion count  
448 (TIC) intensity  $>3,000,000$ ,  $m/z \leq 800$  Da, a mass error  $\leq 0.2$  ppm, and in agreement with  
449 the nitrogen rule (i.e., N containing ions with even mass contain an odd number of N  
450 atoms) and containing Cl and Br atoms were further processed to identify and verify  
451 chlorinated and brominated DBPs, according to the approach followed in a previous  
452 study [26]. Iodine was not considered in formula assignment because an initial search  
453 using in-house developed software did not detect iodine-containing compounds.

454 Furthermore, unrealistic formulae were also discarded according to their C, H and O  
455 proportions, so that only those with C, O and H  $>0$ , O/C  $\leq 1$ , H/C  $\leq 2.5$ , N and S  $\leq 1$  and  
456 double bond equivalents (DBE)  $\geq 0$  were considered. Remaining formulae were verified  
457 as halogenated DBPs after evaluation of their predictable isotopic patterns, i.e., the  
458 presence of  $m/z$  ions expected to occur due to the different combinations of chlorine and  
459 bromine stable isotopes ( $^{35}\text{Cl}/^{37}\text{Cl}$  and  $^{79}\text{Br}/^{81}\text{Br}$ ). Verified formulae containing nitrogen  
460 or sulfur atoms were very few (Tables 7 and 8). Moreover, in the case of S-containing  
461 formulae, the majority was present in non-disinfected and disinfected waters at  
462 comparable intensity, and therefore they were excluded for data analysis.

463 Only verified formulae with CHO and Br and/or Cl occurring in all three sample  
464 replicates of the water samples were further evaluated and interpreted. Finally, the

465 formulae detected after disinfection while not being detected at the point before  
466 disinfection were considered as DBPs. Hence, presence and absence, rather than  
467 differences in relative intensities of individual formulae, was used to define the DBPs  
468 formed. Procedural blanks were used as quality controls because the very few peaks  
469 present in blank samples are usually not seen in real samples due to the suppression  
470 effects caused by the sample matrix components that compete for ionization.

471 Visualization of non-target data was undertaken through three-dimensional van  
472 Krevelen diagrams (H/C vs O/C) that provide information about the degrees of  
473 saturation (y-axis) and oxygenation (x-axis) of the verified formulae [56] and their mass  
474 distribution. Modified Kendrick mass defect ( $-KMD/z^*$ ) plots were also created to show  
475 homologous series of molecules according to increasing number of methylene ( $-CH_2$ )  
476 units in the x-axis and the nominal exchange of  $CH_4$  against O along the y-axis and  $H_2$   
477 along diagonals, since heteroatoms in the verified formulae are limited to oxygens [57].  
478 Diagrams showing DBE [58], modified aromaticity index ( $AI_{mod}$ ) [58], and average  
479 oxidation state of the carbon ( $C_{OS}$ ) [26] against the number of carbons of the verified  
480 formulae were also constructed to evaluate and detect changes in DBP mixtures.

481 The differences in mass distribution, O/C, O/H, DBE,  $AI_{mod}$ ,  $C_{OS}$ , Cl/C and Br/C of the  
482 halogenated mixtures observed in each plant before and after disinfection (after  
483 removing overlapping features) were statistically evaluated using non-parametric tests  
484 (Mann-Whitney U test) with a significance level of 0.05. To evaluate significant  
485 differences among all investigated disinfected waters, the Kruskal-Wallis test, and  
486 Dunn's pairwise *post hoc* tests were applied. Statistics were done using IBM SigmaPlot  
487 12.5.

488

489

490 ***Non-target LC-ESI(-)-Orbitrap MS analysis of halogenated DBPs***

491 The SPE-concentrated fraction was analyzed using an Acquity UPLC system (Waters)  
492 coupled to an Orbitrap mass spectrometer (QExactive, Thermo Scientific).  
493 Chromatographic separation was achieved with a Purospher® STAR RP-18 endcapped  
494 column (2 µm particle size, 150x2.1 mm) and a linear organic gradient of a mobile  
495 phase consisting of water and MeOH both with 0.1% formic acid at a constant flow rate  
496 of 0.2 mL/min.

497 ESI was performed in the negative mode (ESI(-)) for the comparability of FT-ICR MS  
498 results. HRMS acquisition was conducted in data-dependent scan mode. This included a  
499 full scan over the  $m/z$  range 35- 650 at full width at half maximum (FWHM) resolution  
500 of 70,000, and a data-dependent-MS<sup>2</sup> scan at a resolution of 35,000 on the top 10 ions  
501 above an intensity threshold of  $1e^5$ .

502 HRMS data were processed using the Compound Discoverer 3.1 software. Element  
503 constraints for the molecular formulae assignments were <sup>12</sup>C: 0–90, <sup>1</sup>H: 190–∞, <sup>16</sup>O: 0–  
504 15, <sup>14</sup>N: 0–10, <sup>32</sup>S: 0–5, <sup>31</sup>P: 0–3, <sup>23</sup>Na: 0–2, <sup>35</sup>Cl: 0–4, <sup>79</sup>Br: 0–4, <sup>127</sup>I: 0–3, and mass error  
505 was set to ± 5 ppm. The number of oxygen atoms for elemental composition prediction  
506 was restricted to 15 according to the findings of FT-ICR MS data (halogenated formulae  
507 with a maximum of 12 oxygen atoms, Figure 11). Only features above a TIC intensity  
508 of 100,000 were considered. The thousands of peaks found were prioritized for further  
509 identification tasks according to their exclusive occurrence in all three replicates of  
510 disinfected water samples and absence in non-disinfected and blank samples and to the  
511 presence of halogens (i.e., Cl, Br or I) in their structure.

512 Orbitrap MS has a lower FWHM mass resolution (70,000 at  $m/z$  200) than FT-ICR MS  
513 (400,000 at  $m/z$  400), which results in a higher mass error (<5 ppm vs <0.2 ppm). Such  
514 a mass error in Orbitrap MS generally leads to more than one logical elemental



515 composition containing CHO, N, S, I, Br, and/or Cl. Therefore, the isotopic pattern of  
516 the parent ion was used to restrict the number of Br and Cl atoms in the elemental  
517 composition, so that the isotopic cluster includes all ions with an  $m/z$  defect of  $\pm 1.997$ .  
518 Once the elemental composition was established, the MS2 fragmentation of the  
519 prioritized DBP was compared with *in silico* fragmentation of molecules with the same  
520 elemental composition contained in the PubChem database using MetFrag  
521 (<https://msbi.ipb-halle.de/MetFrag/>) [59]. The one with the highest score was provided  
522 as a tentative candidate, and its identity was only confirmed after the comparison of its  
523 retention time and MS2 fragmentation with an analytical standard (when available). The  
524 scoring terms selected were i) fragments match after *in silico* fragmentation and ii)  
525 spectral similarity of structure candidates (Figure 5). This workflow is illustrated in  
526 Figure 5, using halogenated derivatives of hydroxypiranes as an example. The main  
527 limitation of this approach is that structure candidates are limited to the database  
528 content.

529

### 530 ***Transformation of DBP concentrations into Cl-equivalent concentrations***

531 To convert DBP concentrations into Cl-eq concentrations, the following formula was  
532 applied, in which the same atomic weight (35.45 Da) is assigned to all halogens present  
533 in the molecule (chlorine, bromine, and iodine) [60]:

534

$$\frac{\mu\text{g of DBP as Cl - eq}}{L} = \frac{\text{DBP conc } \left(\frac{\mu\text{g}}{L}\right)}{\text{DBP M.W. } \left(\frac{\text{g}}{\text{mol}}\right)} * (\text{No. halogen atoms}) * 35.45$$

535

536 where *DBP conc* is the concentration of the DBP (in  $\mu\text{g/L}$ ) and *DBP M.W.* is the  
537 molecular weight of the DBP (in  $\text{g/mol}$ ).

538

539

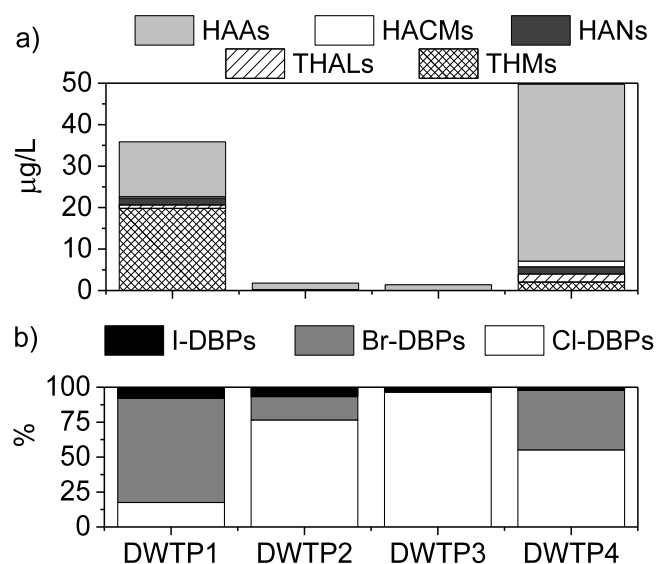


553  
554

**Table 5.** Concentration (in ng/L) of the target halogenated DBPs measured in the disinfected water samples (n.d.= not detected). MRL: method reporting limit.

Class	Analyte	DWTP1	DWTP2	DWTP3	DWTP4	MRL
THMs	DBCM	15	n.d.	n.d.	1.6	<0.10
	TBM	2.6	n.d.	n.d.	<0.1	<0.10
	DCIM	0.97	n.d.	n.d.	0.37	0.10
	BCIM	0.77	n.d.	n.d.	<0.1	0.10
	DBIM	0.19	n.d.	n.d.	n.d.	0.10
	CDIM	n.d.	n.d.	n.d.	n.d.	0.10
	BDIM	n.d.	n.d.	n.d.	n.d.	0.25
	TIM	n.d.	n.d.	n.d.	n.d.	0.10
THALs	TCAL	0.45	n.d.	n.d.	1.7	0.25
	BDCAL	0.41	n.d.	n.d.	0.30	0.25
	DBCAL	n.d.	n.d.	n.d.	n.d.	0.25
	TBAL	n.d.	n.d.	n.d.	n.d.	0.10
HANs	CAN	n.d.	n.d.	n.d.	n.d.	0.25
	BAN	n.d.	n.d.	n.d.	n.d.	0.10
	IAN	n.d.	n.d.	n.d.	n.d.	0.10
	DCAN	0.88	<0.1	n.d.	1.7	0.10
	DBAN	0.71	n.d.	n.d.	n.d.	0.10
	BDCAN	n.d.	n.d.	n.d.	n.d.	0.50
	DBCAN	n.d.	n.d.	n.d.	n.d.	0.25
	TBAN	n.d.	n.d.	n.d.	n.d.	0.25
HACMs	CACM	n.d.	n.d.	n.d.	n.d.	0.25
	BACM	n.d.	n.d.	n.d.	n.d.	0.50
	IACM	n.d.	n.d.	n.d.	n.d.	0.50
	BCACM	0.39	<0.1	n.d.	0.24	0.10
	DCACM	n.d.	<0.25	n.d.	1.1	0.25
	DBACM	n.d.	n.d.	n.d.	n.d.	0.10
	CIACM	n.d.	n.d.	n.d.	n.d.	0.50
	BIACM	n.d.	n.d.	n.d.	n.d.	0.25
	DIACM	n.d.	n.d.	n.d.	n.d.	2.5
	TCACM	n.d.	n.d.	n.d.	<0.05	0.05
	BDCACM	n.d.	n.d.	n.d.	n.d.	0.10
	DBCACM	n.d.	n.d.	n.d.	n.d.	2.5
TBACM	n.d.	n.d.	n.d.	n.d.	0.50	
HAAs	CAA	0.39	n.d.	n.d.	0.57	0.25
	BAA	0.38	n.d.	n.d.	<0.25	0.25
	IAA	<0.05	n.d.	0.05	<0.05	0.05
	BCAA	2.1	n.d.	n.d.	3.3	1.0
	DCAA	3.2	1.2	1.1	12	0.50
	DBAA	1.9	0.25	n.d.	0.49	0.10
	CIAA	0.61	n.d.	n.d.	0.62	0.05
	BIAA	0.12	n.d.	n.d.	n.d.	0.05
	DIAA	0.13	0.12	n.d.	n.d.	0.05
	TCAA	1.4	<0.1	0.30	11	0.10
	BDCAA	2.7	n.d.	n.d.	8.6	2.5
	DBCAA	n.d.	n.d.	n.d.	<10	10
	TBAA	n.d.	n.d.	n.d.	n.d.	10
	DPN	0.25	n.d.	n.d.	1.6	0.05

555



556

557 **Figure 6.** a) Concentrations of the target halogenated DBP classes investigated in  
 558 chemically disinfected waters and b) proportion (%) of iodine-, bromine- and only  
 559 chlorine-containing DBPs to target  $\Sigma\text{DBP}$  concentrations.

560

561 After chemical disinfection, the highest total concentrations of selected DBPs ( $\Sigma\text{DBP}$ )  
 562 were found in chlorinated waters, DWTP1 (36  $\mu\text{g/L}$ ), and DWTP4 (50  $\mu\text{g/L}$ ). On the  
 563 contrary,  $\Sigma\text{DBP}$  in chloraminated waters was always  $<2 \mu\text{g/L}$ . Overall, the halogenated  
 564 DBP classes THMs and HAAs were the dominant groups, with a joint average  
 565 contribution of 92 % to the  $\Sigma\text{DBP}$ . It is well known that the use of chlorine enhances the  
 566 formation of THMs and HAAs as compared to chloramine-based treatments [14, 61,  
 567 62]. The fact that TCM and BDCM, the main THM species formed during chlorination  
 568 of waters with low bromide content [63, 64], were not covered in our study may explain  
 569 that HAAs contributed more than THMs to  $\Sigma\text{DBP}$  in DWTP4, where bromide  
 570 concentration in source water was quite low (0.054 mg/L), and therefore, high  
 571 concentrations of TCM and BDCM could form. According to the measurements of  
 572 regulated THMs conducted by the DWTPs in that period of the year, TCM and BDCM  
 573 may contribute with 73% and 94% to the total THM concentrations present in DWTP1  
 574 and DWTP4, respectively.

575 According to the target approach, the formation of iodine-containing DBPs of the  
576 investigated waters was in general low (< 8%), which is in agreement with the low  
577 iodide levels of the source waters (<limit of quantification (LOQ) of 25 µg/L). As for  
578 the potential of the waters to form bromine-containing DBPs (those compounds with at  
579 least one bromine atom in their structure, excluding iodo-DBPs that contain also  
580 bromine), the highest concentrations were found in waters from DWTP1, where 75% of  
581 the DBP mass found was formed by Br-DBPs, followed by waters from DWTP4, with  
582 43% of Br-DBPs. This can be related to the amounts of bromide present in the  
583 corresponding non-chemically disinfected waters (0.11 mg/L in DWTP1 and 0.054  
584 mg/L in DWTP4). Note that these contributions of Br-DBPs are higher than real due to  
585 failure in capturing TCM and BDCM with the GC-MS conditions used. Because of the  
586 high Br<sup>-</sup> levels of DWTP3 source water (0.21 mg/L), the bromine incorporation into  
587 NOM during chloramination could also be expected, although it was not reflected in the  
588 target analysis, i.e., no Br-DBPs were found. Low bromine incorporation factors into  
589 NOM in the presence of chloramine have been consistently reported in the literature  
590 [65-67]. This could be attributed to the negligible formation of HOBr in the presence of  
591 chloramine via bromamine formation ( $\text{NH}_2\text{Cl} + \text{Br}^- \rightarrow \text{NH}_2\text{Br} + \text{Cl}^-$  with  $k=1.4 \times 10^{-2}$   
592  $\text{M}^{-1}\text{s}^{-1}$  and  $\text{NH}_2\text{Br} + \text{H}_2\text{O} \rightarrow \text{HOBr} + \text{NH}_3$  with  $k=1.5 \times 10^{-3} \text{M}^{-1}\text{s}^{-1}$ ) [68], or  
593 chloramine hydrolysis ( $\text{NH}_2\text{Cl} + \text{H}_2\text{O} \rightarrow \text{HOCl} + \text{NH}_3$ , with a reaction rate constant  
594  $k=3.0 \times 10^{-5} \text{M}^{-1}\text{s}^{-1}$ ) and subsequent reaction of HOCl with bromine [68-70], and/or the  
595 low stability of bromamines in the solution compared to chloramines [70]. Moreover,  
596 the brominated-DBPs formed during chloramination processes may have not been  
597 targeted with our analytical approaches (e.g., amine compounds). This could be the case  
598 of bromochloramine, a reaction product of monochloramine with bromine whose

599 formation exceeds its decay after 24 h chloramine contact time in a typical drinking  
600 water distribution system, as predicted by Liu and Mariñas [71].

601 Among the HANs and HACMs, only trace levels (<1 µg/L) of dihalogenated species  
602 (HANs: dichloroacetonitrile (DCAN) and dibromoacetonitrile (DBAN); HACMs:  
603 dichloroacetamide (DCACM) and bromochloroacetamide (BCACM)) were formed after  
604 chemical disinfection in all plants, except in DWTP3 (Table 5). THALs were only  
605 present in chlorinated waters.

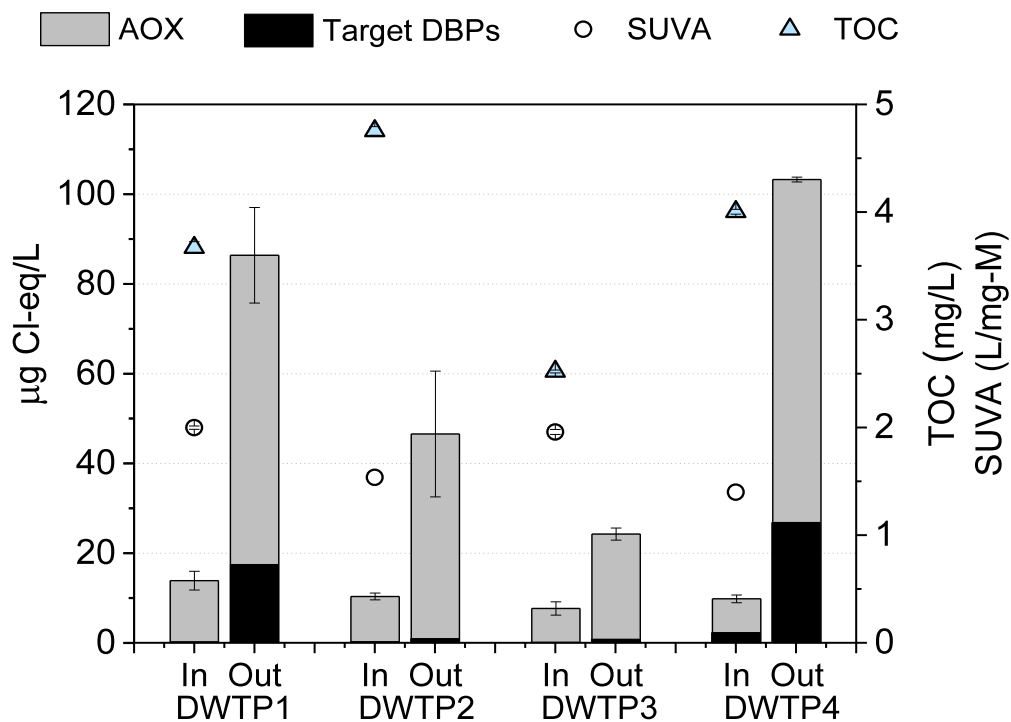
606

#### 607 *AOX as a surrogate measurement of halogenated DBP mixtures*

608 AOX is a bulk measurement of known and unknown DBPs in a sample [72, 73]. AOX  
609 concentrations of disinfected waters (Figure 7) were in line with the total target DBP  
610 concentrations measured, with decreasing levels in the order DWTP4 > DWTP1 >  
611 DWTP2 > DWTP3. The AOX level of water collected at DWTP2 was about half of the  
612 levels observed in DWTP1 and DWTP4, in spite a higher TOC content (Table 2). This  
613 is consistent with previous studies reporting that chloramine (used at DWTP2) has a  
614 lower reactivity towards NOM and hence, results in the formation of lower DBP levels,  
615 as compared to chlorine (used at DWTP1 and DWTP4) [14, 73, 74]. In the present  
616 study, chlorination increased background AOX levels (<14 µg Cl-eq/L) by a factor of 6  
617 and 10 in DWTP1 and DWTP4, respectively, while the AOX increase was only a factor  
618 of 3 (DWTP3) or 4 (DWTP2) during chloramination (Figure 7).

619 After transforming the concentration of targeted DBPs present in waters into µg Cl-  
620 eq/L, it can be concluded that only 27% of the halogenated material formed during the  
621 chemical disinfection processes can be explained by the target DBP analysis (in the  
622 best-case scenario; DWTP4). This value is similar to, or below the percentage of AOX

623 explained by known DBPs reported in chlorinated waters in the peer-reviewed literature  
 624 [14, 75-77]. Note that the inclusion of TCM and BDCM in the list of targeted DBPs  
 625 would slightly increase the proportion of AOX explained by targeted approaches in  
 626 chlorinated waters. Considering the contribution of each THM species to total THM  
 627 concentrations in each plant in that time of the year (data provided by the DWTPs) and  
 628 the levels of TBM and DBCM measured in our study, the percentage of AOX explained  
 629 by known DBPs might increase to 74% and 48% in DWTP1 and DWTP4, respectively.  
 630 The AOX formed in chloraminated DBP mixtures was poorly explained by targeted  
 631 DBPs, being the Cl-eq DBP concentrations <1% of the AOX. Our results are in  
 632 agreement with previous studies that reported a larger unknown fraction of AOX in  
 633 chloraminated than in chlorinated waters [14].



634  
 635 **Figure 7.** AOX concentrations ( $\mu\text{g Cl-eq/L}$ ) in waters before and after chemical  
 636 disinfection. The fraction of AOX explained by target DBP analysis is indicated with  
 637 the black bars (note that TCM and DCBM were not included in the target analysis).  
 638 SUVA and TOC levels of source waters are also indicated.

639 *Non-target FT-ICR MS analysis of halogenated DBP mixtures*

640 The molecular composition of the DBPs detected by FT-ICR MS in the investigated  
 641 disinfected waters is summarized in Table 6, and in Figures 8-11. DBP formulae have  
 642 been listed in Tables 7-22.

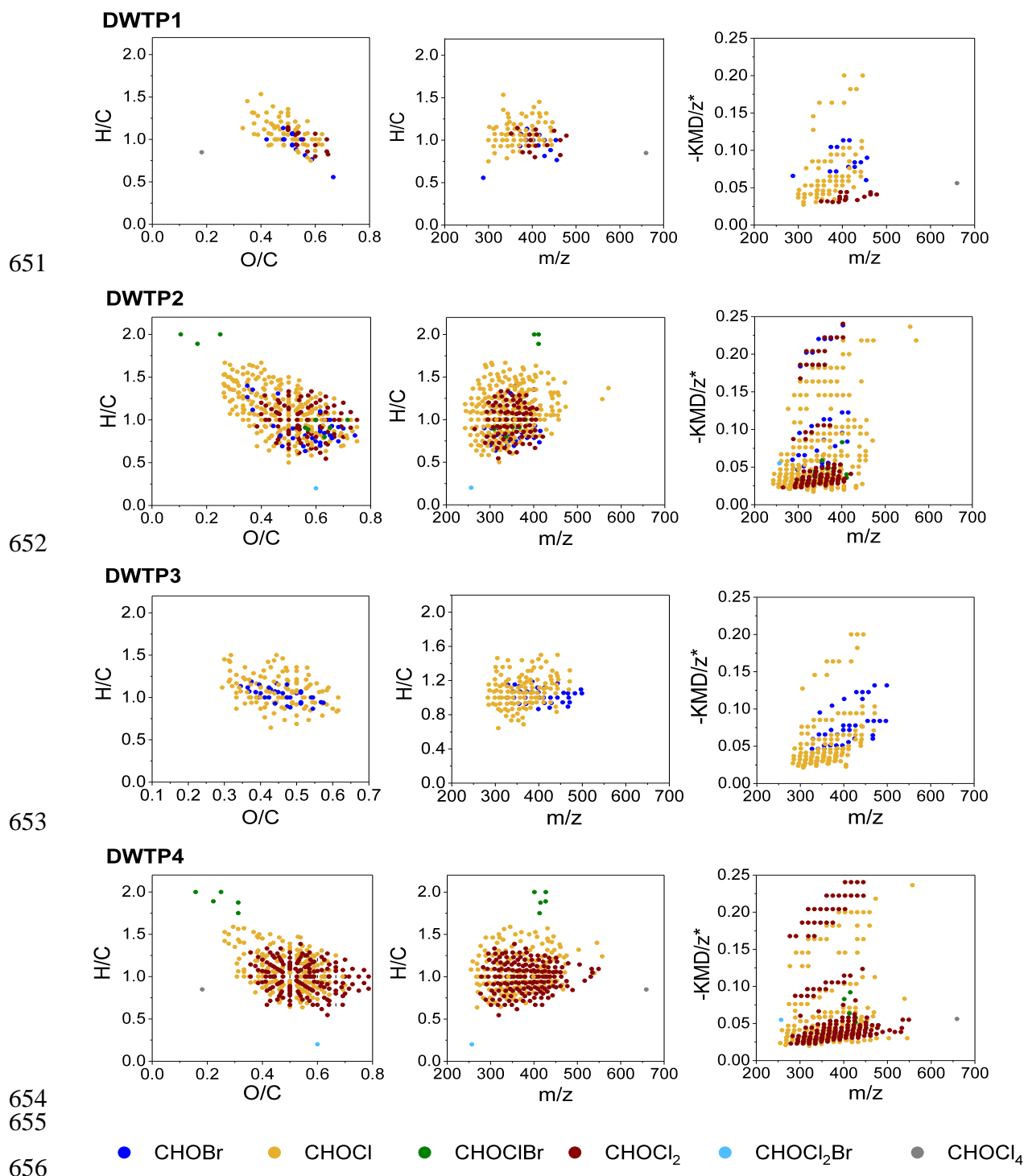
643

644 **Table 6.** Counts and average neutral mass, elemental proportion, aromaticity, and  
 645 oxidation degree, weighted by the relative abundance of each verified DBP present in  
 646 disinfected waters as computed from ESI(-)-FT-ICR mass spectra for singly charged  
 647 ions. Computations are based on formulae in neutral form and are restricted to formulae  
 648 present in three technical replicates.

	DWTP1	DWTP2	DWTP3	DWTP4
<b># of verified formulae</b>	95	349	151	335
<b>Neutral mass (Da)</b>	388.0 (288.9-660.1)	349.0 (244.0-572.2)	375.4 (284.0-500.0)	376.5 (256.1-600.1)
<i>Element proportion in formulae</i>				
<b>C [%]</b>	37.9	37.0	38.3	37.3
<b>H [%]</b>	41.4	42.7	42.2	41.0
<b>O [%]</b>	18.1	17.5	17.2	18.5
<b>Cl [%]</b>	2.5	2.7	2.0	3.2
<b>Br [%]</b>	0.1	0.1	0.3	0
<b>H/C</b>	1.09 (0.56-1.53)	1.13 (0.20-2.00)	1.09 (0.64-1.50)	1.09 (0.20-2.00)
<b>O/C</b>	0.49 (0.18-0.67)	0.48 (0.11-0.75)	0.45 (0.29-0.62)	0.50 (0.16-0.79)
<b>Cl/C</b>	0.07 (0-0.15)	0.08 (0-0.40)	0.05 (0-0.08)	0.09 (0.04-0.40)
<b>Br/C</b>	0.004 (0-0.11)	0.005 (0-0.20)	0.008 (0-0.08)	0.002 (0-0.20)
<i>Aromaticity and oxidation degree<sup>a</sup></i>				
<b>DBE</b>	8.0 (4-18)	6.7 (0-11)	7.9 (4-11)	7.3 (0-18)
<b>DBE/C</b>	0.48 (0-0.78)	0.47 (0-0.80)	0.48 (0.27-0.71)	0.48 (0-0.80)
<b>AI<sub>mod</sub></b>	0.36 (0.13-0.75)	0.35 (-0.07-1.14)	0.37 (-0.11-0.68)	0.37 (-0.07-1.14)
<b>C<sub>os</sub></b>	-0.05 (-0.7-0.89)	-0.089 (-1.68-1.60)	-0.13 (-0.82-0.46)	-0.02 (-1.58-1.60)

649 <sup>a</sup> DBE/C: double bond equivalent relative to the number of carbon atoms, AI<sub>mod</sub>:  
 650 modified aromaticity index; C<sub>os</sub>: carbon oxidation state.

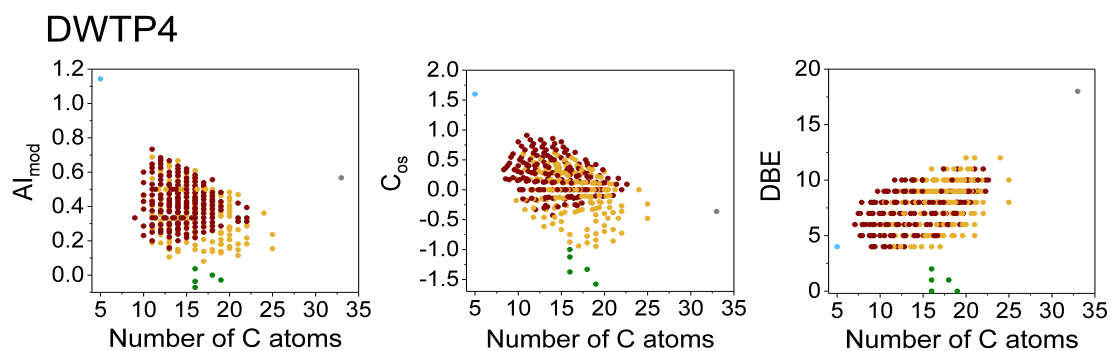
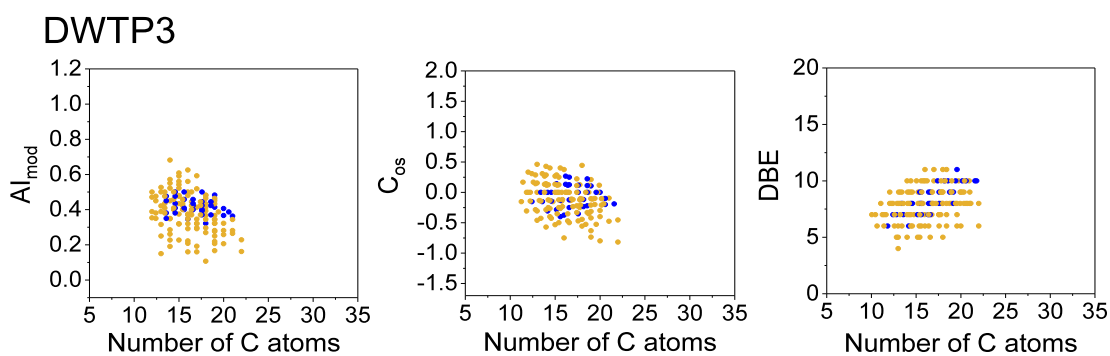
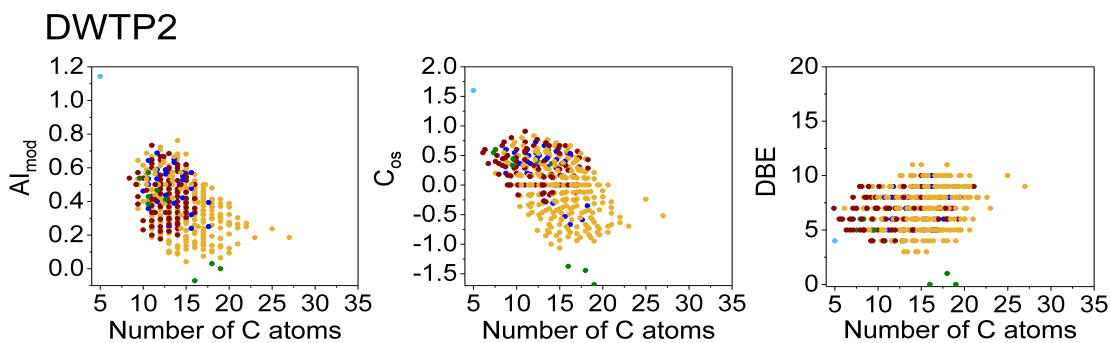
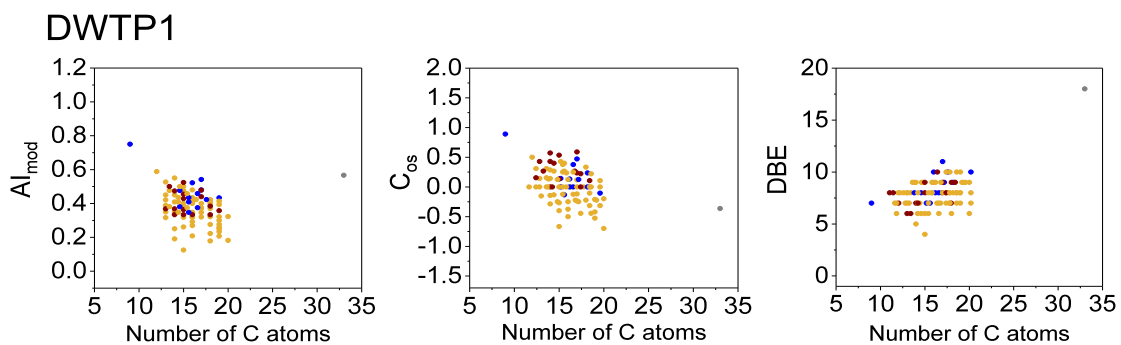




657 **Figure 8.** Molecular composition of the DBP mixtures according to ESI(-)-FT-ICR MS  
 658 analysis visualized by van Krevelen diagrams (left panel), mass edited H/C ratios  
 659 (middle panel), and modified Kendrick mass defect plots (right panel). Only formulae  
 660 present in all three replicates are shown.

661

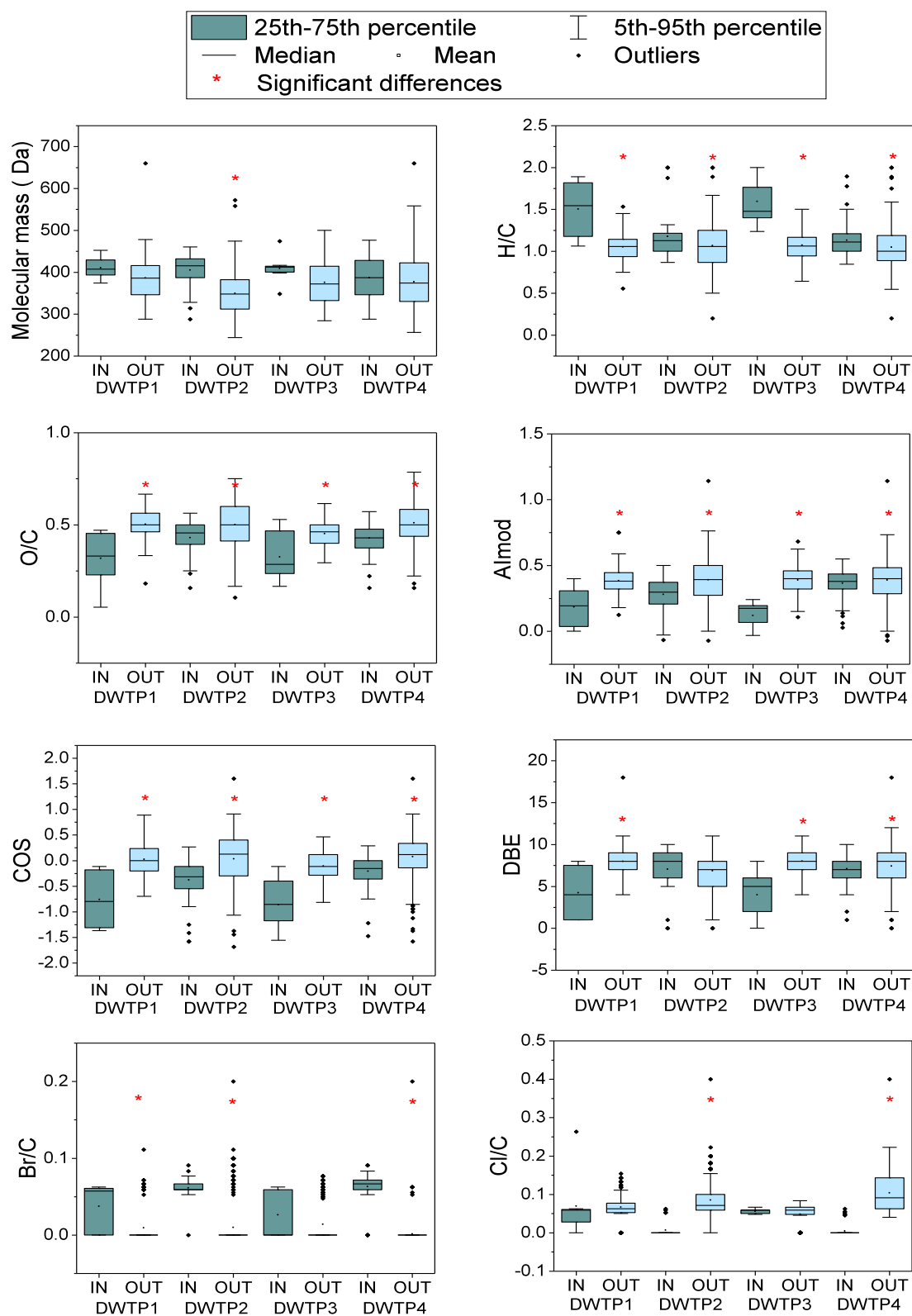
662  
663



669 ● CHOBr    ● CHOCl    ● CHOCIBr    ● CHOCl<sub>2</sub>    ● CHOCl<sub>2</sub>Br    ● CHOCl<sub>4</sub>

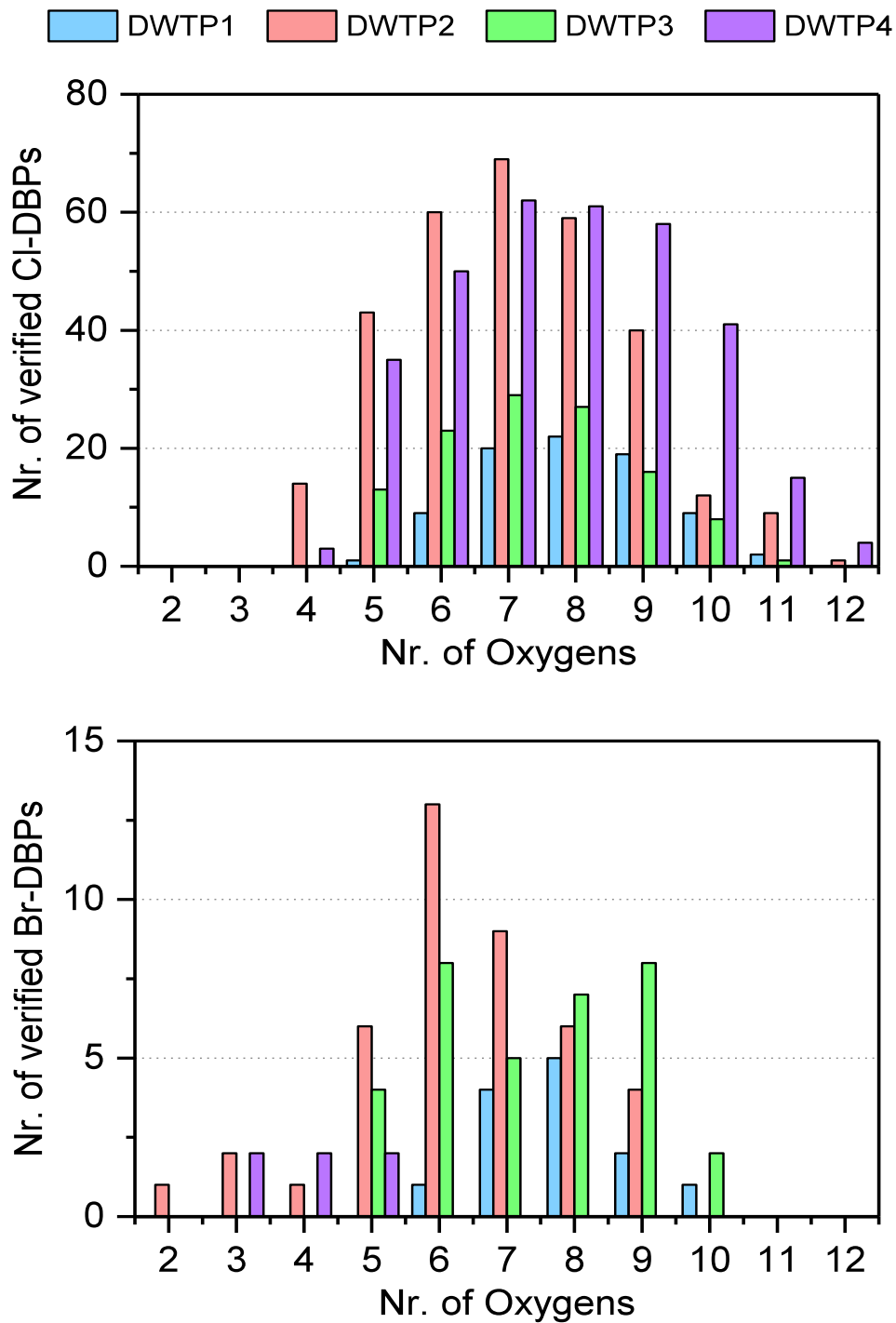
669  
670

671 **Figure 9.** Plots showing DBE, AI<sub>mod</sub>, and C<sub>os</sub> versus the number of carbon for verified  
672 DBPs (*m/z* ions only present in disinfected water) according to negative ESI-FT-ICR  
673 MS analysis.



675  
676  
677  
678

**Figure 10.** Box plots showing the properties of verified formulas in IN and OUT samples, after FT-ICR MS analysis.



679  
680  
681  
682  
683  
684

**Figure 11.** The number of verified chlorinated and brominated DBPs (CHO-type) in the investigated DBP mixtures against the number of oxygen atoms of each DBP composition according to negative ESI-FT-ICR MS analysis.

685 **Table 7.** Nitrogen-containing formulae in the investigated samples after search and  
 686 formula filtration <sup>a</sup>.  
 687

Sample code	No. of formulas in the 3 sample replicates	No. of verified formulas (in all replicates)	Theoretical mass (Da) [M-H] <sup>-</sup>	Molecular formula [M]	DBE
DWTP1 IN	19	1	326.09725	C <sub>12</sub> H <sub>26</sub> O <sub>4</sub> BrN	0
OUT	24	0	-	-	-
DWTP2 IN	28	0	-	-	-
OUT	28	3	288.02804	C <sub>11</sub> H <sub>12</sub> O <sub>6</sub> ClN	6
			302.04369	C <sub>12</sub> H <sub>14</sub> O <sub>6</sub> ClN	6
			314.04369	C <sub>13</sub> H <sub>14</sub> O <sub>6</sub> ClN	7
DWTP3 IN	24	0	-	-	-
OUT	22	0	-	-	-
DWTP4 IN	50	3	610.14959	C <sub>30</sub> H <sub>40</sub> O <sub>3</sub> Cl <sub>2</sub> BrN	10
			638.21727	C <sub>33</sub> H <sub>48</sub> O <sub>2</sub> Cl <sub>2</sub> BrN	9
			652.19654	C <sub>33</sub> H <sub>46</sub> O <sub>3</sub> Cl <sub>2</sub> BrN	10
OUT	67	5	300.02804	C <sub>12</sub> H <sub>12</sub> O <sub>6</sub> Cl <sub>1</sub> N	7
			302.04369	C <sub>12</sub> H <sub>14</sub> O <sub>6</sub> Cl <sub>1</sub> N	6
			312.02804	C <sub>13</sub> H <sub>12</sub> O <sub>6</sub> Cl <sub>1</sub> N	8
			314.04369	C <sub>13</sub> H <sub>14</sub> O <sub>6</sub> Cl <sub>1</sub> N	7
			316.05934	C <sub>13</sub> H <sub>16</sub> O <sub>6</sub> Cl <sub>1</sub> N	6

688 <sup>a</sup> Masses with equal intensity in IN and OUT are highlighted in *IN* and *OUT* are highlighted in grey.

689  
 690

691 **Table 8.** Sulfur-containing formulae in the investigated samples after search and  
 692 formulae filtration <sup>a</sup>.

Sample code	No. of formulas in the 3 sample replicates	No. of verified formulas (in all replicates)	Theoretical mass (Da) [M-H] <sup>-</sup>	Molecular formula [M]	DBE	
DWTP1	IN	30	5	413.0922	<b>C<sub>17</sub>H<sub>32</sub>O<sub>2</sub>ClBrS</b>	1
				<i>425.0922</i>	<i>C<sub>18</sub>H<sub>32</sub>O<sub>2</sub>ClBrS</i>	2
				<i>427.10787</i>	<i>C<sub>18</sub>H<sub>34</sub>O<sub>2</sub>ClBrS</i>	1
				<i>427.14425</i>	<i>C<sub>19</sub>H<sub>38</sub>OClBrS</i>	0
				<i>453.15990</i>	<i>C<sub>21</sub>H<sub>40</sub>OClBrS</i>	1
	OUT	30	5	346.73820	<b>C<sub>5</sub>H<sub>3</sub>OBr<sub>3</sub>S</b>	3
				<i>427.10787</i>	<i>C<sub>18</sub>H<sub>34</sub>O<sub>2</sub>ClBrS</i>	1
				<i>427.14425</i>	<i>C<sub>19</sub>H<sub>38</sub>OClBrS</i>	0
				439.14425	<b>C<sub>20</sub>H<sub>38</sub>OClBrS</b>	1
				<i>453.1599</i>	<i>C<sub>21</sub>H<sub>40</sub>OClBrS</i>	1
DWTP2	IN	22	6	<i>411.11295</i>	<i>C<sub>18</sub>H<sub>34</sub>OClBrS</i>	1
				<i>413.09222</i>	<i>C<sub>17</sub>H<sub>32</sub>O<sub>2</sub>ClBrS</i>	1
				<i>413.12860</i>	<i>C<sub>18</sub>H<sub>36</sub>OClBrS</i>	0
				425.09222	<b>C<sub>18</sub>H<sub>32</sub>O<sub>2</sub>ClBrS</b>	2
				<i>427.10787</i>	<i>C<sub>18</sub>H<sub>34</sub>O<sub>2</sub>ClBrS</i>	1
	OUT	55	5	346.73820	<b>C<sub>5</sub>H<sub>3</sub>OBr<sub>3</sub>S</b>	3
				<i>411.11295</i>	<i>C<sub>18</sub>H<sub>34</sub>OClBrS</i>	1
				<i>413.09222</i>	<i>C<sub>17</sub>H<sub>32</sub>O<sub>2</sub>ClBrS</i>	1
				<i>413.12860</i>	<i>C<sub>18</sub>H<sub>36</sub>OClBrS</i>	0
				<i>427.14425</i>	<i>C<sub>18</sub>H<sub>34</sub>O<sub>2</sub>ClBrS</i>	0
DWTP3	IN	23	5	425.09222	<b>C<sub>18</sub>H<sub>32</sub>O<sub>2</sub>ClBrS</b>	2
				<i>427.10787</i>	<i>C<sub>18</sub>H<sub>34</sub>O<sub>2</sub>ClBrS</i>	1
				<i>427.14425</i>	<i>C<sub>18</sub>H<sub>34</sub>O<sub>2</sub>ClBrS</i>	0
				<i>451.14425</i>	<i>C<sub>21</sub>H<sub>40</sub>OClBrS</i>	2
				<i>453.1599</i>	<i>C<sub>21</sub>H<sub>40</sub>OClBrS</i>	1
	OUT	59	8	413.09222	<b>C<sub>17</sub>H<sub>32</sub>O<sub>2</sub>ClBrS</b>	1
				<i>427.10787</i>	<i>C<sub>18</sub>H<sub>34</sub>O<sub>2</sub>ClBrS</i>	1
				<i>427.14425</i>	<i>C<sub>18</sub>H<sub>34</sub>O<sub>2</sub>ClBrS</i>	0
				439.14425	<b>C<sub>20</sub>H<sub>38</sub>OClBrS</b>	1
				<i>451.14425</i>	<i>C<sub>21</sub>H<sub>40</sub>OClBrS</i>	2
				<i>453.1599</i>	<i>C<sub>21</sub>H<sub>40</sub>OClBrS</i>	1
				477.00526	<b>C<sub>21</sub>H<sub>15</sub>O<sub>9</sub>ClS</b>	14
				507.01582	<b>C<sub>22</sub>H<sub>17</sub>O<sub>10</sub>ClS</b>	14
DWTP4	IN	18	5	<i>413.09222</i>	<i>C<sub>17</sub>H<sub>32</sub>O<sub>2</sub>ClBrS</i>	1
				<i>413.12860</i>	<i>C<sub>18</sub>H<sub>36</sub>OClBrS</i>	0
				425.09222	<b>C<sub>18</sub>H<sub>32</sub>O<sub>2</sub>ClBrS</b>	2
				<i>427.10787</i>	<i>C<sub>18</sub>H<sub>34</sub>O<sub>2</sub>ClBrS</i>	1
				<i>427.14425</i>	<i>C<sub>18</sub>H<sub>34</sub>O<sub>2</sub>ClBrS</i>	0
	OUT	24	4	413.09222	<b>C<sub>17</sub>H<sub>32</sub>O<sub>2</sub>ClBrS</b>	1
				<i>413.12860</i>	<i>C<sub>18</sub>H<sub>36</sub>OClBrS</i>	0
				<i>427.10787</i>	<i>C<sub>18</sub>H<sub>34</sub>O<sub>2</sub>ClBrS</i>	1
				<i>427.14425</i>	<i>C<sub>18</sub>H<sub>34</sub>O<sub>2</sub>ClBrS</i>	0

693 <sup>a</sup> Masses with equal intensity in IN and OUT are highlighted in italics and grey.

694 **Table 9.** List of verified formulae of the 19 DBPs common to all four disinfected water  
 695 samples according to negative ESI-FT-ICR MS analysis (only present in all three  
 696 replicates of disinfected water).  
 697

<b>Common to all DWTPs</b>	
<b><i>Molecular formula</i></b>	<b><i>Theoretical mass of the negative ion</i></b>
C14 H13 O6 Cl1	311.03279
C13 H11 O7 Cl1	313.01206
C13 H13 O7 Cl1	315.02771
C13 H15 O7 Cl1	317.04336
C14 H13 O7 Cl1	327.02771
C13 H13 O8 Cl1	331.02262
C14 H11 O8 Cl1	341.00697
C14 H13 O8 Cl1	343.02262
C14 H15 O8 Cl1	345.03827
C16 H15 O7 Cl1	353.04336
C15 H13 O8 Cl1	355.02262
C16 H17 O7 Cl1	355.05901
C15 H15 O8 Cl1	357.03827
C16 H15 O8 Cl1	369.03827
C15 H13 O9 Cl1	371.01754
C18 H19 O7 Cl1	381.07466
C17 H17 O8 Cl1	383.05392
C16 H15 O9 Cl1	385.03319
C17 H17 O9 Cl1	399.04884
C18 H19 O9 Cl1	413.06449

698

699 **Table 10.** List of verified formulae of the 23 DBPs unique to DWTP1 according to  
700 negative ESI-FT-ICR MS analysis (only present in all three replicates of disinfected  
701 water).

702  
703

<b>DWTP1-unique</b>	
<b><i>Molecular formula</i></b>	<b><i>Theoretical mass of the negative ion</i></b>
C9 H5 O6 Br1	286.91968
C15 H23 O6 Cl1	333.11104
C15 H17 O7 Cl1	343.05901
C16 H21 O6 Cl1	343.09539
C15 H19 O7 Cl1	345.07466
C15 H15 O7 Br1	384.99284
C18 H23 O7 Cl1	385.10596
C15 H17 O7 Br1	387.00849
C18 H21 O8 Cl1	399.08522
C19 H25 O7 Cl1	399.12161
C18 H25 O8 Cl1	403.11652
C19 H23 O8 Cl1	413.10087
C16 H17 O8 Br1	415.00341
C19 H25 O8 Cl1	415.11652
C20 H29 O7 Cl1	415.15291
C18 H23 O9 Cl1	417.09579
C16 H13 O9 Br1	426.96702
C17 H15 O9 Br1	440.98267
C19 H19 O10 Cl1	441.05940
C19 H19 O8 Br1	453.01906
C17 H13 O10 Br1	454.96194
C17 H14 O11 Cl2	462.98405
C19 H20 O10 Cl2	477.03608

704  
705  
706



707 **Table 11.** List of verified formulae of the 124 DBPs unique to DWTP2 according to  
 708 negative ESI-FT-ICR MS analysis (only present in all three replicates of disinfected  
 709 water).

<b>DWTP2-unique</b>		<b>DWTP2-unique (continued)</b>	
<b><i>Molecular formula</i></b>	<b><i>Theoretical mass of the negative ion</i></b>	<b><i>Molecular formula</i></b>	<b><i>Theoretical mass of the negative ion</i></b>
C10 H9 O5 Cl1	243.00658	C12 H12 O5 Cl2	304.99891
C11 H13 O4 Cl1	243.04296	C11 H11 O8 Cl1	305.00697
C10 H11 O5 Cl1	245.02223	C14 H23 O5 Cl1	305.11613
C11 H9 O5 Cl1	255.00658	C9 H8 O5 Cl1 Br1	308.91709
C10 H7 O6 Cl1	256.98584	C11 H7 O6 Br1	312.93533
C11 H11 O5 Cl1	257.02223	C11 H9 O6 Br1	314.95098
C12 H15 O4 Cl1	257.05861	C12 H9 O8 Cl1	314.99132
C10 H9 O6 Cl1	259.00149	C12 H11 O8 Cl1	317.00697
C10 H11 O6 Cl1	261.01714	C15 H23 O5 Cl1	317.11613
C11 H15 O5 Cl1	261.05353	C10 H9 O7 Br1	318.94589
C9 H8 O5 Cl2	264.96761	C14 H7 O7 Cl1	320.98076
C12 H9 O5 Cl1	267.00658	C12 H16 O6 Cl2	325.02512
C10 H7 O7 Cl1	272.98076	C13 H9 O8 Cl1	326.99132
C13 H19 O4 Cl1	273.08991	C11 H9 O7 Br1	330.94589
C11 H13 O6 Cl1	275.03279	C12 H9 O9 Cl1	330.98624
C12 H17 O5 Cl1	275.06918	C11 H11 O7 Br1	332.96154
C13 H9 O5 Cl1	279.00658	C12 H11 O9 Cl1	333.00189
C12 H7 O6 Cl1	280.98584	C14 H21 O7 Cl1	335.09031
C13 H11 O5 Cl1	281.02223	C15 H25 O6 Cl1	335.12669
C14 H15 O4 Cl1	281.05861	C10 H8 O6 Cl1 Br1	336.91201
C14 H17 O4 Cl1	283.07426	C10 H10 O6 Cl1 Br1	338.92766
C11 H7 O7 Cl1	284.98076	C13 H9 O6 Br1	338.95098
C14 H19 O4 Cl1	285.08991	C14 H9 O8 Cl1	338.99132
C10 H9 O5 Br1	286.95606	C17 H21 O5 Cl1	339.10048
C11 H9 O7 Cl1	286.99641	C12 H16 O7 Cl2	341.02004
C14 H21 O4 Cl1	287.10556	C17 H23 O5 Cl1	341.11613
C14 H23 O4 Cl1	289.12121	C12 H9 O7 Br1	342.94589
C13 H21 O5 Cl1	291.10048	C13 H9 O9 Cl1	342.98624
C10 H8 O6 Cl2	292.96252	C17 H25 O5 Cl1	343.13178
C12 H7 O7 Cl1	296.98076	C13 H8 O7 Cl2	344.95744
C15 H19 O4 Cl1	297.08991	C11 H9 O8 Br1	346.94081
C11 H9 O5 Br1	298.95606	C13 H17 O6 Br1	347.01358
C15 H21 O4 Cl1	299.10556	C13 H13 O9 Cl1	347.01754
C10 H7 O6 Br1	300.93533	C15 H21 O7 Cl1	347.09031
C15 H23 O4 Cl1	301.12121	C11 H10 O6 Cl1 Br1	350.92766
C10 H9 O6 Br1	302.95098	C15 H9 O8 Cl1	350.99132
C11 H9 O8 Cl1	302.99132	C10 H10 O7 Cl1 Br1	354.92257
C15 H25 O4 Cl1	303.13686	C13 H9 O7 Br1	354.94589
C10 H11 O6 Br1	304.96663	C15 H19 O5 Br1	357.03431

710 **Table 11. (cont.)**  
711

<i>DWTP2-unique (continued)</i>	
<i>Molecular formula</i>	<i>Theoretical mass of the negative ion</i>
C17 H23 O6 Cl1	357.11104
C12 H9 O8 Br1	358.94081
C15 H21 O5 Br1	359.04996
C17 H25 O6 Cl1	359.12669
C12 H11 O8 Br1	360.95646
C15 H21 O8 Cl1	363.08522
C11 H10 O7 Cl1 Br1	366.92257
C19 H25 O5 Cl1	367.13178
C14 H11 O7 Br1	368.96154
C18 H23 O6 Cl1	369.11104
C13 H11 O8 Br1	372.95646
C14 H11 O10 Cl1	372.9968
C17 H23 O7 Cl1	373.10596
C13 H13 O8 Br1	374.97211
C17 H25 O7 Cl1	375.12161
C18 H29 O6 Cl1	375.15799
C16 H23 O8 Cl1	377.10087
C17 H27 O7 Cl1	377.13726
C12 H12 O7 Cl1 Br1	380.93822
C14 H11 O8 Br1	384.95646
C15 H13 O10 Cl1	387.01245
C17 H25 O8 Cl1	391.11652
C19 H21 O7 Cl1	395.09031
C14 H11 O9 Br1	400.95137
C17 H23 O6 Br1	401.06053
C14 H13 O9 Br1	402.96702
C15 H13 O11 Cl1	403.00737
C17 H21 O9 Cl1	403.08014
C19 H31 O7 Cl1	405.16856
C18 H34 O3 Cl1 Br1	411.13071
C19 H38 O2 Cl1 Br1	411.1671
C15 H11 O9 Br1	412.95137
C15 H13 O9 Br1	414.96702
C16 H13 O11 Cl1	415.00737
C20 H31 O7 Cl1	417.16856
C17 H15 O11 Cl1	429.02302
C20 H31 O8 Cl1	433.16347
C22 H29 O7 Cl1	439.15291

<i>DWTP2-unique (continued)</i>	
<i>Molecular formula</i>	<i>Theoretical mass of the negative ion</i>
C18 H19 O11 Cl1	445.05432
C21 H25 O9 Cl1	455.11144
C22 H29 O8 Cl1	455.14782
C19 H19 O11 Cl1	457.05432
C21 H27 O9 Cl1	457.12709
C19 H21 O11 Cl1	459.06997
C23 H33 O8 Cl1	471.17912
C27 H37 O11 Cl1	571.19517

712

713 **Table 12.** List of verified formulae of the 44 DBPs unique to DWTP3 according to  
 714 negative ESI-FT-ICR MS analysis (only present in all three replicates of disinfected  
 715 water).

<b>DWTP3-unique</b>		<b>DWTP3-unique (continued)</b>	
<b><i>Molecular formula</i></b>	<b><i>Theoretical mass of the negative ion</i></b>	<b><i>Molecular formula</i></b>	<b><i>Theoretical mass of the negative ion</i></b>
C14 H17 O5 Cl1	299.06918	C18 H17 O10 Br1	470.99324
C13 H17 O6 Cl1	303.06409	C21 H25 O10 Cl1	471.10635
C15 H13 O5 Cl1	307.03788	C22 H29 O9 Cl1	471.14274
C14 H19 O6 Cl1	317.07974	C20 H21 O9 Br1	483.02962
C16 H19 O5 Cl1	325.08483	C21 H23 O9 Br1	497.04527
C13 H13 O5 Br1	326.98736	C20 H21 O10 Br1	499.02454
C13 H15 O5 Br1	329.00301		
C14 H15 O5 Br1	341.00301		
C13 H13 O6 Br1	342.98228		
C13 H15 O6 Br1	344.99793		
C15 H17 O5 Br1	355.01866		
C14 H15 O6 Br1	356.99793		
C17 H13 O7 Cl1	363.02771		
C16 H11 O8 Cl1	365.00697		
C15 H15 O6 Br1	368.99793		
C17 H21 O7 Cl1	371.09031		
C16 H17 O6 Br1	383.01358		
C18 H21 O7 Cl1	383.09031		
C16 H19 O6 Br1	385.02923		
C19 H27 O6 Cl1	385.14234		
C19 H19 O7 Cl1	393.07466		
C15 H13 O8 Br1	398.97211		
C16 H17 O7 Br1	399.00849		
C19 H19 O8 Cl1	409.06957		
C17 H17 O7 Br1	411.00849		
C17 H19 O7 Br1	413.02414		
C19 H27 O8 Cl1	417.13217		
C17 H15 O8 Br1	424.98776		
C16 H15 O9 Br1	428.98267		
C17 H17 O9 Br1	442.99832		
C18 H21 O8 Br1	443.03471		
C22 H33 O7 Cl1	443.18421		
C18 H17 O9 Br1	454.99832		
C18 H19 O9 Br1	457.01397		
C19 H17 O9 Br1	466.99832		
C20 H21 O8 Br1	467.03471		
C19 H19 O9 Br1	469.01397		
C21 H23 O10 Cl1	469.0907		

716

717 **Table 13.** List of verified formulae of the 121 DBPs unique to DWTP4 according to  
 718 negative ESI-FT-ICR MS analysis (only present in all three replicates of disinfected  
 719 water).

<b>DWTP4-unique</b>		<b>DWTP4-unique (continued)</b>	
<b>Molecular formula</b>	<b>Theoretical mass of the negative ion</b>	<b>Molecular formula</b>	<b>Theoretical mass of the negative ion</b>
C13 H13 O4 Cl1	267.04296	C16 H12 O8 Cl2	400.98365
C10 H9 O7 Cl1	274.99641	C17 H16 O7 Cl2	401.02004
C10 H8 O5 Cl2	276.96761	C17 H18 O7 Cl2	403.03569
C10 H10 O5 Cl2	278.98326	C16 H19 O10 Cl1	405.05940
C9 H10 O6 Cl2	282.97817	C17 H25 O9 Cl1	407.11144
C13 H19 O5 Cl1	289.08483	C14 H12 O10 Cl2	408.97348
C11 H10 O5 Cl2	290.98326	C16 H20 O8 Cl2	409.04625
C11 H14 O5 Cl2	295.01456	C14 H14 O10 Cl2	410.98913
C12 H8 O5 Cl2	300.96761	C15 H18 O9 Cl2	411.02552
C12 H10 O5 Cl2	302.98326	C17 H15 O10 Cl1	413.02810
C12 H16 O5 Cl2	309.03021	C16 H28 O5 Cl1 Br1	413.07359
C13 H14 O5 Cl2	319.01456	C17 H14 O8 Cl2	414.99930
C13 H16 O5 Cl2	321.03021	C16 H30 O5 Cl1 Br1	415.08924
C14 H14 O5 Cl2	331.01456	C16 H12 O9 Cl2	416.97857
C14 H16 O5 Cl2	333.03021	C17 H16 O8 Cl2	417.01495
C16 H13 O6 Cl1	335.03279	C15 H10 O10 Cl2	418.95783
C14 H18 O5 Cl2	335.04586	C16 H14 O9 Cl2	418.99422
C14 H10 O6 Cl2	342.97817	C17 H18 O8 Cl2	419.03060
C14 H12 O6 Cl2	344.99382	C17 H21 O10 Cl1	419.07505
C12 H8 O8 Cl2	348.95235	C18 H25 O9 Cl1	419.11144
C14 H16 O6 Cl2	349.02512	C16 H16 O9 Cl2	421.00987
C14 H19 O8 Cl1	349.06957	C17 H20 O8 Cl2	421.04625
C13 H18 O7 Cl2	355.03569	C15 H14 O10 Cl2	422.98913
C15 H14 O6 Cl2	359.00947	C16 H18 O9 Cl2	423.02552
C12 H10 O9 Cl2	366.96292	C19 H17 O9 Cl1	423.04884
C16 H13 O8 Cl1	367.02262	C20 H21 O8 Cl1	423.08522
C15 H14 O7 Cl2	375.00439	C14 H12 O11 Cl2	424.96840
C16 H18 O6 Cl2	375.04077	C15 H16 O10 Cl2	425.00478
C13 H10 O9 Cl2	378.96292	C18 H15 O10 Cl1	425.02810
C16 H11 O9 Cl1	381.00189	C16 H20 O9 Cl2	425.04117
C15 H20 O7 Cl2	381.05134	C20 H23 O8 Cl1	425.10087
C16 H14 O7 Cl2	387.00439	C14 H14 O11 Cl2	426.98405
C16 H16 O7 Cl2	389.02004	C18 H34 O4 Cl1 Br1	427.12563
C15 H15 O10 Cl1	389.02810	C19 H38 O3 Cl1 Br1	427.16201
C16 H21 O9 Cl1	391.08014	C17 H14 O9 Cl2	430.99422
C16 H20 O7 Cl2	393.05134	C18 H18 O8 Cl2	431.03060
C15 H18 O8 Cl2	395.03060	C20 H29 O8 Cl1	431.14782
C13 H12 O10 Cl2	396.97348	C21 H33 O7 Cl1	431.18421
C13 H14 O10 Cl2	398.98913	C16 H12 O10 Cl2	432.97348

720

721 **Table 13.** (cont).  
722

<i>DWTP4-unique (continued)</i>	
<i>Molecular formula</i>	<i>Theoretical mass of the negative ion</i>
C18 H20 O8 Cl2	433.04625
C16 H14 O10 Cl2	434.98913
C17 H18 O9 Cl2	435.02552
C18 H22 O8 Cl2	435.06190
C16 H16 O10 Cl2	437.00478
C17 H20 O9 Cl2	437.04117
C20 H19 O9 Cl1	437.06449
C21 H25 O8 Cl1	439.11652
C22 H31 O7 Cl1	441.16856
C18 H14 O9 Cl2	442.99422
C18 H16 O9 Cl2	445.00987
C19 H20 O8 Cl2	445.04625
C18 H18 O9 Cl2	447.02552
C17 H16 O10 Cl2	449.00478
C16 H14 O11 Cl2	450.98405
C17 H18 O10 Cl2	451.02043
C18 H22 O9 Cl2	451.05682
C17 H20 O10 Cl2	453.03608
C20 H19 O10 Cl1	453.05940
C20 H25 O10 Cl1	459.10635
C21 H29 O9 Cl1	459.14274
C18 H16 O10 Cl2	461.00478
C19 H20 O9 Cl2	461.04117
C20 H27 O10 Cl1	461.12200
C18 H20 O10 Cl2	465.03608
C21 H19 O10 Cl1	465.05940
C20 H17 O11 Cl1	467.03867
C22 H27 O9 Cl1	469.12709
C20 H21 O11 Cl1	471.06997
C19 H18 O10 Cl2	475.02043
C20 H25 O11 Cl1	475.10127
C18 H16 O11 Cl2	476.99970
C19 H22 O10 Cl2	479.05173
C19 H16 O11 Cl2	488.99970
C22 H29 O11 Cl1	503.13257
C21 H24 O10 Cl2	505.06738
C21 H20 O11 Cl2	517.03100
C18 H20 O8 Cl2	476.99970

<i>DWTP4-unique (continued)</i>	
<i>Molecular formula</i>	<i>Theoretical mass of the negative ion</i>
C22 H22 O11 Cl2	531.04665
C22 H24 O11 Cl2	533.06230
C21 H22 O12 Cl2	535.04156
C24 H25 O12 Cl1	539.09618
C25 H35 O11 Cl1	545.17952
C22 H24 O12 Cl2	549.05721

723

724 **Table 14.** List of verified formulae of the 49 DBPs common to DWTP1 and DWTP2  
 725 according to negative ESI-FT-ICR MS analysis (only present in all three replicates of  
 726 disinfected water).

<b>DWTP1+DWTP2</b>		<b>DWTP1+DWTP2 (continued)</b>	
<b><i>Molecular formula</i></b>	<b><i>Theoretical mass of the negative ion</i></b>	<b><i>Molecular formula</i></b>	<b><i>Theoretical mass of the negative ion</i></b>
C12 H9 O7 Cl1	298.99641	C17 H17 O9 Cl1	399.04884
C13 H13 O6 Cl1	299.03279	C16 H15 O10 Cl1	401.02810
C13 H15 O6 Cl1	301.04844	C17 H19 O9 Cl1	401.06449
C14 H13 O6 Cl1	311.03279	C16 H17 O10 Cl1	403.04375
C15 H17 O5 Cl1	311.06918	C15 H12 O9 Cl2	404.97857
C13 H11 O7 Cl1	313.01206	C16 H18 O8 Cl2	407.03060
C13 H13 O7 Cl1	315.02771	C18 H19 O9 Cl1	413.06449
C13 H15 O7 Cl1	317.04336	C17 H17 O10 Cl1	415.04375
C14 H13 O7 Cl1	327.02771	C19 H19 O9 Cl1	425.06449
C13 H13 O8 Cl1	331.02262	C20 H23 O9 Cl1	441.09579
C16 H17 O6 Cl1	339.06409	C19 H21 O10 Cl1	443.07505
C14 H11 O8 Cl1	341.00697		
C14 H13 O8 Cl1	343.02262		
C14 H15 O8 Cl1	345.03827		
C14 H17 O8 Cl1	347.05392		
C13 H14 O7 Cl2	351.00439		
C16 H15 O7 Cl1	353.04336		
C15 H13 O8 Cl1	355.02262		
C16 H17 O7 Cl1	355.05901		
C15 H15 O8 Cl1	357.03827		
C15 H17 O8 Cl1	359.05392		
C14 H16 O7 Cl2	365.02004		
C16 H15 O8 Cl1	369.03827		
C17 H19 O7 Cl1	369.07466		
C15 H13 O9 Cl1	371.01754		
C15 H15 O9 Cl1	373.03319		
C16 H19 O8 Cl1	373.06957		
C16 H21 O8 Cl1	375.08522		
C14 H12 O8 Cl2	376.98365		
C18 H19 O7 Cl1	381.07466		
C17 H17 O8 Cl1	383.05392		
C16 H15 O9 Cl1	385.03319		
C17 H19 O8 Cl1	385.06957		
C16 H17 O9 Cl1	387.04884		
C15 H14 O8 Cl2	390.99930		
C14 H12 O9 Cl2	392.97857		
C15 H16 O8 Cl2	393.01495		
C14 H14 O9 Cl2	394.99422		

727

728 **Table 15.** List of verified formulae of the 48 DBPs common to DWTP1 and DWTP3  
 729 according to negative ESI-FT-ICR MS analysis (only present in all three replicates of  
 730 disinfected water).  
 731

<b>DWTP1+DWTP3</b>		<b>DWTP1+DWTP3 (continued)</b>	
<b><i>Molecular formula</i></b>	<b><i>Theoretical mass of the negative ion</i></b>	<b><i>Molecular formula</i></b>	<b><i>Theoretical mass of the negative ion</i></b>
C13 H13 O6 Cl1	299.03279	C15 H15 O8 Br1	400.98776
C13 H15 O6 Cl1	301.04844	C17 H19 O9 Cl1	401.06449
C14 H13 O6 Cl1	311.03279	C16 H15 O8 Br1	412.98776
C15 H17 O5 Cl1	311.06918	C18 H19 O9 Cl1	413.06449
C13 H11 O7 Cl1	313.01206	C17 H17 O8 Br1	427.00341
C14 H15 O6 Cl1	313.04844	C18 H17 O10 Cl1	427.04375
C13 H13 O7 Cl1	315.02771	C19 H23 O9 Cl1	429.09579
C13 H15 O7 Cl1	317.04336	C19 H25 O9 Cl1	431.11144
C14 H13 O7 Cl1	327.02771	C20 H23 O9 Cl1	441.09579
C14 H15 O7 Cl1	329.04336	C19 H21 O10 Cl1	443.07505
C13 H13 O8 Cl1	331.02262	C19 H23 O10 Cl1	445.09070
C14 H19 O7 Cl1	333.07466		
C16 H17 O6 Cl1	339.06409		
C14 H11 O8 Cl1	341.00697		
C15 H15 O7 Cl1	341.04336		
C14 H13 O8 Cl1	343.02262		
C14 H15 O8 Cl1	345.03827		
C16 H15 O7 Cl1	353.04336		
C15 H13 O8 Cl1	355.02262		
C16 H17 O7 Cl1	355.05901		
C15 H15 O8 Cl1	357.03827		
C16 H19 O7 Cl1	357.07466		
C15 H17 O8 Cl1	359.05392		
C16 H15 O8 Cl1	369.03827		
C17 H19 O7 Cl1	369.07466		
C14 H13 O7 Br1	370.97719		
C15 H13 O9 Cl1	371.01754		
C16 H17 O8 Cl1	371.05392		
C14 H15 O7 Br1	372.99284		
C16 H19 O8 Cl1	373.06957		
C16 H21 O8 Cl1	375.08522		
C18 H19 O7 Cl1	381.07466		
C17 H17 O8 Cl1	383.05392		
C16 H15 O9 Cl1	385.03319		
C17 H19 O8 Cl1	385.06957		
C16 H17 O9 Cl1	387.04884		
C17 H17 O9 Cl1	399.04884		

732

733 **Table 16.** List of verified formulae of the 47 DBPs common to DWTP1 and DWTP4  
 734 according to negative ESI-FT-ICR MS analysis (only present in all three replicates of  
 735 disinfected water).

<b>DWTP1+DWTP4</b>		<b>DWTP1+DWTP4 (continued)</b>	
<b><i>Molecular formula</i></b>	<b><i>Theoretical mass of the negative ion</i></b>	<b><i>Molecular formula</i></b>	<b><i>Theoretical mass of the negative ion</i></b>
C12 H9 O7 Cl1	298.99641	C18 H17 O10 Cl1	427.04375
C14 H13 O6 Cl1	311.03279	C19 H25 O9 Cl1	431.11144
C13 H11 O7 Cl1	313.01206	C17 H16 O9 Cl2	433.00987
C13 H13 O7 Cl1	315.02771	C18 H17 O11 Cl1	443.03867
C13 H15 O7 Cl1	317.04336	C19 H23 O10 Cl1	445.09070
C14 H13 O7 Cl1	327.02771	C18 H20 O9 Cl2	449.04117
C13 H13 O8 Cl1	331.02262	C18 H18 O10 Cl2	463.02043
C14 H11 O8 Cl1	341.00697	C33 H28 O6 Cl4	659.05673
C16 H19 O6 Cl1	341.07974		
C14 H13 O8 Cl1	343.02262		
C14 H15 O8 Cl1	345.03827		
C14 H17 O8 Cl1	347.05392		
C13 H14 O7 Cl2	351.00439		
C16 H15 O7 Cl1	353.04336		
C15 H13 O8 Cl1	355.02262		
C16 H17 O7 Cl1	355.05901		
C15 H15 O8 Cl1	357.03827		
C14 H16 O7 Cl2	365.02004		
C16 H15 O8 Cl1	369.03827		
C15 H13 O9 Cl1	371.01754		
C16 H17 O8 Cl1	371.05392		
C15 H15 O9 Cl1	373.03319		
C14 H12 O8 Cl2	376.98365		
C18 H19 O7 Cl1	381.07466		
C16 H15 O9 Cl1	385.03319		
C15 H14 O8 Cl2	390.99930		
C14 H12 O9 Cl2	392.97857		
C15 H16 O8 Cl2	393.01495		
C14 H14 O9 Cl2	394.99422		
C17 H17 O9 Cl1	399.04884		
C16 H15 O10 Cl1	401.02810		
C16 H17 O10 Cl1	403.04375		
C15 H12 O9 Cl2	404.97857		
C15 H14 O9 Cl2	406.99422		
C16 H18 O8 Cl2	407.03060		
C15 H16 O9 Cl2	409.00987		
C18 H19 O9 Cl1	413.06449		
C17 H17 O10 Cl1	415.04375		
C19 H19 O9 Cl1	425.06449		

736



737 **Table 17.** List of verified formulae of the 80 DBPs common to DWTP2 and DWTP3  
 738 according to negative ESI-FT-ICR MS analysis (only present in all three replicates of  
 739 disinfected water).  
 740

<b>DWTP2+DWTP3</b>		<b>DWTP2+DWTP3 (continued)</b>	
<b><i>Molecular formula</i></b>	<b><i>Theoretical mass of the negative ion</i></b>	<b><i>Molecular formula</i></b>	<b><i>Theoretical mass of the negative ion</i></b>
C12 H11 O6 Cl1	285.01714	C14 H13 O6 Br1	354.98228
C13 H15 O5 Cl1	285.05353	C15 H13 O8 Cl1	355.02262
C12 H13 O6 Cl1	287.03279	C16 H17 O7 Cl1	355.05901
C14 H13 O5 Cl1	295.03788	C17 H21 O6 Cl1	355.09539
C14 H15 O5 Cl1	297.05353	C15 H15 O8 Cl1	357.03827
C13 H13 O6 Cl1	299.03279	C15 H17 O8 Cl1	359.05392
C12 H11 O7 Cl1	301.01206	C15 H19 O8 Cl1	361.06957
C13 H15 O6 Cl1	301.04844	C16 H23 O7 Cl1	361.10596
C14 H19 O5 Cl1	301.08483	C17 H17 O7 Cl1	367.05901
C12 H13 O7 Cl1	303.02771	C18 H21 O6 Cl1	367.09539
C13 H19 O6 Cl1	305.07974	C16 H15 O8 Cl1	369.03827
C14 H9 O6 Cl1	307.00149	C17 H19 O7 Cl1	369.07466
C15 H15 O5 Cl1	309.05353	C15 H13 O9 Cl1	371.01754
C14 H13 O6 Cl1	311.03279	C16 H19 O8 Cl1	373.06957
C15 H17 O5 Cl1	311.06918	C16 H21 O8 Cl1	375.08522
C13 H11 O7 Cl1	313.01206	C17 H15 O8 Cl1	381.03827
C15 H19 O5 Cl1	313.08483	C18 H19 O7 Cl1	381.07466
C13 H13 O7 Cl1	315.02771	C17 H17 O8 Cl1	383.05392
C13 H15 O7 Cl1	317.04336	C19 H25 O6 Cl1	383.12669
C15 H13 O6 Cl1	323.03279	C16 H15 O9 Cl1	385.03319
C14 H11 O7 Cl1	325.01206	C17 H19 O8 Cl1	385.06957
C15 H15 O6 Cl1	325.04844	C16 H17 O9 Cl1	387.04884
C14 H13 O7 Cl1	327.02771	C17 H23 O8 Cl1	389.10087
C15 H17 O6 Cl1	327.06409	C17 H19 O6 Br1	397.02923
C13 H11 O8 Cl1	329.00697	C18 H19 O8 Cl1	397.06957
C16 H23 O5 Cl1	329.11613	C19 H23 O7 Cl1	397.10596
C13 H13 O8 Cl1	331.02262	C17 H17 O9 Cl1	399.04884
C14 H17 O7 Cl1	331.05901	C20 H29 O6 Cl1	399.15799
C15 H11 O7 Cl1	337.01206	C17 H19 O9 Cl1	401.06449
C16 H15 O6 Cl1	337.04844	C17 H23 O9 Cl1	405.09579
C17 H19 O5 Cl1	337.08483	C18 H27 O8 Cl1	405.13217
C15 H13 O7 Cl1	339.02771	C18 H19 O9 Cl1	413.06449
C16 H17 O6 Cl1	339.06409	C18 H21 O9 Cl1	415.08014
C14 H11 O8 Cl1	341.00697	C17 H19 O10 Cl1	417.0594
C14 H13 O8 Cl1	343.02262	C20 H21 O9 Cl1	439.08014
C14 H15 O8 Cl1	345.03827	C18 H15 O11 Cl1	441.02302
C16 H13 O7 Cl1	351.02771	C20 H23 O9 Cl1	441.09579
C15 H11 O8 Cl1	353.00697	C21 H27 O8 Cl1	441.13217
C16 H15 O7 Cl1	353.04336	C19 H21 O10 Cl1	443.07505
C17 H19 O6 Cl1	353.07974	C20 H25 O9 Cl1	443.11144

741 **Table 18.** List of verified formulae of the 190 DBPs common to DWTP2 and DWTP4  
 742 according to negative ESI-FT-ICR MS analysis (only present in all three replicates of  
 743 disinfected water).

<i>DWTP2+DWTP4 (continued)</i>		<i>DWTP2+DWTP4 (continued)</i>	
<i>Molecular formula</i>	<i>Theoretical mass of the negative ion</i>	<i>Molecular formula</i>	<i>Theoretical mass of the negative ion</i>
C12 H13 O4 Cl1	255.04296	C11 H14 O6 Cl2	311.00947
C5 H1 O3 Cl2 Br1	256.84134	C14 H13 O6 Cl1	311.03279
C11 H13 O5 Cl1	259.03788	C10 H12 O7 Cl2	312.98874
C11 H7 O6 Cl1	268.98584	C13 H11 O7 Cl1	313.01206
C12 H11 O5 Cl1	269.02223	C15 H19 O5 Cl1	313.08483
C13 H15 O4 Cl1	269.05861	C13 H13 O7 Cl1	315.02771
C11 H9 O6 Cl1	271.00149	C15 H21 O5 Cl1	315.10048
C12 H13 O5 Cl1	271.03788	C12 H8 O6 Cl2	316.96252
C11 H11 O6 Cl1	273.01714	C13 H12 O5 Cl2	316.99891
C12 H15 O5 Cl1	273.05353	C13 H15 O7 Cl1	317.04336
C11 H15 O6 Cl1	277.04844	C11 H6 O7 Cl2	318.94179
C12 H9 O6 Cl1	283.00149	C12 H10 O6 Cl2	318.97817
C12 H11 O6 Cl1	285.01714	C12 H13 O8 Cl1	319.02262
C12 H13 O6 Cl1	287.03279	C13 H17 O7 Cl1	319.05901
C13 H17 O5 Cl1	287.06918	C14 H21 O6 Cl1	319.09539
C11 H8 O5 Cl2	288.96761	C11 H8 O7 Cl2	320.95744
C11 H11 O7 Cl1	289.01206	C12 H12 O6 Cl2	320.99382
C12 H15 O6 Cl1	289.04844	C12 H15 O8 Cl1	321.03827
C11 H13 O7 Cl1	291.02771	C13 H19 O7 Cl1	321.07466
C11 H12 O5 Cl2	292.99891	C11 H10 O7 Cl2	322.97309
C10 H10 O6 Cl2	294.97817	C14 H9 O7 Cl1	322.99641
C13 H9 O6 Cl1	295.00149	C12 H14 O6 Cl2	323.00947
C14 H13 O5 Cl1	295.03788	C15 H13 O6 Cl1	323.03279
C10 H12 O6 Cl2	296.99382	C16 H17 O5 Cl1	323.06918
C13 H11 O6 Cl1	297.01714	C11 H12 O7 Cl2	324.98874
C12 H9 O7 Cl1	298.99641	C14 H11 O7 Cl1	325.01206
C12 H11 O7 Cl1	301.01206	C15 H15 O6 Cl1	325.04844
C12 H13 O7 Cl1	303.02771	C11 H14 O7 Cl2	327.00439
C11 H8 O6 Cl2	304.96252	C14 H13 O7 Cl1	327.02771
C12 H15 O7 Cl1	305.04336	C15 H17 O6 Cl1	327.06409
C13 H19 O6 Cl1	305.07974	C13 H11 O8 Cl1	329.00697
C11 H10 O6 Cl2	306.97817	C15 H19 O6 Cl1	329.07974
C12 H14 O5 Cl2	307.01456	C16 H23 O5 Cl1	329.11613
C10 H8 O7 Cl2	308.95744	C13 H10 O6 Cl2	330.97817
C11 H12 O6 Cl2	308.99382	C13 H13 O8 Cl1	331.02262
C14 H11 O6 Cl1	309.01714	C16 H25 O5 Cl1	331.13178
C15 H15 O5 Cl1	309.05353	C12 H8 O7 Cl2	332.95744
C10 H10 O7 Cl2	310.97309	C13 H12 O6 Cl2	332.99382
C13 H9 O7 Cl1	310.99641	C13 H15 O8 Cl1	333.03827

744

745  
746

**Table 18.** (cont.)

<b>DWTP2+DWTP4 (continued)</b>		<b>DWTP2+DWTP4 (continued)</b>	
<b>Molecular formula</b>	<b>Theoretical mass of the negative ion</b>	<b>Molecular formula</b>	<b>Theoretical mass of te negative ion</b>
C12 H10 O7 Cl2	334.97309	C15 H16 O6 Cl2	361.02512
C13 H14 O6 Cl2	335.00947	C14 H15 O9 Cl1	361.03319
C13 H17 O8 Cl1	335.05392	C15 H19 O8 Cl1	361.06957
C12 H12 O7 Cl2	336.98874	C14 H14 O7 Cl2	363.00439
C15 H11 O7 Cl1	337.01206	C15 H18 O6 Cl2	363.04077
C13 H16 O6 Cl2	337.02512	C13 H12 O8 Cl2	364.98365
C16 H15 O6 Cl1	337.04844	C14 H16 O7 Cl2	365.02004
C11 H10 O8 Cl2	338.96800	C13 H14 O8 Cl2	366.99930
C12 H14 O7 Cl2	339.00439	C14 H18 O7 Cl2	367.03569
C15 H13 O7 Cl1	339.02771	C17 H17 O7 Cl1	367.05901
C11 H12 O8 Cl2	340.98365	C12 H12 O9 Cl2	368.97857
C14 H11 O8 Cl1	341.00697	C15 H11 O9 Cl1	369.00189
C14 H13 O8 Cl1	343.02262	C13 H16 O8 Cl2	369.01495
C13 H11 O9 Cl1	345.00189	C16 H15 O8 Cl1	369.03827
C14 H15 O8 Cl1	345.03827	C19 H27 O5 Cl1	369.14743
C17 H27 O5 Cl1	345.14743	C15 H13 O9 Cl1	371.01754
C13 H10 O7 Cl2	346.97309	C19 H29 O5 Cl1	371.16308
C14 H14 O6 Cl2	347.00947	C15 H12 O7 Cl2	372.98874
C14 H17 O8 Cl1	347.05392	C15 H15 O9 Cl1	373.03319
C13 H12 O7 Cl2	348.98874	C14 H10 O8 Cl2	374.96800
C12 H10 O8 Cl2	350.96800	C15 H17 O9 Cl1	375.04884
C13 H14 O7 Cl2	351.00439	C14 H12 O8 Cl2	376.98365
C16 H13 O7 Cl1	351.02771	C15 H16 O7 Cl2	377.02004
C14 H18 O6 Cl2	351.04077	C15 H19 O9 Cl1	377.06449
C17 H17 O6 Cl1	351.06409	C14 H14 O8 Cl2	378.99930
C12 H12 O8 Cl2	352.98365	C15 H18 O7 Cl2	379.03569
C15 H11 O8 Cl1	353.00697	C13 H12 O9 Cl2	380.97857
C13 H16 O7 Cl2	353.02004	C14 H16 O8 Cl2	381.01495
C16 H15 O7 Cl1	353.04336	C17 H15 O8 Cl1	381.03827
C12 H14 O8 Cl2	354.99930	C18 H19 O7 Cl1	381.07466
C15 H13 O8 Cl1	355.02262	C13 H14 O9 Cl2	382.99422
C16 H17 O7 Cl1	355.05901	C16 H13 O9 Cl1	383.01754
C18 H25 O5 Cl1	355.13178	C14 H18 O8 Cl2	383.03060
C14 H11 O9 Cl1	357.00189	C16 H15 O9 Cl1	385.03319
C15 H15 O8 Cl1	357.03827	C15 H12 O8 Cl2	388.98365
C18 H27 O5 Cl1	357.14743	C16 H19 O9 Cl1	389.06449
C14 H10 O7 Cl2	358.97309	C18 H27 O7 Cl1	389.13726
C14 H13 O9 Cl1	359.01754	C14 H10 O9 Cl2	390.96292
C13 H8 O8 Cl2	360.95235	C15 H14 O8 Cl2	390.99930
C14 H12 O7 Cl2	360.98874	C16 H18 O7 Cl2	391.03569

747

748 **Table 18.** (cont.)  
 749

<b>DWTP2+DWTP4 (continued)</b>	
<b><i>Molecular formula</i></b>	<b><i>Theoretical mass of the negative ion</i></b>
C14 H12 O9 Cl2	392.97857
C15 H16 O8 Cl2	393.01495
C14 H14 O9 Cl2	394.99422
C14 H16 O9 Cl2	397.00987
C17 H15 O9 Cl1	397.03319
C18 H19 O8 Cl1	397.06957
C20 H27 O6 Cl1	397.14234
C16 H13 O10 Cl1	399.01245
C17 H17 O9 Cl1	399.04884
C16 H15 O10 Cl1	401.02810
C16 H32 O4 Cl1 Br1	401.10998
C15 H10 O9 Cl2	402.96292
C16 H14 O8 Cl2	402.99930
C16 H17 O10 Cl1	403.04375
C19 H29 O7 Cl1	403.15291
C15 H12 O9 Cl2	404.97857
C16 H16 O8 Cl2	405.01495
C16 H18 O8 Cl2	407.03060
C18 H19 O9 Cl1	413.06449
C17 H17 O10 Cl1	415.04375
C17 H19 O10 Cl1	417.05940
C15 H12 O10 Cl2	420.97348
C19 H19 O9 Cl1	425.06449
C18 H19 O10 Cl1	429.05940
C19 H27 O9 Cl1	433.12709
C20 H21 O9 Cl1	439.08014
C21 H27 O8 Cl1	441.13217
C21 H31 O8 Cl1	445.16347
C19 H25 O10 Cl1	447.10635
C20 H21 O10 Cl1	455.07505
C20 H23 O11 Cl1	473.08562
C25 H31 O12 Cl1	557.14313

750

751 **Table 19.** List of verified formulae of the 61 DBPs common to DWTP3 and DWTP4  
 752 according to negative ESI-FT-ICR MS analysis (only present in all three replicates of  
 753 disinfected water).

<b>DWTP3+DWTP4</b>		<b>DWTP3+DWTP4</b>	
<b><i>Molecular formula</i></b>	<b><i>Theoretical mass of the negative ion</i></b>	<b><i>Molecular formula</i></b>	<b><i>Theoretical mass of the negative ion</i></b>
C13 H13 O5 Cl1	283.03788	C16 H15 O8 Cl1	369.03827
C12 H11 O6 Cl1	285.01714	C15 H13 O9 Cl1	371.01754
C12 H13 O6 Cl1	287.03279	C16 H17 O8 Cl1	371.05392
C14 H13 O5 Cl1	295.03788	C18 H17 O7 Cl1	379.05901
C12 H11 O7 Cl1	301.01206	C17 H15 O8 Cl1	381.03827
C12 H13 O7 Cl1	303.02771	C18 H19 O7 Cl1	381.07466
C13 H19 O6 Cl1	305.07974	C19 H23 O6 Cl1	381.11104
C15 H15 O5 Cl1	309.05353	C16 H15 O9 Cl1	385.03319
C14 H13 O6 Cl1	311.03279	C18 H17 O8 Cl1	395.05392
C13 H11 O7 Cl1	313.01206	C18 H19 O8 Cl1	397.06957
C15 H19 O5 Cl1	313.08483	C17 H17 O9 Cl1	399.04884
C13 H13 O7 Cl1	315.02771	C18 H17 O9 Cl1	411.04884
C13 H15 O7 Cl1	317.04336	C19 H21 O8 Cl1	411.08522
C15 H13 O6 Cl1	323.03279	C18 H19 O9 Cl1	413.06449
C14 H11 O7 Cl1	325.01206	C17 H19 O10 Cl1	417.05940
C15 H15 O6 Cl1	325.04844	C18 H17 O10 Cl1	427.04375
C14 H13 O7 Cl1	327.02771	C19 H21 O9 Cl1	427.08014
C15 H17 O6 Cl1	327.06409	C20 H25 O8 Cl1	427.11652
C13 H11 O8 Cl1	329.00697	C18 H21 O10 Cl1	431.07505
C16 H23 O5 Cl1	329.11613	C19 H25 O9 Cl1	431.11144
C13 H13 O8 Cl1	331.02262	C19 H17 O10 Cl1	439.04375
C15 H11 O7 Cl1	337.01206	C20 H21 O9 Cl1	439.08014
C16 H15 O6 Cl1	337.04844	C21 H27 O8 Cl1	441.13217
C15 H13 O7 Cl1	339.02771	C19 H23 O10 Cl1	445.09070
C14 H11 O8 Cl1	341.00697	C16 H17 O8 Cl1	371.05392
C14 H13 O8 Cl1	343.02262		
C14 H15 O8 Cl1	345.03827		
C16 H13 O7 Cl1	351.02771		
C15 H11 O8 Cl1	353.00697		
C16 H15 O7 Cl1	353.04336		
C15 H13 O8 Cl1	355.02262		
C16 H17 O7 Cl1	355.05901		
C15 H15 O8 Cl1	357.03827		
C15 H19 O8 Cl1	361.06957		
C17 H15 O7 Cl1	365.04336		
C18 H19 O6 Cl1	365.07974		
C17 H17 O7 Cl1	367.05901		

754

755 **Table 20.** List of verified formulae of the 33 DBPs common to DWTP1, DWTP2, and  
 756 DWTP3 according to negative ESI-FT-ICR MS analysis (only present in all three  
 757 replicates of disinfected water).  
 758

<b>DWTP1+DWTP2+DWTP3</b>	
<b><i>Molecular formula</i></b>	<b><i>Theoretical mass of the negative ion</i></b>
C13 H13 O6 Cl1	299.03279
C13 H15 O6 Cl1	301.04844
C14 H13 O6 Cl1	311.03279
C15 H17 O5 Cl1	311.06918
C13 H11 O7 Cl1	313.01206
C13 H13 O7 Cl1	315.02771
C13 H15 O7 Cl1	317.04336
C14 H13 O7 Cl1	327.02771
C13 H13 O8 Cl1	331.02262
C16 H17 O6 Cl1	339.06409
C14 H11 O8 Cl1	341.00697
C14 H13 O8 Cl1	343.02262
C14 H15 O8 Cl1	345.03827
C16 H15 O7 Cl1	353.04336
C15 H13 O8 Cl1	355.02262
C16 H17 O7 Cl1	355.05901
C15 H15 O8 Cl1	357.03827
C15 H17 O8 Cl1	359.05392
C16 H15 O8 Cl1	369.03827
C17 H19 O7 Cl1	369.07466
C15 H13 O9 Cl1	371.01754
C16 H19 O8 Cl1	373.06957
C16 H21 O8 Cl1	375.08522
C18 H19 O7 Cl1	381.07466
C17 H17 O8 Cl1	383.05392
C16 H15 O9 Cl1	385.03319
C17 H19 O8 Cl1	385.06957
C16 H17 O9 Cl1	387.04884
C17 H17 O9 Cl1	399.04884
C17 H19 O9 Cl1	401.06449
C18 H19 O9 Cl1	413.06449
C20 H23 O9 Cl1	441.09579
C19 H21 O10 Cl1	443.07505

759

760 **Table 21.** List of verified formulae of the 23 DBPs common to DWTP1, DWTP3, and  
 761 DWTP4 according to negative ESI-FT-ICR MS analysis (only present in all three  
 762 replicates of disinfected water).  
 763

<b>DWTP1+DWTP3+DWTP4</b>	
<b><i>Molecular formula</i></b>	<b><i>Theoretical mass of the negative ion</i></b>
C14 H13 O6 Cl1	311.03279
C13 H11 O7 Cl1	313.01206
C13 H13 O7 Cl1	315.02771
C13 H15 O7 Cl1	317.04336
C14 H13 O7 Cl1	327.02771
C13 H13 O8 Cl1	331.02262
C14 H11 O8 Cl1	341.00697
C14 H13 O8 Cl1	343.02262
C14 H15 O8 Cl1	345.03827
C16 H15 O7 Cl1	353.04336
C15 H13 O8 Cl1	355.02262
C16 H17 O7 Cl1	355.05901
C15 H15 O8 Cl1	357.03827
C16 H15 O8 Cl1	369.03827
C15 H13 O9 Cl1	371.01754
C16 H17 O8 Cl1	371.05392
C18 H19 O7 Cl1	381.07466
C16 H15 O9 Cl1	385.03319
C17 H17 O9 Cl1	399.04884
C18 H19 O9 Cl1	413.06449
C18 H17 O10 Cl1	427.04375
C19 H25 O9 Cl1	431.11144
C19 H23 O10 Cl1	445.09070

764

765 **Table 22.** List of verified formulae of the 45 DBPs common to DWTP2, DWTP3, and  
 766 DWTP4 according to negative ESI-FT-ICR MS analysis (only present in all three  
 767 replicates of disinfected water).  
 768

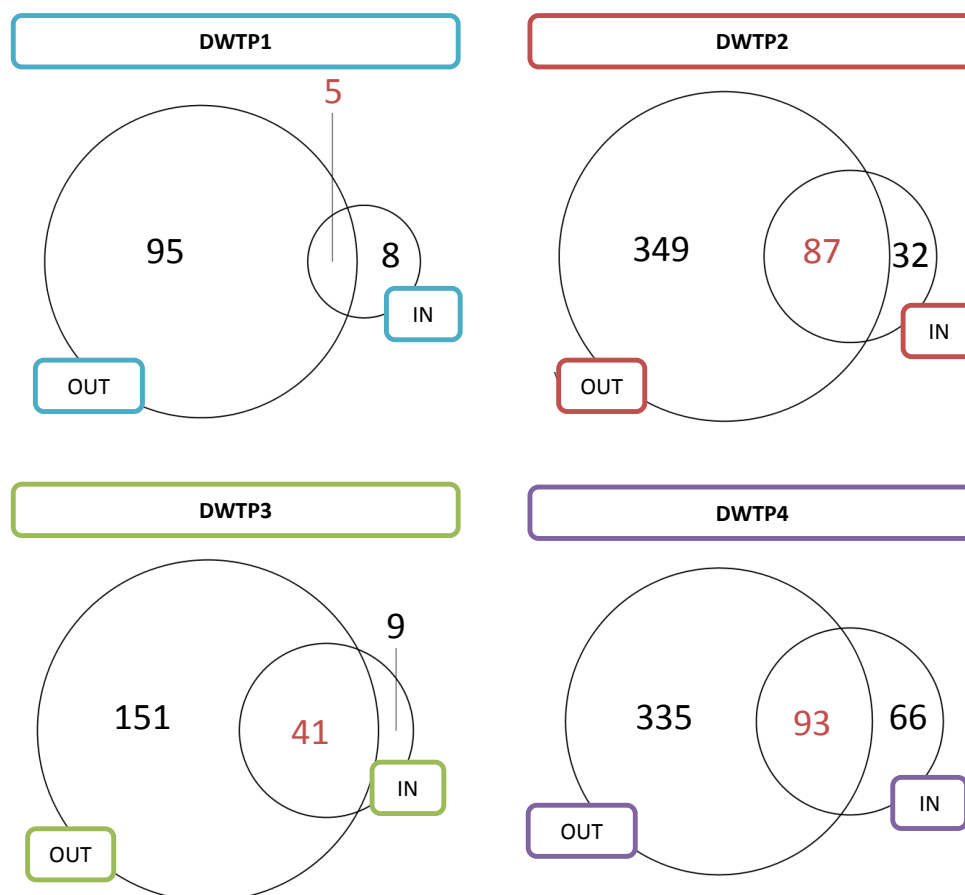
<b>DWTP2+DWTP3+DWTP4</b>		<b>DWTP2+DWTP3+DWTP4 (cont.)</b>	
<b><i>Molecular formula</i></b>	<b><i>Theoretical mass of the negative ion</i></b>	<b><i>Molecular formula</i></b>	<b><i>Theoretical mass of the negative ion</i></b>
C12 H11 O6 Cl1	285.01714	C18 H19 O7 Cl1	381.07466
C12 H13 O6 Cl1	287.03279	C16 H15 O9 Cl1	385.03319
C14 H13 O5 Cl1	295.03788	C18 H19 O8 Cl1	397.06957
C12 H11 O7 Cl1	301.01206	C17 H17 O9 Cl1	399.04884
C12 H13 O7 Cl1	303.02771	C18 H19 O9 Cl1	413.06449
C13 H19 O6 Cl1	305.07974	C17 H19 O10 Cl1	417.0594
C15 H15 O5 Cl1	309.05353	C20 H21 O9 Cl1	439.08014
C14 H13 O6 Cl1	311.03279	C21 H27 O8 Cl1	441.13217
C13 H11 O7 Cl1	313.01206		
C15 H19 O5 Cl1	313.08483		
C13 H13 O7 Cl1	315.02771		
C13 H15 O7 Cl1	317.04336		
C15 H13 O6 Cl1	323.03279		
C14 H11 O7 Cl1	325.01206		
C15 H15 O6 Cl1	325.04844		
C14 H13 O7 Cl1	327.02771		
C15 H17 O6 Cl1	327.06409		
C13 H11 O8 Cl1	329.00697		
C16 H23 O5 Cl1	329.11613		
C13 H13 O8 Cl1	331.02262		
C15 H11 O7 Cl1	337.01206		
C16 H15 O6 Cl1	337.04844		
C15 H13 O7 Cl1	339.02771		
C14 H11 O8 Cl1	341.00697		
C14 H13 O8 Cl1	343.02262		
C14 H15 O8 Cl1	345.03827		
C16 H13 O7 Cl1	351.02771		
C15 H11 O8 Cl1	353.00697		
C16 H15 O7 Cl1	353.04336		
C15 H13 O8 Cl1	355.02262		
C16 H17 O7 Cl1	355.05901		
C15 H15 O8 Cl1	357.03827		
C15 H19 O8 Cl1	361.06957		
C17 H17 O7 Cl1	367.05901		
C16 H15 O8 Cl1	369.03827		
C15 H13 O9 Cl1	371.01754		
C17 H15 O8 Cl1	381.03827		

769



770 Changes of the molecular composition of halogenated NOM during disinfection

771 In the case of DWTP1, 5% of the substances verified in disinfected water were also  
772 identified in the water before disinfection. In the case of the other investigated DWTPs  
773 the formulae overlay in non-disinfected and disinfected waters ranged between 20 and  
774 22% (Figure 12).



775 **Figure 12.** Venn diagrams showing the number of molecular formulae unique and  
776 common to non-disinfected (IN) and disinfected water (OUT) in each investigated  
777 drinking water treatment plant, after non-target FT-ICR MS analysis.  
778  
779

780 The weighted average molecular mass (weighted against relative intensities) of Cl- and  
781 Br-containing substances decreased during the chemical disinfection of water. However,  
782 this decrease was statistically significant only in DWTP2 and DWTP3 ( $p < 0.05$ , Table  
783 23). Verified halogenated formulae in chemically-disinfected water samples had a lower  
784 H/C ratio and a higher O/C ratio,  $AI_{mod}$ , and  $C_{OS}$  than those in non-disinfected waters.

785 These differences were statistically significant in most cases (except for H/C ratio,  
 786 DBE, and  $AI_{mod}$  in DWTP2 and DBE and  $AI_{mod}$  in DWTP4) with a confidence level of  
 787 95% ( $p < 0.05$ , Tables 24-28). These differences can be explained by the specific  
 788 reactivity of the chemical disinfectants with NOM, forming aromatic halogenated  
 789 compounds with high C-C double bond density and DBE (Figure 10).

790 **Table 23.** Statistics for comparison of the molecular mass of verified Cl and Br  
 791 formulae in the investigated samples, after negative ESI-FT-ICR MS analysis.

		Mann-Whitney U* (2 independent groups: IN vs OUT)				Kruskal-Wallis** (various independent groups: DWTP_OUT samples)			
		n	Median	U	p-value	Median	$\chi^2_{(3)}$	p-value	Post-hoc Dunn's test ( $p < 0.05$ )
DWTP1	IN	8	407	555	0.088	386	59.1	<b>&lt;0.001</b>	<i>DWTP1 vs DWTP2</i> <i>DWTP3 vs DWTP2</i> <i>DWTP4 vs DWTP2</i>
	OUT	95	386						
DWTP2	IN	32	415	9533	<b>&lt;0.001</b>	348			
	OUT	349	348						
DWTP3	IN	9	412	1017	<b>0.031</b>	372			
	OUT	151	372						
DWTP4	IN	66	387	14530	0.142	374			
	OUT	335	374						

793 \*When  $p$ -value  $< 0.05$ , the molecular mass of the Cl and Br-formulae before and after  
 794 disinfection are significantly different with a significance level of 5%. Overlapping features  
 795 between IN and OUT were removed.

796 \*\*When  $p$ -value  $< 0.05$ , the molecular mass of the Cl and Br-formulae in disinfected water of  
 797 the different DWTPs are significantly different with a significance level of 5%. Pairwise  
 798 comparison with a posthoc Dunn's test allows identification of the differences.

799

800  
801  
802  
803

**Table 24.** Statistics for comparison of the H/C content of verified Cl and Br formulae in the investigated samples, after negative ESI-FT-ICR MS analysis.

	n	Mann-Whitney U* (2 independent groups: IN vs OUT)			Kruskal-Wallis** (various independent groups: DWTP_OUT samples)			
		Median	U	p-value	Median	$\chi^2_{(3)}$	p-value	Post-hoc Dunn's test (p<0.05)
DWTP1 IN	8	1.55	706	<b>&lt;0.001</b>	1.06	2.81	0.422	-
OUT	95	1.06						
DWTP2 IN	32	1.13	7262	0.054	1.06			
OUT	349	1.06						
DWTP3 IN	9	1.48	1348	<b>&lt;0.001</b>	1.06			
OUT	151	1.06						
DWTP4 IN	66	1.11	16001	<b>0.001</b>	1.00			
OUT	335	1.00						

804 \*When p-value <0.05, the H/C content of verified Cl and Br-formulae before and after  
805 disinfection are significantly different with a significance level of 5%. Overlapping features  
806 between IN and OUT were removed.

807 \*\*When p-value <0.05, the H/C content of verified DBPs in disinfected water of the different  
808 DWTPs are significantly different with a significance level of 5%. Pairwise comparison with a  
809 posthoc Dunn's test allows identification of the differences.

810  
811

**Table 25.** Statistics for comparison of the O/C content of verified Cl and Br formulae in the investigated samples, after negative ESI-FT-ICR MS analysis.

814

	n	Mann-Whitney U* (2 independent groups: IN vs OUT)			Kruskal-Wallis** (various independent groups: DWTP_OUT samples)			
		Median	U	p-value	Median	$\chi^2_{(3)}$	p-value	Post-hoc Dunn's test (p<0.05)
DWTP1 IN	8	0.33	128	<b>&lt;0.001</b>	0.50	38.9	<b>&lt;0.001</b>	<i>DWTP4 vs DWTP3</i> <i>DWTP1 vs DWTP3</i> <i>DWTP2 vs DWTP3</i>
OUT	95	0.50						
DWTP2 IN	32	0.46	4175	<b>0.001</b>	0.50			
OUT	349	0.50						
DWTP3 IN	9	0.29	362	<b>0.007</b>	0.46			
OUT	151	0.46						
DWTP4 IN	66	0.43	8145	<b>&lt;0.001</b>	0.50			
OUT	335	0.50						

815 \*When p-value <0.05, the O/C content of verified Cl and Br-formulae before and after  
816 disinfection are significantly different with a significance level of 5%. Overlapping features  
817 between IN and OUT were removed.

818 \*\*When p-value <0.05, the O/C content of verified DBPs in disinfected water of the different  
819 DWTPs are significantly different with a significance level of 5%. Pairwise comparison with a  
820 posthoc Dunn's test allows identification of the differences.

821  
822  
823  
824

825 **Table 26.** Statistics for comparison of the  $AI_{mod}$  of verified Cl and Br formulae in the  
 826 investigated samples, after negative ESI-FT-ICR MS analysis.  
 827

		Mann-Whitney U* (2 independent groups: IN vs OUT)				Kruskal-Wallis** (various independent groups: DWTP_OUT samples)			
		n	Median	U	p-value	Median	$\chi^2_{(3)}$	p-value	Post-hoc Dunn's test (p<0.05)
DWTP1	IN	8	0.19	139	<b>&lt;0.001</b>	0.38	0.38	0.945	-
	OUT	95	0.38						
DWTP2	IN	32	0.36	5213	0.132	0.39			
	OUT	349	0.39						
DWTP3	IN	9	0.17	93	<b>&lt;0.001</b>	0.40			
	OUT	151	0.40						
DWTP4	IN	66	0.38	12270	0.247	0.4			
	OUT	335	0.40						

828 \*When p-value <0.05, the  $AI_{mod}$  content of verified Cl and Br-formulae before and after  
 829 disinfection are significantly different with a significance level of 5%. Overlapping features  
 830 between IN and OUT were removed.

831 \*\*When p-value <0.05, the  $AI_{mod}$  content of verified DBPs in disinfected water of the different  
 832 DWTPs are significantly different with a significance level of 5%. Pairwise comparison with a  
 833 posthoc Dunn's test allows identification of the differences.

834

835

836 **Table 27.** Statistics for comparison of the  $C_{OS}$  of verified Cl and Br formulae in the  
 837 investigated samples, after negative ESI-FT-ICR MS analysis.

838

		Mann-Whitney U* (2 independent groups: IN vs OUT)				Kruskal-Wallis** (various independent groups: DWTP_OUT samples)			
		n	Median	U	p-value	Median	$\chi^2_{(3)}$	p-value	Post-hoc Dunn's test (p<0.05)
DWTP1	IN	8	-0.80	115	<b>&lt;0.001</b>	0	34.2	<b>&lt;0.001</b>	<i>DWTP4 vs DWTP3</i> <i>DWTP1 vs DWTP3</i> <i>DWTP2 vs DWTP3</i>
	OUT	95	0						
DWTP2	IN	32	-0.13	4129	<b>&lt;0.001</b>	0.13			
	OUT	349	0.13						
DWTP3	IN	9	-0.86	184	<b>&lt;0.001</b>	-0.12			
	OUT	151	-0.12						
DWTP4	IN	66	-0.15	8015	<b>&lt;0.001</b>	0.12			
	OUT	335	0.12						

839 \*When p-value <0.05, the  $C_{OS}$  content of verified Cl and Br-formulae before and after  
 840 disinfection are significantly different with a significance level of 5%. Overlapping features  
 841 between IN and OUT were removed.

842 \*\*When p-value <0.05, the  $C_{OS}$  content of verified DBPs in disinfected water of the different  
 843 DWTPs are significantly different with a significance level of 5%. Pairwise comparison with a  
 844 posthoc Dunn's test allows identification of the differences.

845

846

847  
848  
849  
850

**Table 28.** Statistics for comparison of the DBE of verified Cl and Br formulae in the investigated samples, after negative ESI-FT-ICR MS analysis.

		Mann-Whitney U* (2 independent groups: IN vs OUT)				Kruskal-Wallis** (various independent groups: DWTP_OUT samples)			
		n	Median	U	p-value	Median	$\chi^2_{(3)}$	p-value	Post-hoc Dunn's test (p<0.05)
DWTP1	IN	8	4	168	<b>0.002</b>	8	49.7	<b>&lt;0.001</b>	<i>DWTP3 vs DWTP2</i> <i>DWTP3 vs DWTP4</i> <i>DWTP1 vs DWTP2</i> <i>DWTP4 vs DWTP2</i>
	OUT	95	8						
DWTP2	IN	32	8	7013	0.126	7			
	OUT	349	7						
DWTP3	IN	9	5	196	<b>&lt;0.001</b>	8			
	OUT	151	8						
DWTP4	IN	66	7	12294	0.253	8			
	OUT	335	8						

851 \*When p-value <0.05, the DBE content of verified Cl and Br-formulae before and after  
852 disinfection are significantly different with a significance level of 5%. Overlapping features  
853 between IN and OUT were removed.

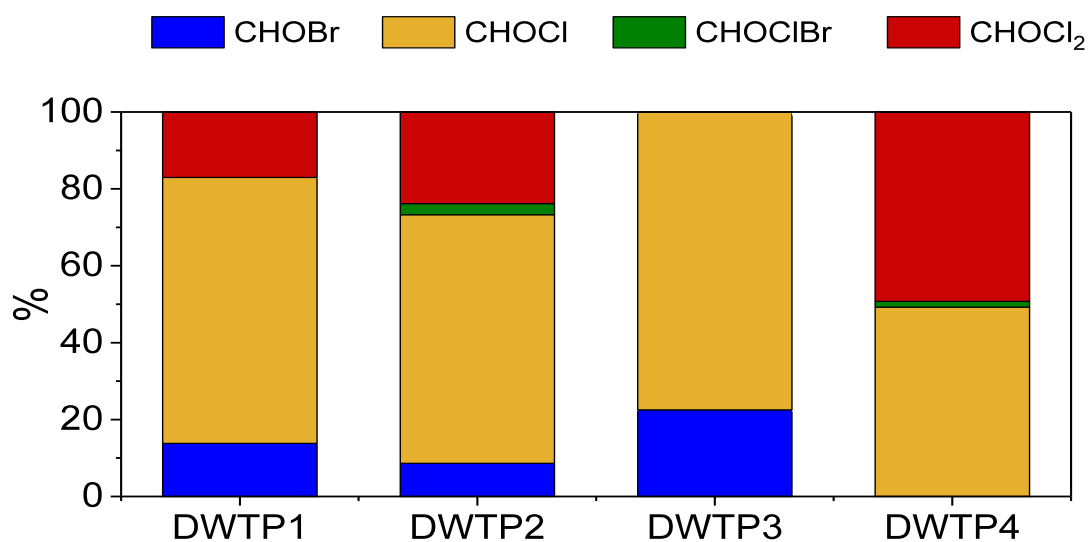
854 \*\*When p-value <0.05, the DBE content of verified DBPs in disinfected water of the different  
855 DWTPs are significantly different with a significance level of 5%. Pairwise comparison with a  
856 posthoc Dunn's test allows identification of the differences.  
857

858 *Cl- and Br- compounds in DBP mixtures*

859 The contribution of different groups of halogenated substances to the DBP mixture  
860 chemodiversity in all disinfected waters is summarized in Figure 13. Monochlorinated  
861 compounds (CHOC1) contributed the most to the total DBP mixture chemodiversity in  
862 all disinfected waters (65-75%) except in DWTP4, where both CHOC1 and CHOC1<sub>2</sub>  
863 were equally relevant (49% each). Bromine incorporation into NOM led to the  
864 formation of monobrominated substances (CHOBr) in the order DWTP3 (23%) >  
865 DWTP1 (14%) > DWTP2 (9%) > DWTP4 (2%). Even higher bromination rates were  
866 expected to occur in DWTP3, according to the results of a previous study, where  
867 chloramination of source waters with a slightly higher concentration of bromide (0.28  
868 mg/L) than in DWTP3 (0.22 mg/L) resulted mainly in the formation of CHOBr  
869 compounds [26]. This finding, which has also been confirmed by target analyses in this  
870 study, could be associated with a dominant presence of aromatic DBP precursors in

871 DWTP3 source water (as indicated by SUVA measurements, Table 2). Thus, this could  
872 result in low incorporation of bromine into NOM during chloramination, as reported  
873 elsewhere [78].

874 Dichlorinated compounds ( $\text{CHOCl}_2$ ) were not present in DWTP3, but were the second  
875 most abundant group formed in the remaining DWTPs. As previously mentioned,  
876  $\text{CHOCl}_2$  make up 49% of the formulae found in DWTP4, where chlorination of the  
877 source water with the lowest amount of bromide (0.05 mg/L) occurred, but accounted  
878 for less than 24% of the halogenated substances found in DWTP1 and DWTP2  
879 disinfected waters (Figure 13). In this regard, the halogenated chemical space covered  
880 by the FT-ICR MS analysis in DWTP4 gives evidence that substances highly  
881 substituted with chlorine are formed during the chlorination of waters with low bromide  
882 content in agreement with previous studies [64, 79]. This is also confirmed by the DBPs  
883 found in DWTP4 waters with the target approach (Figure 6 and Table 5).



884  
885  
886  
887  
888  
889

**Figure 13.** Contribution of each group of halogenated compounds to the chemodiversity of the investigated disinfected waters, after FT-ICR MS analysis. Y-axis shows the percent of verified molecular formulae.

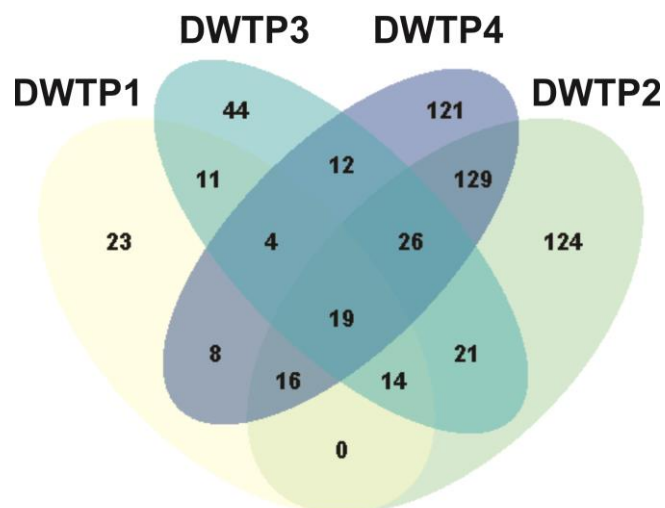
890 Finally, a small group of halogenated DBPs containing one Br and one Cl atom  
891 (CHOCIBr) was also found in DWTP2 and DWTP4, and constituted 3% and 1.5%,  
892 respectively, of the total formulae verified in these samples. In DWTP4, these formulae  
893 have DBE between 0 and 1, very low  $AI_{mod}$  ( $<0$ ), high H/C ratio (1.8-2), and low O/C  
894 ratio (0.2-0.3). Consequently, they correspond to aliphatic compounds (Figures 8 and  
895 10). In DWTP2, most of the verified CHOCIBr DBPs have an aromatic character (DBE  
896 of 5 or 6,  $AI_{mod}$  between 0.38 and 0.57, H/C ratio  $\leq 1$ , and relatively high O/C ratio of  
897 0.6-0.7).

898 The investigated DBP mixtures contained only two highly halogenated formulae, *viz.*  
899  $C_{33}H_{28}O_6Cl_4$  in DWTP1 and DWTP4 and  $C_5HO_3Cl_2Br$  in DWTP2. The  $CHOC_4$   
900 formula corresponded with the verified DBP of the highest molecular weight. This and  
901 the non-detection of additional highly halogenated formulae may suggest that these type  
902 of compounds are unstable or intermediate DBPs that may rapidly alter via hydrolysis to  
903 smaller compounds; or that the specific precursors of this type of DBPs, required for  
904 their formation, were not abundant in these source waters [80].

905

#### 906 *Specific molecular composition of DBP mixtures of each water treatment plant*

907 In total, 19 formulae, all of them corresponding with monochlorinated compounds were  
908 observed to occur in all disinfected waters; whereas 23, 124, 44, and 121 were unique to  
909 DWTP1, DWTP2, DWTP3, and DWTP4, respectively (Figure 14, and Tables 7-22).  
910 The molecular composition of the common DBPs and DBPs unique to each water  
911 treatment plant is summarized in Figures 15-18. In the case of DWTP3, unique DBPs  
912 were mainly CHOBBr compounds, whereas in DWTP4 unique DBPs were dominated by  
913  $CHOC_2$  formulae.

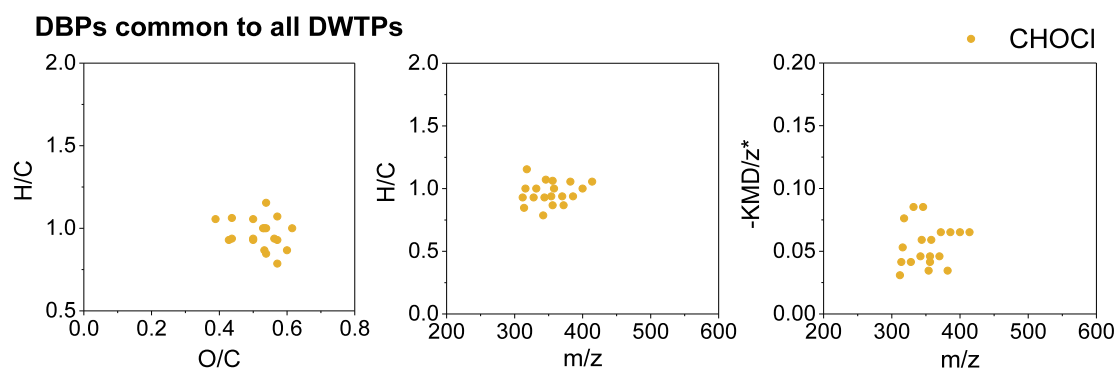


914

915 **Figure 14.** Venn diagram showing the chemodiversity of the investigated DBP mixtures  
 916 according to ESI(-)-FT-ICR MS analysis.

917

918

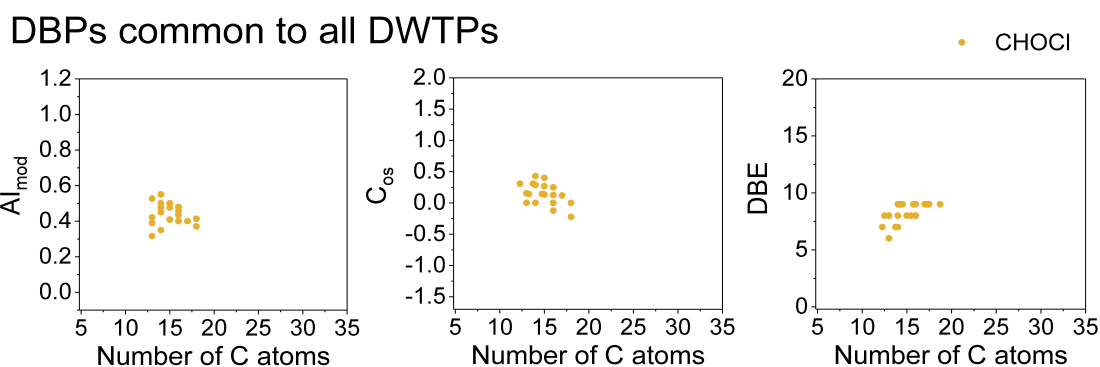


919

920 **Figure 15.** Molecular composition of the DBPs formed in all DWTPs according to  
 921 ESI(-)-FT-ICR MS analysis visualized by van Krevelen diagrams (left panel), mass  
 922 edited H/C ratios (middle panel), and modified Kendrick mass defect (right panel). Only  
 923 formulae present in all three replicates are shown.

924





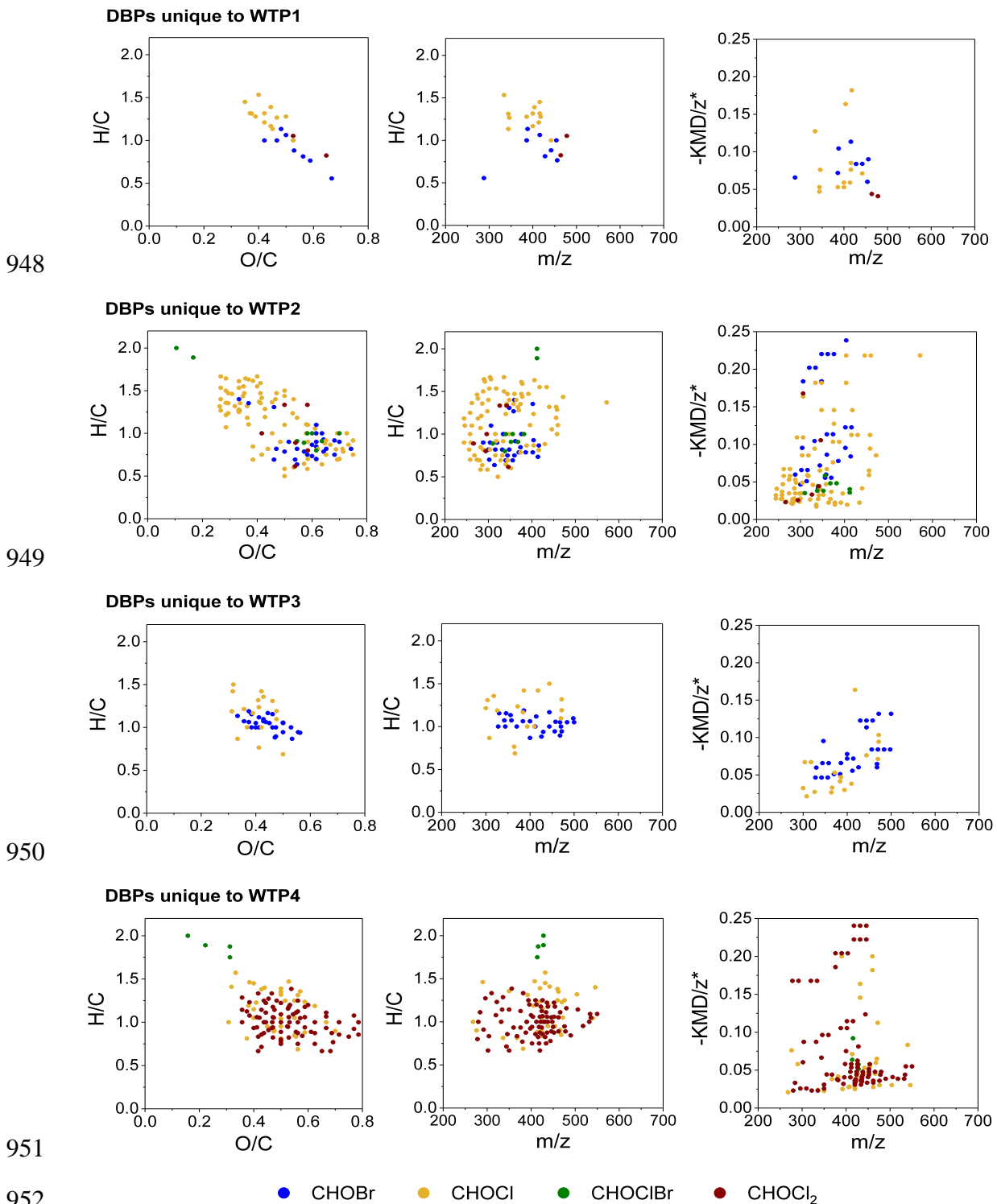
925  
926

927 **Figure 16.** Plots showing DBE,  $Al_{mod}$ , and  $C_{OS}$  versus the number of carbon for verified  
928 DBPs ( $m/z$  ions only present in disinfected water) common to all DWTPs according to  
929 negative ESI-FT-ICR MS analysis.

930

931 The weighted average molecular mass of DBPs was very similar in all disinfected  
932 waters, being all distributed within the mass range of 244 - 660 Da (Table 6). However,  
933 the distribution of the molecular mass of the  $m/z$  ions in DWTP2 was slightly lower than  
934 that observed in the other plants ( $p < 0.001$ ). This was also true for the distribution of  
935 DBE in the DBPs identified in DWTP2. DWTP2, together with DWTP4, presented the  
936 highest diversity of bromine and chlorine-containing features identified as DBPs  
937 (Figures 8 and 17). Thus, heterogeneity of the mixture seems to be associated to the  
938 properties and amount of NOM in the source water rather than the disinfectant applied.  
939 It is worthy to highlight that the number of molecular formulae verified in one sample is  
940 subject to a very conservative verification approach (i.e., the  $m/z$  ion should appear  
941 above an established threshold in all three replicates). In this regard, samples yielding  
942 more verified formulae are more representative of the true chemodiversity of the  
943 mixture than samples with fewer formulae. However, this does not necessarily translate  
944 into a higher mixture heterogeneity, since the intensity of an  $m/z$  ion in a sample is  
945 highly depending on matrix effects and intensities of other formulae in the sample, and  
946 as a result, the number of formulae present in the sample may be underestimated.

947

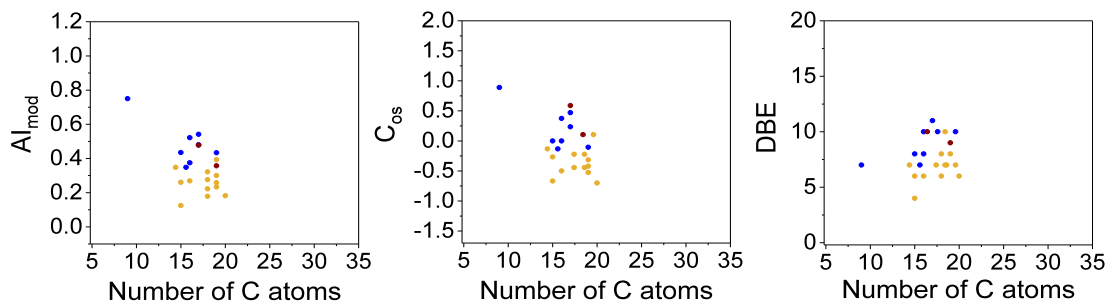


953 **Figure 17.** Molecular composition of the DBPs unique to each DWTP according to  
954 ESI(-)-FT-ICR MS analysis visualized by van Krevelen diagrams (left panel), mass  
955 edited H/C ratios (middle panel), and modified Kendrick mass defect plots (right panel).  
956 Only formulae present in all three replicates are shown.

957

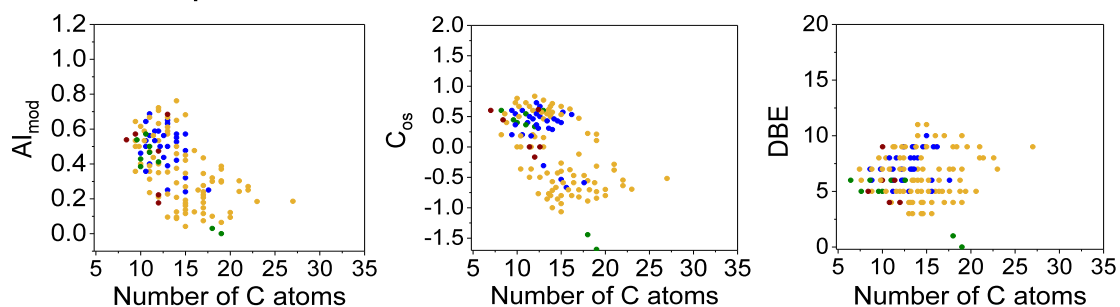
958  
959

### DBPs unique to DWTP1



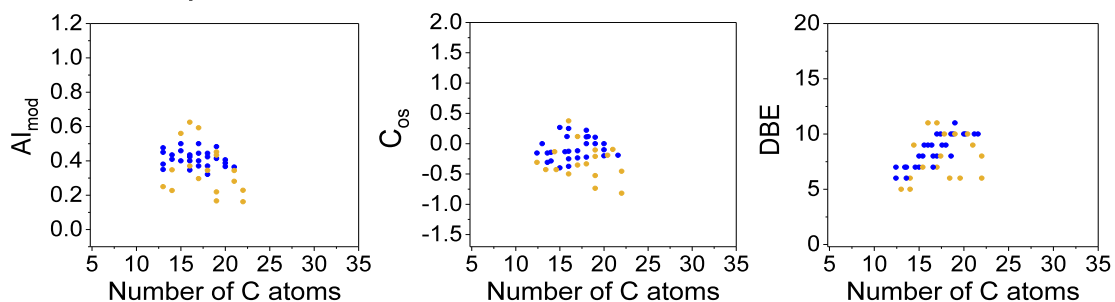
960

### DBPs unique to DWTP2



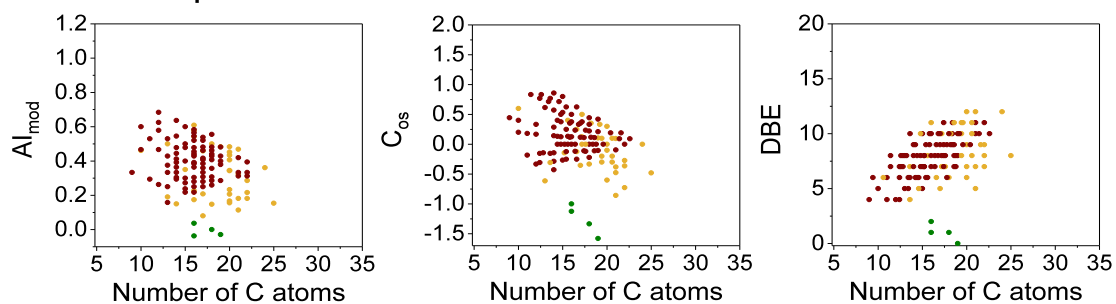
961

### DBPs unique to DWTP3



962

### DBPs unique to DWTP4



963

● CHOBr ● CHOCl ● CHOCIBr ● CHOCl<sub>2</sub>

964  
965

966 **Figure 18.** Plots showing DBE, AI<sub>mod</sub>, and C<sub>OS</sub> versus the number of carbon for unique  
967 verified DBPs (*m/z* ions only present in disinfected water) according to negative ESI-  
968 FT-ICR MS analysis.

969

970 While mono and diCl-DBPs were dominant in DWTP4 disinfected water, the DBP  
971 mixture in DWTP3 was dominated by monohalogenated Br- and Cl-DBPs. Besides  
972  $C_{33}H_{28}O_6Cl_4$  and  $C_{17}H_{34}O_4ClBr$ , no other di- or higher halogenated formulae were  
973 present in DWTP3 disinfected water. The computed weighted average O/C ratio and  
974  $C_{OS}$  of the formulae verified in DWTP3 were significantly different (lower) compared  
975 to the formulae verified in the other investigated DBP mixtures ( $p < 0.001$ ). This could  
976 be partially attributed to the use of chloramine for disinfection that has a lower  
977 oxidation potential than chlorine.

978 The  $-KMD/z^*$  diagrams revealed two major groups of DBPs in each DBP mixture  
979 (Figure 8); one group located in the lower region of the diagram ( $-KMD/z^* < 0.12$ ),  
980 characterized by unsaturated compounds, and one group, located in the upper region of  
981 the diagram ( $-KMD/z^* > 0.12$ ), mainly formed by highly oxygenated and unsaturated  
982 compounds. Specifically,  $CHCl_2$  formulae distribute in three regions in DWTP2 and  
983 DWTP4 ( $-KMD/z^* < 0.05$ ,  $-KMD/z^*$  around 0.10 and  $-KMD/z^* > 0.12$ ), which could  
984 indicate that each of these groups arises from different precursors.

985 The average Cl/C ratio of the verified formulae decreased in the order  
986 DWTP4 > DWTP2 > DWTP1 > DWTP3, while the average Br/C ratio decreased as follows  
987 DWTP3 > DWTP2 > DWTP1 > DWTP4 (Table 2).

988

989 ***Non-target LC-ESI(-)-Orbitrap MS analysis to identify DBPs in halogenated DBP***  
990 ***mixtures***

991 Using LC-ESI(-)-Orbitrap MS, a total of 81, 129, 54, and 116 newly formed  
992 halogenated and non-halogenated features with abundances above 100,000 counts were  
993 found in all three triplicate samples of DWTP1, DWTP2, DWTP3, and DWTP4. The  
994 halogenated features were compared to those detected by FT-ICR MS. Only few  
995 formulae were detected using both techniques (i.e., 286.91968; 243.00658, 259.00149;  
996 300.96761; 335.04586; 255.04296; 256.84134; 318.94179). The low percentage of  
997 agreement between the halogenated features detected with both techniques could be  
998 attributed to: (i) the chromatographic column including retention factor, selectivity  
999 and/or efficiency, and (ii) the incompatibility of some DBPs with the mobile phase used  
1000 in the LC-ESI(-)-Orbitrap MS approach, (iii) the loss of some DBPs during the second  
1001 SPE preconcentration process for Orbitrap MS analysis, (iv) interference problems  
1002 related to the ion suppression phenomenon (that may vary between the ESI ion source  
1003 configurations used, and reduce after chromatographic separation of sample  
1004 components), (v) the use of different data processing tools (e.g., the algorithm used for  
1005 peak deconvolution of LC-Orbitrap MS data) [81], or (vi) a mixture of all these factors.  
1006 Besides, the DBP with the lowest  $m/z$  confirmed with FT-ICR MS had a nominal  $m/z$  of  
1007 243, whereas many of the DBPs detected with Orbitrap MS were below this value. This  
1008 could be attributed to on the one hand the higher mass cutoff set in FT-ICR MS  
1009 compared to LC-Orbitrap MS, and also the low capability of the direct infusion  
1010 approach to detect ions in the low  $m/z$  range. Direct infusion is highly affected by ion  
1011 suppression effects as all matrix components are analyzed at once, and this may

1012 condition the detection of low  $m/z$  ions. The implementation of LC before FT-ICR MS  
1013 is limited by the acquisition speed of the ICR cell operated.

1014 Contrary to FT-ICR MS instruments, the Q-Exactive, due to its hybrid nature  
1015 (Quadrupole-Orbitrap MS) provides structural information of the different ions in the  
1016 mixture. Thus, it allows assigning a molecular structure for most of the halogenated  
1017 DBPs present in the investigated disinfected samples.

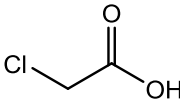
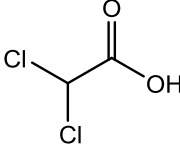
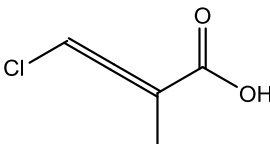
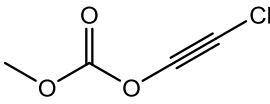
1018 Despite that the iodo-acids found in the target approach are indeed amenable to ESI(-)  
1019 [82, 83], iodo-DBPs were not detected in the samples using LC-Orbitrap MS. This can  
1020 be attributed to the fact that their concentrations were below the limit of detection of the  
1021 technique, or they were not captured with the extraction method used (water pH during  
1022 extraction was equal to the highest  $pK_a$  of iodo-acids that were detected).

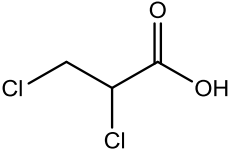
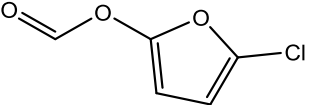
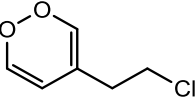
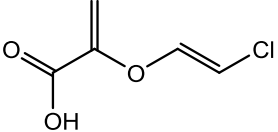
1023 The workflow used (Figure 5) allowed identifying in total 86 DBPs (including isobaric  
1024 species), which corresponded with 43% (DWTP1) - 70% (DWTP3) of the newly  
1025 formed features. Most of the identifications were obtained with a confidence level of 3,  
1026 according to Schimanski's scale [84], i.e., there were identification pieces of evidence  
1027 from MS2 data for proposing a specific molecular structure, but this could not be  
1028 confirmed. A confidence level of 1 was achieved for 4 compounds, specifically, for 4  
1029 HAAs after injection of an extract aliquot fortified with pure analytical standards, and  
1030 comparison of their retention time and fragmentation pattern.

1031 The DBPs tentatively identified are listed in Table 29. According to the structures  
1032 proposed, most DBPs identified are highly unsaturated and phenolic compounds, which  
1033 is in agreement with their properties, summarized in Table 30 and Figures 19-21.

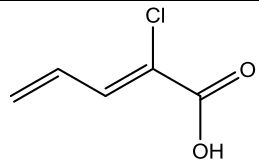
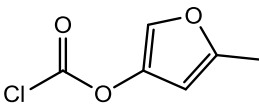
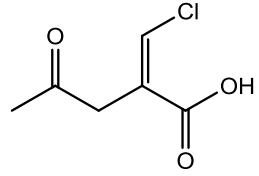
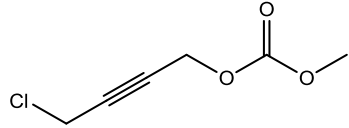
1034  
1035

**Table 29.** DBPs identified after LC-ESI(-)MS/MS analyses with QExactive MS.

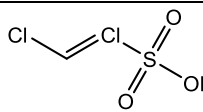
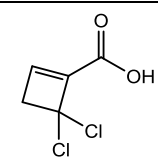
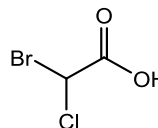
Parent ion				Presence in extracts					Suspect DBP (Level of confidence)	Identification evidence
Theor. mass [M-H] <sup>-</sup>	Elemental comp [M]	RDB E	Δ error (ppm)	Rt (min)	DW TP1	DW TP2	DW TP3	DW TP4		
92.9751	C <sub>2</sub> H <sub>3</sub> ClO <sub>2</sub>	1.5	3.438	7.95	√	√	T	√	 <i>2-chloroacetic acid</i> (CL 1)	<ul style="list-style-type: none"> <li>- Isotopic pattern of Cl</li> <li>- CONFIRMED with analytical standard</li> </ul>
126.9359	C <sub>2</sub> H <sub>2</sub> Cl <sub>2</sub> O <sub>2</sub>	1.5	2.067	6.9	√√	√√√	√√	√√√	 <i>2,2-dichloroacetic acid</i> (CL 1)	<ul style="list-style-type: none"> <li>- Isotopic pattern of Cl<sub>2</sub></li> <li>- Characteristic fragments: 126.9361 (C<sub>2</sub>HCl<sub>2</sub>O<sub>2</sub>) 82.9462 (CHCl<sub>2</sub>)</li> <li>- The highest score in MetFrag</li> <li>- CONFIRMED with analytical standard</li> </ul>
130.9905	C <sub>5</sub> H <sub>5</sub> ClO <sub>2</sub>	3.5	2.287	9.73	√	√√	√√	√	 <i>4-chloro-2-methyl-but-2,3-dienoic acid</i> (CL 3)	<ul style="list-style-type: none"> <li>- Isotopic pattern of Cl</li> <li>- Characteristic fragments: 130.9908 (C<sub>5</sub>H<sub>4</sub>ClO<sub>2</sub>) 113.0247 (C<sub>5</sub>H<sub>5</sub>O<sub>3</sub>) 95.0140 (C<sub>5</sub>H<sub>3</sub>O<sub>2</sub>) 87.0453 (C<sub>4</sub>H<sub>7</sub>O<sub>2</sub>)</li> <li>- The highest score in MetFrag</li> </ul>
132.9698	C <sub>4</sub> H <sub>3</sub> ClO <sub>3</sub>	3.5	2.595	7.82	√	√√√	√√	√	 <i>chloroethynyl methyl carbonate</i> (CL 3)	<ul style="list-style-type: none"> <li>- Isotopic pattern of Cl</li> <li>- Characteristic fragments: 132.9701 (C<sub>4</sub>H<sub>2</sub>ClO<sub>3</sub>) 74.9643 (C<sub>2</sub>ClO) 68.9982 (C<sub>3</sub>H<sub>2</sub>O) 58.9692 (C<sub>2</sub>Cl)</li> <li>- The highest score in MetFrag</li> </ul>

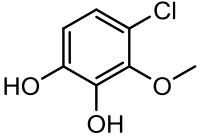
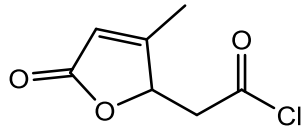
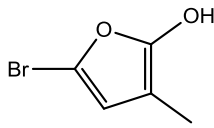
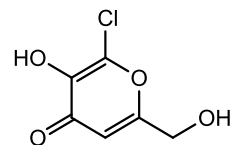
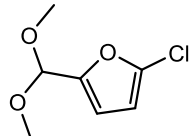
134.9413	C <sub>4</sub> H <sub>2</sub> Cl <sub>2</sub> O	3.5	2.124	14.1	x	x	x	√	n/a (CL 4)	- Isotopic pattern of Cl <sub>2</sub> - No MS2 available
140.9518	C <sub>3</sub> H <sub>4</sub> Cl <sub>2</sub> O <sub>2</sub>	1.5	2.851	13.1	√	x	x	√√	 2,3-dichloropropanoic acid (CL 3)	- Isotopic pattern of Cl <sub>2</sub> - Characteristic fragments: 140.9520 (C <sub>3</sub> H <sub>3</sub> Cl <sub>2</sub> O <sub>2</sub> ) 104.9751 (C <sub>3</sub> H <sub>2</sub> ClO <sub>2</sub> ) 96.9617 (C <sub>2</sub> H <sub>3</sub> Cl) 71.0139 (C <sub>3</sub> H <sub>3</sub> O <sub>2</sub> ) - The highest score in MetFrag
144.9698	C <sub>5</sub> H <sub>3</sub> ClO <sub>3</sub>	4.5	1.414	6.85	√√	√√√	√√	√√	 5-chlorofuran-2-yl formate (CL 3)	- Isotopic pattern of Cl - Characteristic fragments: 144.9700 (C <sub>5</sub> H <sub>2</sub> ClO <sub>3</sub> ) 116.9799 (C <sub>4</sub> H <sub>2</sub> ClO <sub>2</sub> ) 100.9799 (C <sub>4</sub> H <sub>2</sub> ClO) 74.9643 (C <sub>2</sub> ClO) 65.0032 (C <sub>4</sub> HO) - The highest score in MetFrag
145.0065	C <sub>6</sub> H <sub>7</sub> ClO <sub>2</sub>	3.5	2.066	11.7	X	√√	√	x	 4-(2-chloroethyl)-1,2-dioxine (CL 3)	- Isotopic pattern of Cl - Characteristic fragments: 145.0065 (C <sub>6</sub> H <sub>6</sub> ClO <sub>2</sub> ) 83.0143 (C <sub>4</sub> H <sub>3</sub> O <sub>2</sub> ) 81.0143 (C <sub>5</sub> H <sub>5</sub> O) - The highest score in MetFrag
146.9854	C <sub>5</sub> H <sub>5</sub> ClO <sub>3</sub>	3.5	2.483	9.5	√	√√√	√√	√	 2-((2-chlorovinyl)oxy)acrylic acid (CL 3)	- Isotopic pattern of Cl - Characteristic fragments: 146.9857 (C <sub>5</sub> H <sub>4</sub> ClO <sub>3</sub> ) 102.9958 (C <sub>4</sub> H <sub>4</sub> ClO) 67.0189 (C <sub>4</sub> H <sub>3</sub> O) 58.9692 (C <sub>2</sub> Cl) - The highest score in MetFrag

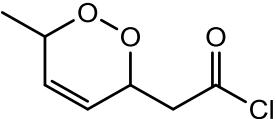
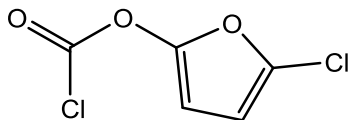
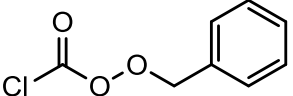
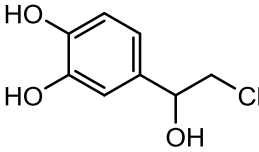


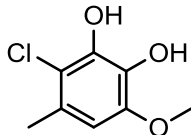
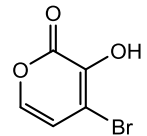
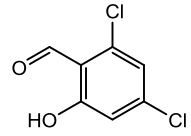
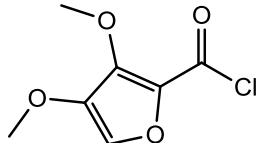
146.9854	C <sub>5</sub> H <sub>5</sub> ClO <sub>3</sub>	3.5	1.829	5.47	√	√	x	√	 <p><i>2-chloropenta-2,4-dienoic acid</i> (CL 3)</p>	<ul style="list-style-type: none"> <li>- Isotopic pattern of Cl</li> <li>- Characteristic fragments: 146.9857 (C<sub>5</sub>H<sub>4</sub>ClO<sub>3</sub>) 104.9753 (C<sub>3</sub>H<sub>2</sub>ClO<sub>2</sub>) 67.0189 (C<sub>4</sub>H<sub>3</sub>O) 58.9692 (C<sub>2</sub>Cl)</li> <li>- The highest score in MetFrag</li> </ul>
157.0063	C <sub>7</sub> H <sub>7</sub> ClO <sub>2</sub>	4.5	0.952	13.1	x	x	x	√	n/a (CL 4)	<ul style="list-style-type: none"> <li>- Isotopic pattern of Cl</li> <li>- No MS2 available</li> </ul>
158.9857	C <sub>6</sub> H <sub>5</sub> ClO <sub>3</sub>	4.5	1.101	9.23	X	√√	√	√	 <p><i>(5-methyl-3-furyl) carbonochloridate</i> (CL 3)</p>	<ul style="list-style-type: none"> <li>- Isotopic pattern of Cl</li> <li>- Characteristic fragments: 158.9857 (C<sub>6</sub>H<sub>4</sub>ClO<sub>3</sub>) 143.9623 (C<sub>5</sub>HClO<sub>3</sub>) 130.9544 (C<sub>4</sub>ClO<sub>3</sub>) 114.9960 (C<sub>5</sub>H<sub>4</sub>ClO) 79.0190 (C<sub>5</sub>H<sub>3</sub>O) 83.0140 (C<sub>4</sub>H<sub>3</sub>O<sub>2</sub>)</li> <li>- The highest score in MetFrag</li> </ul>
161.0012	C <sub>6</sub> H <sub>7</sub> ClO <sub>3</sub>	3.5	0.776	8.38	T	√√	√	√	 <p><i>2-(chloromethylene)-4-oxopentanoic acid</i> (CL 3)</p>	<ul style="list-style-type: none"> <li>- Isotopic pattern of Cl</li> <li>- Characteristic fragments: 161.0012 (C<sub>6</sub>H<sub>6</sub>ClO<sub>3</sub>) 118.9906 (C<sub>4</sub>H<sub>4</sub>ClO<sub>2</sub>) 125.0245 (C<sub>6</sub>H<sub>5</sub>O<sub>3</sub>) 83.0140 (C<sub>4</sub>H<sub>3</sub>O) 57.0342 (C<sub>3</sub>H<sub>5</sub>O)</li> <li>- The highest score in MetFrag</li> </ul>
161.0012	C <sub>6</sub> H <sub>7</sub> ClO <sub>3</sub>	3.5	0.776	8.8	T	√√	√	√	 <p><i>4-chlorobut-2-ynyl methyl carbonate</i> (CL 3)</p>	<ul style="list-style-type: none"> <li>- Isotopic pattern of Cl</li> <li>- Characteristic fragments: 160.0012 (C<sub>6</sub>H<sub>6</sub>ClO<sub>3</sub>) 128.9751 (C<sub>5</sub>H<sub>2</sub>ClO<sub>2</sub>) 110.0011 (C<sub>5</sub>H<sub>2</sub>O<sub>3</sub>) 95.0141 (C<sub>5</sub>H<sub>3</sub>O<sub>2</sub>) 72.9930 (C<sub>2</sub>HO<sub>3</sub>)</li> </ul>

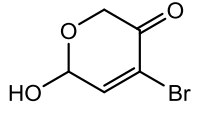
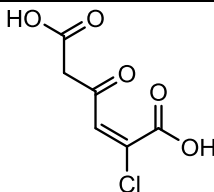
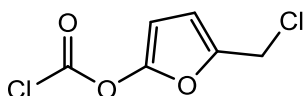
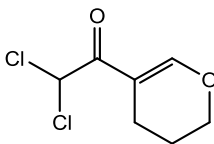
- The highest score in MetFrag

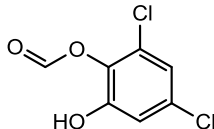
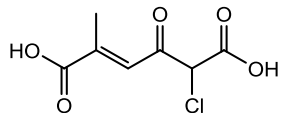
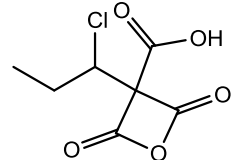
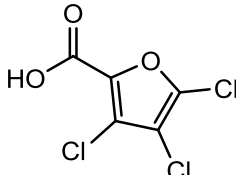
161.0012	C <sub>6</sub> H <sub>7</sub> ClO <sub>3</sub>	3.5	0.776	11.8	T	√√	T	T	n/a (CL 4)	- Isotopic pattern of Cl - No MS2 available
162.9032	CH <sub>2</sub> Cl <sub>2</sub> O <sub>3</sub> S	0.5	2.067	6.24	√	x	x	√√	 <i>Chloro-(sulfoλ3-chloranylidene)methane</i> (CL 3)	- Isotopic pattern of Cl <sub>2</sub> - Characteristic fragments: 162.9032 (CHCl <sub>2</sub> O <sub>3</sub> S) 98.9315 (O <sub>2</sub> ClS) 79.9575 (O <sub>3</sub> S) - The highest score in MetFrag
164.9517	C <sub>5</sub> H <sub>4</sub> Cl <sub>2</sub> O <sub>2</sub>	3.5	0.678	8.79	√	√√	√	√	 <i>4,4-dichlorocyclobutene-1-carboxylic acid</i> (CL 3)	- Isotopic pattern of Cl <sub>2</sub> - Characteristic fragments: 164.9516 (C <sub>5</sub> H <sub>3</sub> Cl <sub>2</sub> O <sub>2</sub> ) 128.9751 (C <sub>5</sub> H <sub>2</sub> ClO <sub>2</sub> ) 92.9982 (C <sub>5</sub> HO <sub>2</sub> ) 96.9604 (C <sub>2</sub> H <sub>3</sub> Cl <sub>2</sub> ) - The highest score in MetFrag
170.8854	C <sub>2</sub> H <sub>2</sub> BrClO <sub>2</sub>	1.5	1.621	8.05	√√	√√√	√√	√√√	 <i>2-bromo,2-chloroacetic acid</i> (CL 1)	- Isotopic pattern of BrCl - Characteristic fragments: 170.8855(C <sub>2</sub> HBrClO <sub>2</sub> ) 126.8958(CHBrCl) 78.9189 (Br) - Unique score in MetFrag - CONFIRMED with analytical std
170.9857	C <sub>7</sub> H <sub>5</sub> ClO <sub>3</sub>	5.5	1.140	20.2	x	x	x	√	n/a (CL 4)	- Isotopic pattern of Cl - No MS2 available

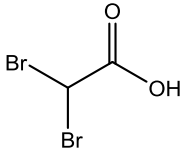
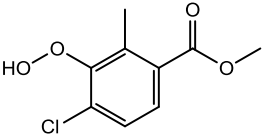
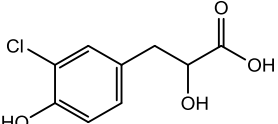
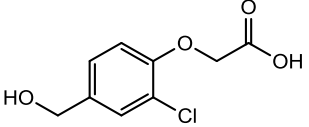
173.0011	C <sub>7</sub> H <sub>7</sub> ClO <sub>3</sub>	4.5	1.184	9.6	x	√	x	x	 <p>4-chloro-3-methoxy-benzene-1,2-diol (CL 3)</p>	<ul style="list-style-type: none"> <li>- Isotopic pattern of Cl</li> <li>- Characteristic fragments:               <ul style="list-style-type: none"> <li>173.0012(C<sub>7</sub>H<sub>6</sub>ClO<sub>3</sub>)</li> <li>142.9907(C<sub>6</sub>H<sub>4</sub>ClO<sub>2</sub>)</li> <li>111.0458 (C<sub>6</sub>H<sub>7</sub>O<sub>2</sub>)</li> <li>65.0032 (C<sub>4</sub>HO)</li> </ul> </li> <li>- -The highest score in MetFrag</li> </ul>
173.0011	C <sub>7</sub> H <sub>7</sub> ClO <sub>3</sub>	4.5	3.834	10.9	√	√√	x	√	 <p>2-(3-methyl-5-oxo-2H-furan-2-yl)acetyl chloride (CL 3)</p>	<ul style="list-style-type: none"> <li>- Isotopic pattern of Cl</li> <li>- Characteristic fragments:               <ul style="list-style-type: none"> <li>173.0012 (C<sub>7</sub>H<sub>6</sub>ClO<sub>3</sub>)</li> <li>157.9778 (C<sub>6</sub>H<sub>3</sub>ClO<sub>3</sub>)</li> <li>129.298 (C<sub>6</sub>H<sub>5</sub>O<sub>2</sub>)</li> <li>97.0297 (C<sub>5</sub>H<sub>5</sub>O<sub>2</sub>)</li> </ul> </li> <li>- The highest score in MetFrag</li> </ul>
174.9400	C <sub>5</sub> H <sub>5</sub> BrO <sub>2</sub>	3.5	-0.259	10.2	x	√√	√√	x	 <p>5-bromo-3-methyl-furan-2-ol (CL3)</p>	<ul style="list-style-type: none"> <li>- Isotopic pattern of Br</li> <li>- Characteristic fragments:               <ul style="list-style-type: none"> <li>174.9401 (C<sub>5</sub>H<sub>4</sub>BrO<sub>2</sub>)</li> <li>95.0141 (C<sub>5</sub>H<sub>3</sub>O<sub>2</sub>)</li> <li>78.9189 (Br)</li> </ul> </li> <li>- The highest score in MetFrag</li> </ul>
174.9803	C <sub>6</sub> H <sub>5</sub> ClO <sub>4</sub>	4.5	-0.284	7.15	x	√	x	√	 <p>2-chloro-3-hydroxy-6-(hydroxymethyl)pyran-4-one (CL 3)</p>	<ul style="list-style-type: none"> <li>- Isotopic pattern of Cl</li> <li>- Characteristic fragments:               <ul style="list-style-type: none"> <li>174.9803 (C<sub>6</sub>H<sub>4</sub>ClO<sub>4</sub>)</li> <li>139.0037 (C<sub>6</sub>H<sub>3</sub>O<sub>4</sub>)</li> <li>111.0090 (C<sub>5</sub>H<sub>3</sub>O<sub>3</sub>)</li> <li>83.0139 (C<sub>4</sub>H<sub>3</sub>O<sub>2</sub>)</li> <li>67.0188 (C<sub>4</sub>H<sub>3</sub>O)</li> </ul> </li> <li>- The highest score in MetFrag</li> </ul>
175.0167	C <sub>7</sub> H <sub>9</sub> ClO <sub>3</sub>	3.5	0.256	8.90	x	√√	√	√		<ul style="list-style-type: none"> <li>- Isotopic pattern of Cl</li> <li>- Characteristic fragments:               <ul style="list-style-type: none"> <li>173.0012 (C<sub>7</sub>H<sub>8</sub>ClO<sub>3</sub>)</li> <li>142.9906 (C<sub>6</sub>H<sub>4</sub>ClO<sub>2</sub>)</li> <li>109.0298 (C<sub>6</sub>H<sub>5</sub>O<sub>2</sub>)</li> </ul> </li> </ul>

175.0167	C <sub>7</sub> H <sub>9</sub> ClO <sub>3</sub>	3.5	0.256	9.26	x	√√	T	√	<p><i>2-chloro-5-(dimethoxymethyl)furan (CL 3)</i></p>  <p><i>2-6-methyl-3,6-dihydro-1,2-dioxin-3-yl]acetyl chloride (CL 3)</i></p>	<p>65.0032 (C<sub>4</sub>HO)</p> <p>- The highest score in MetFrag</p> <p>- Isotopic pattern of Cl</p> <p>- Characteristic fragments:</p> <p>175.0168 (C<sub>7</sub>H<sub>8</sub>ClO<sub>3</sub>)</p> <p>139.0403 (C<sub>7</sub>H<sub>7</sub>O<sub>3</sub>)</p> <p>111.0454 (C<sub>6</sub>H<sub>7</sub>O<sub>2</sub>)</p> <p>104.9750 (C<sub>3</sub>H<sub>2</sub>ClO<sub>2</sub>)</p> <p>83.0503 (C<sub>5</sub>H<sub>7</sub>O)</p> <p>55.0185 (C<sub>3</sub>H<sub>3</sub>O)</p>
178.9308	C <sub>5</sub> H <sub>2</sub> Cl <sub>2</sub> O <sub>3</sub>	4.5	2.668	9.5/ 11.4 5	√√	√√√	√√	√√	 <p><i>5-chlorofuran-2-yl carbonochloridate (CL 3)</i></p>	<p>- -The highest score in MetFrag</p> <p>- Isotopic pattern of Cl<sub>2</sub></p> <p>- Characteristic fragments:</p> <p>178.9311 (C<sub>5</sub>HCl<sub>2</sub>O<sub>3</sub>)</p> <p>142.9546 (C<sub>5</sub>ClO<sub>3</sub>)</p> <p>98.9646 (C<sub>4</sub>ClO)</p> <p>70.9694 (C<sub>3</sub>ClO)</p>
185.0014	C <sub>8</sub> H <sub>7</sub> ClO <sub>3</sub>	5.5	1.756	7.98	X	√	√	X	 <p><i>benzyloxy carbonochloridate (CL 3)</i></p>	<p>- The highest score in MetFrag</p> <p>- Isotopic pattern of Cl</p> <p>- Characteristic fragments:</p> <p>185.0015 (C<sub>8</sub>H<sub>6</sub>ClO<sub>3</sub>)</p> <p>149.0248 (C<sub>8</sub>H<sub>5</sub>O<sub>3</sub>)</p> <p>105.0348 (C<sub>7</sub>H<sub>5</sub>O)</p> <p>81.0347 (C<sub>5</sub>H<sub>5</sub>O)</p> <p>78.9592 (CClO<sub>2</sub>)</p>
186.9802	C <sub>7</sub> H <sub>5</sub> ClO <sub>4</sub>	5.5	-0.105	11.9	X	√	√	X	n/a (CL 4)	<p>- Isotopic pattern of Cl</p> <p>- No MS2 available</p>
187.0168	C <sub>8</sub> H <sub>9</sub> ClO <sub>3</sub>	4.5	0.400	9.7	x	√√	x	x		<p>- Isotopic pattern of Cl</p> <p>- Characteristic fragments:</p> <p>187.0168 (C<sub>8</sub>H<sub>8</sub>ClO<sub>3</sub>)</p> <p>125.0611 (C<sub>7</sub>H<sub>9</sub>ClO<sub>2</sub>)</p> <p>109.0296 (C<sub>6</sub>H<sub>5</sub>O<sub>2</sub>)</p>

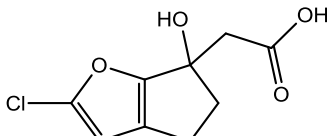
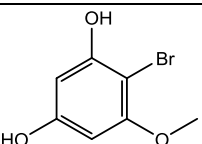
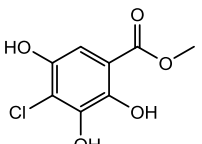
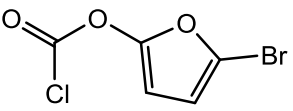
187.0168	$C_8H_9ClO_3$	4.5	0.293	10.8	x	√√	x	√	<p>4-[2-chloro-1-hydroxy-ethyl]benzene-1,2-diol (CL 3)</p>  <p>3-chloro-6-methoxy-4-methylbenzene-1,2-diol (CL 3)</p>	<p>68.9981 (<math>C_3HO_2</math>)</p> <ul style="list-style-type: none"> <li>- The highest score in MetFrag</li> <li>- Isotopic pattern of Cl</li> <li>- Characteristic fragments: <ul style="list-style-type: none"> <li>187.0168 (<math>C_8H_8ClO_3</math>)</li> <li>157.0063 (<math>C_7H_6ClO_2</math>)</li> <li>154.9907 (<math>C_7H_4ClO_2</math>)</li> <li>121.0297 (<math>C_7H_5O_2</math>)</li> <li>79.0190 (<math>C_5H_3O</math>)</li> <li>65.0031 (<math>C_4HO</math>)</li> </ul> </li> </ul>
188.9193	$C_5H_3BrO_3$	4.5	1.906	7.12	√	√√	√√	x	 <p>4-bromo-3-hydroxy-pyran-2-one (CL:3)</p>	<ul style="list-style-type: none"> <li>- The highest score in MetFrag</li> <li>- Isotopic pattern of Br</li> <li>- Characteristic fragments: <ul style="list-style-type: none"> <li>188.9195 (<math>C_5H_2BrO_3</math>)</li> <li>87.0089 (<math>C_3HO_3</math>)</li> <li>78.9190 (Br)</li> <li>65.0033 (<math>C_4HO</math>)</li> </ul> </li> </ul>
188.9516	$C_7H_4Cl_2O_2$	5.5	1.545	19.0	√	x	x	T	 <p>2,4-dichloro-6-hydroxybenzaldehyde (CL 3)</p>	<ul style="list-style-type: none"> <li>- The highest score in MetFrag</li> <li>- Isotopic pattern of <math>Cl_2</math></li> <li>- Characteristic fragments: <ul style="list-style-type: none"> <li>188.9520 (<math>C_7H_3Cl_2O_2</math>)</li> </ul> </li> </ul>
188.9963	$C_7H_7ClO_4$	4.5	0.901	8.82	√	√√	√	√	 <p>3,4-dimethoxyfuran-2-carbonyl chloride (CL 3)</p>	<ul style="list-style-type: none"> <li>- The highest score in MetFrag</li> <li>- Isotopic pattern of Cl</li> <li>- Characteristic fragments: <ul style="list-style-type: none"> <li>188.9961 (<math>C_7H_6ClO_4</math>)</li> <li>158.9854 (<math>C_6H_4ClO_3</math>)</li> <li>144.9698 (<math>C_5H_2ClO_3</math>)</li> <li>123.0089 (<math>C_6H_3O_3</math>)</li> <li>95.0141 (<math>C_5H_3O_2</math>)</li> <li>79.0190 (<math>C_5H_3O</math>)</li> </ul> </li> </ul>

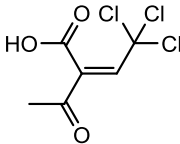
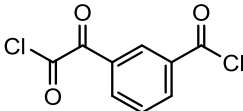
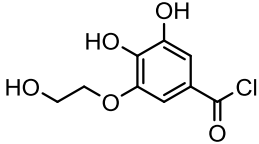
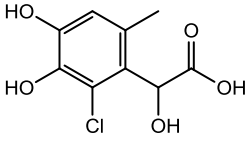
190.9352	C <sub>5</sub> H <sub>5</sub> BrO <sub>3</sub>	3.5	1.048	9.76	x	√√	x	x	 <p><i>4-bromo-6-hydroxy-2H-pyran-3(6H)-one (CL 3)</i></p>	<ul style="list-style-type: none"> <li>- Isotopic pattern of Br</li> <li>- Characteristic fragments: <ul style="list-style-type: none"> <li>190.9351 (C<sub>5</sub>H<sub>4</sub>BrO<sub>3</sub>)</li> <li>146.9450 (C<sub>4</sub>H<sub>4</sub>BrO)</li> <li>102.9190 (C<sub>2</sub>Br)</li> <li>78.9190 (Br)</li> <li>67.0188 (C<sub>4</sub>H<sub>3</sub>O)</li> </ul> </li> </ul>
190.9751	C <sub>6</sub> H <sub>5</sub> ClO <sub>5</sub>	4.5	-0.703	7.37	X	√√	x	x	 <p><i>(E)-2-chloro-4-oxo-hex-2-enedioic acid (CL 3)</i></p>	<ul style="list-style-type: none"> <li>- Isotopic pattern of Cl</li> <li>- Characteristic fragments: <ul style="list-style-type: none"> <li>190.9751 (C<sub>6</sub>H<sub>4</sub>ClO<sub>5</sub>)</li> <li>146.9856 (C<sub>5</sub>H<sub>4</sub>ClO<sub>3</sub>)</li> <li>111.0090 (C<sub>5</sub>H<sub>3</sub>O<sub>3</sub>)</li> <li>83.0139 (C<sub>4</sub>H<sub>3</sub>O<sub>2</sub>)</li> <li>67.0188 (C<sub>4</sub>H<sub>3</sub>O)</li> </ul> </li> <li>- The highest score in MetFrag</li> </ul>
192.9466	C <sub>6</sub> H <sub>4</sub> Cl <sub>2</sub> O <sub>3</sub>	4.5	0.245	11.1	√	√√	x	√√	 <p><i>[5-(chloromethyl)-2-furyl] carbonochloridate (CL 3)</i></p>	<ul style="list-style-type: none"> <li>- Isotopic pattern of Cl<sub>2</sub></li> <li>- Characteristic fragments: <ul style="list-style-type: none"> <li>192.9464 (C<sub>6</sub>H<sub>3</sub>Cl<sub>2</sub>O<sub>3</sub>)</li> <li>156.9698 (C<sub>6</sub>H<sub>2</sub>ClO<sub>3</sub>)</li> <li>128.9750 (C<sub>5</sub>H<sub>2</sub>ClO<sub>2</sub>)</li> <li>93.0347 (C<sub>6</sub>H<sub>5</sub>O)</li> <li>65.0030 (C<sub>4</sub>HO)</li> </ul> </li> <li>- The highest score in MetFrag</li> </ul>
192.9830	C <sub>7</sub> H <sub>8</sub> Cl <sub>2</sub> O <sub>2</sub>	3.5	0.527	13.1	x	√√	x	x	 <p><i>2,2-dichloro-1-(3,4-dihydro-2H-pyran-5-yl)ethanone (CL 3)</i></p>	<ul style="list-style-type: none"> <li>- Isotopic pattern of Cl<sub>2</sub></li> <li>- Characteristic fragments: <ul style="list-style-type: none"> <li>192.9830 (C<sub>7</sub>H<sub>7</sub>Cl<sub>2</sub>O<sub>2</sub>)</li> <li>121.0663 (C<sub>8</sub>H<sub>9</sub>O)</li> <li>107.0504 (C<sub>7</sub>H<sub>7</sub>O)</li> <li>93.0347 (C<sub>6</sub>H<sub>5</sub>O)</li> <li>65.0394 (C<sub>5</sub>H<sub>5</sub>)</li> </ul> </li> <li>- The highest score in MetFrag</li> </ul>

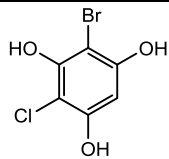
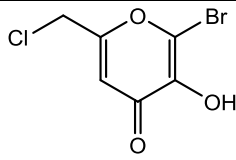
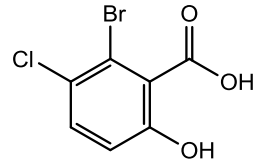
204.9465	C <sub>7</sub> H <sub>4</sub> Cl <sub>2</sub> O <sub>3</sub>	5.5	1.646	20.5	√	x	x	√	 <p>(2,4-dichloro-6-hydroxyphenyl) formate (CL 3)</p>	<ul style="list-style-type: none"> <li>- Isotopic pattern of Cl<sub>2</sub></li> <li>- Characteristic fragments: 204.9468 (C<sub>7</sub>H<sub>3</sub>Cl<sub>2</sub>O<sub>3</sub>) 160.9571 (C<sub>6</sub>H<sub>3</sub>Cl<sub>2</sub>O) 124.9803 (C<sub>6</sub>H<sub>2</sub>ClO) 113.0251 (C<sub>5</sub>H<sub>5</sub>O<sub>3</sub>) 89.0035 (C<sub>6</sub>HO)</li> <li>- The highest score in MetFrag</li> </ul>
204.9911	C <sub>7</sub> H <sub>7</sub> ClO <sub>5</sub>	4.5	0.467	9.5	x	√√	√	√	 <p>5-chloro-2-methyl-4-oxo-hex-2-enedioic acid (CL 3)</p>	<ul style="list-style-type: none"> <li>- Isotopic pattern of Cl</li> <li>- Characteristic fragments: 204.9910 (C<sub>7</sub>H<sub>6</sub>ClO<sub>5</sub>) 125.0247 (C<sub>5</sub>H<sub>6</sub>O<sub>3</sub>) 117.0115 (C<sub>5</sub>H<sub>6</sub>ClO) 69.0345 (C<sub>4</sub>H<sub>5</sub>O)</li> <li>- The highest score in MetFrag</li> </ul>
204.9911	C <sub>7</sub> H <sub>7</sub> ClO <sub>5</sub>	4.5	0.467	10.8	√	√	√	√	 <p>3-(1-chloropropyl)-2,4-dioxo-oxetane-3-carboxylic acid (CL 3)</p>	<ul style="list-style-type: none"> <li>- Isotopic pattern of Cl</li> <li>- Characteristic fragments: 204.9910 (C<sub>7</sub>H<sub>6</sub>ClO<sub>5</sub>) 125.0246 (C<sub>6</sub>H<sub>5</sub>O<sub>3</sub>) 169.0144 (C<sub>7</sub>H<sub>5</sub>O<sub>5</sub>) 97.0298 (C<sub>5</sub>H<sub>5</sub>O<sub>2</sub>)</li> <li>- The highest score in MetFrag</li> </ul>
212.8921	C <sub>5</sub> HCl <sub>3</sub> O <sub>3</sub>	4.5	2.997	13.5	√√√	√√√	x	√√√	 <p>3,4,5-trichlorofuran-2-carboxylic acid (CL 3)</p>	<ul style="list-style-type: none"> <li>- Isotopic pattern of Cl<sub>3</sub></li> <li>- Characteristic fragments: 212.8919 (C<sub>5</sub>Cl<sub>3</sub>O<sub>3</sub>) 177.9231 (C<sub>5</sub>Cl<sub>2</sub>O<sub>3</sub>) 168.9021 (C<sub>4</sub>Cl<sub>3</sub>O) 149.9282 (C<sub>4</sub>Cl<sub>2</sub>O<sub>2</sub>)</li> <li>- The highest score in MetFrag</li> </ul>
212.8921	C <sub>5</sub> HCl <sub>3</sub> O <sub>3</sub>	4.5	0.468	14.5	T	x	x	√√	n/a (CL 4)	<ul style="list-style-type: none"> <li>- Isotopic pattern of Cl<sub>3</sub></li> <li>- No MS2 available</li> </ul>

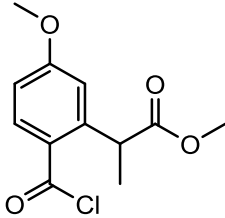
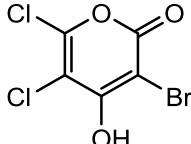
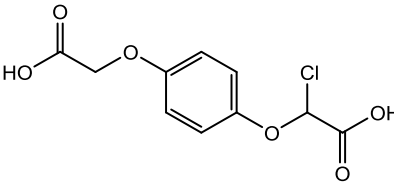
214.8349	C <sub>2</sub> H <sub>2</sub> Br <sub>2</sub> O <sub>2</sub>	1.5	1.407	9.56	√√√	√√	√√	√√	 <p><i>2,2-dibromoacetic acid (CL 1)</i></p>	<ul style="list-style-type: none"> <li>- Isotopic pattern of Br<sub>2</sub></li> <li>- Characteristic fragments: 170.8453(CHBr<sub>2</sub>) 78.9190 )</li> <li>- The highest score in MetFrag</li> <li>- CONFIRMED with analytical standard</li> </ul>
215.0117	C <sub>9</sub> H <sub>9</sub> ClO <sub>4</sub>	5.5	2.420	5.5	x	√	x	x	 <p><i>methyl 4-chloro-3-hydroperoxy-2-methylbenzoate (CL 3)</i></p>	<ul style="list-style-type: none"> <li>- Isotopic pattern of Cl</li> <li>- Characteristic fragments: 215.0118 (C<sub>9</sub>H<sub>8</sub>ClO<sub>4</sub>) 197.0013 (C<sub>9</sub>H<sub>6</sub>ClO<sub>3</sub>) 169.0067 (C<sub>8</sub>H<sub>6</sub>ClO<sub>2</sub>)</li> <li>- The highest score in MetFrag</li> </ul>
215.0117	C <sub>9</sub> H <sub>9</sub> ClO <sub>4</sub>	5.5	3.808	8.8	x	√	x	x	 <p><i>3-(3-chloro-4-hydroxyphenyl)-2-hydroxypropanoic acid (CL 3)</i></p>	<ul style="list-style-type: none"> <li>- Isotopic pattern of Cl</li> <li>- Characteristic fragments: 215.0118 (C<sub>9</sub>H<sub>8</sub>ClO<sub>4</sub>) 171.0221 (C<sub>8</sub>H<sub>8</sub>ClO<sub>2</sub>) 155.9986 (C<sub>7</sub>H<sub>5</sub>ClO<sub>2</sub>) 135.0455 (C<sub>8</sub>H<sub>7</sub>O<sub>2</sub>) 127.0406 (C<sub>6</sub>H<sub>7</sub>O<sub>3</sub>) 91.0192 (C<sub>6</sub>H<sub>3</sub>O)</li> <li>- The highest score in MetFrag</li> </ul>
215.0117	C <sub>9</sub> H <sub>9</sub> ClO <sub>4</sub>	5.5	1.815	10.1	X	√	X	√	 <p><i>2-[2-chloro-4-(hydroxymethyl)phenoxy]acetic acid (CL 3)</i></p>	<ul style="list-style-type: none"> <li>- Isotopic pattern of Cl</li> <li>- Characteristic fragments: 215.0120 (C<sub>9</sub>H<sub>8</sub>ClO<sub>4</sub>) 171.0224 (C<sub>8</sub>H<sub>8</sub>ClO<sub>2</sub>) 155.9982 (C<sub>7</sub>H<sub>5</sub>ClO<sub>2</sub>) 135.0456 (C<sub>8</sub>H<sub>7</sub>O<sub>2</sub>) 107.0506 (C<sub>7</sub>H<sub>7</sub>O) 91.0193 (C<sub>6</sub>H<sub>3</sub>O)</li> <li>- The highest score in MetFrag</li> </ul>

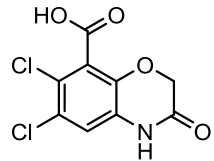
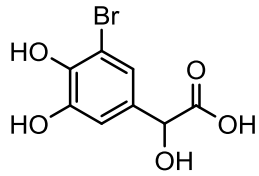
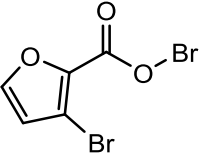
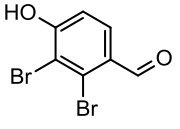


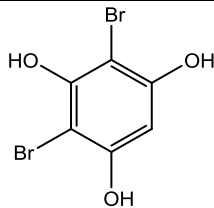
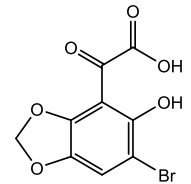
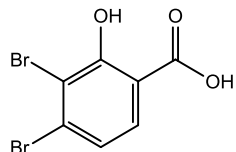
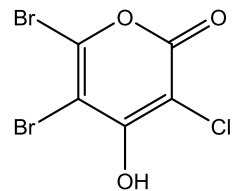
215.0117	C <sub>9</sub> H <sub>9</sub> ClO <sub>4</sub>	5.5	3.342	13.9	x	√√	x	x	 <p><i>2-(2-chloro-6-hydroxy-4,5-dihydrocyclopenta[b]furan-6-yl)acetic acid (CL 3)</i></p>	<ul style="list-style-type: none"> <li>- Isotopic pattern of Cl</li> <li>- Characteristic fragments: <ul style="list-style-type: none"> <li>215.0120 (C<sub>9</sub>H<sub>8</sub>ClO<sub>4</sub>)</li> <li>187.9884 (C<sub>7</sub>H<sub>5</sub>ClO<sub>4</sub>)</li> <li>171.0224 (C<sub>8</sub>H<sub>8</sub>ClO<sub>2</sub>)</li> <li>155.9982 (C<sub>7</sub>H<sub>5</sub>ClO<sub>2</sub>)</li> <li>141.9828 (C<sub>6</sub>H<sub>3</sub>ClO<sub>2</sub>)</li> <li>135.0456 (C<sub>8</sub>H<sub>7</sub>O<sub>2</sub>)</li> <li>109.0662 (C<sub>7</sub>H<sub>9</sub>O)</li> </ul> </li> </ul>
216.9505	C <sub>7</sub> H <sub>7</sub> BrO <sub>3</sub>	4.5	-0.230	11.1	√	√√	√	√	 <p><i>4-bromo-5-methoxy-benzene-1,3-diol (CL 3)</i></p>	<ul style="list-style-type: none"> <li>- Isotopic pattern of Br</li> <li>- Characteristic fragments: <ul style="list-style-type: none"> <li>216.9507 (C<sub>7</sub>H<sub>6</sub>BrO<sub>3</sub>)</li> <li>137.0248 (C<sub>7</sub>H<sub>5</sub>O<sub>3</sub>)</li> <li>117.0115 (C<sub>5</sub>H<sub>6</sub>ClO)</li> <li>78.9190 (Br)</li> </ul> </li> <li>- The highest score in MetFrag</li> </ul>
216.9909	C <sub>8</sub> H <sub>7</sub> ClO <sub>5</sub>	5.5	-0.066	10	x	√√	x	√	 <p><i>methyl 4-chloro-2,3,5-trihydroxy-benzoate (CL 3)</i></p>	<ul style="list-style-type: none"> <li>- Isotopic pattern of Cl</li> <li>- Characteristic fragments: <ul style="list-style-type: none"> <li>219.9909 (C<sub>8</sub>H<sub>6</sub>ClO<sub>5</sub>)</li> <li>173.0012 (C<sub>7</sub>H<sub>6</sub>ClO<sub>3</sub>)</li> <li>137.246 (C<sub>6</sub>H<sub>3</sub>ClO<sub>3</sub>)</li> <li>137.0246 (C<sub>7</sub>H<sub>5</sub>O<sub>3</sub>)</li> <li>109.02976 (C<sub>6</sub>H<sub>5</sub>O<sub>2</sub>)</li> </ul> </li> <li>- The highest score in MetFrag</li> </ul>
222.8805	C <sub>5</sub> H <sub>2</sub> BrClO <sub>3</sub>	4.5	1.716	10.3/	√√	√√√	√√	√√	 <p><i>5-bromofuran-2-yl carbonochloridate (CL 3)</i></p>	<ul style="list-style-type: none"> <li>- Isotopic pattern of BrCl</li> <li>- Characteristic fragments: <ul style="list-style-type: none"> <li>222.8803 (C<sub>5</sub>HBrClO<sub>3</sub>)</li> <li>147.9571 (C<sub>4</sub>HClO<sub>4</sub>)</li> <li>143.9622 (C<sub>5</sub>HClO<sub>3</sub>)</li> <li>98.9645 (C<sub>4</sub>ClO)</li> <li>78.9190 (Br)</li> </ul> </li> <li>- The highest score in MetFrag</li> </ul>

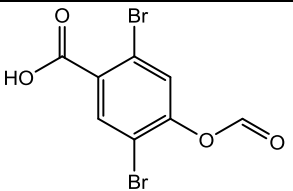
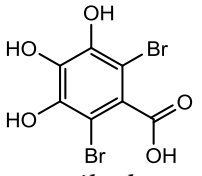
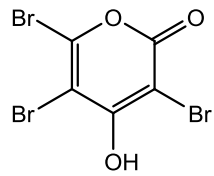
		4.5	2.299	11.7	√	X	X	√	n/a (CL 4)	<ul style="list-style-type: none"> <li>- Isotopic pattern of BrCl</li> <li>- Equal fragmentation pattern than the one eluting at 10.3</li> </ul>
228.9232	C <sub>6</sub> H <sub>5</sub> Cl <sub>3</sub> O <sub>3</sub>	3.5	1.541	11.9	√	√√	X	√√	 <p><i>(E)</i>-2-acetyl-4,4,4-trichlorobut-2-enoic acid (CL 3)</p>	<ul style="list-style-type: none"> <li>- Isotopic pattern of Cl<sub>3</sub></li> <li>- Characteristic fragments: <ul style="list-style-type: none"> <li>192.9468 (C<sub>6</sub>H<sub>3</sub>Cl<sub>2</sub>O<sub>3</sub>)</li> <li>177.9234 (C<sub>5</sub>Cl<sub>2</sub>O<sub>3</sub>)</li> <li>149.9283 (C<sub>4</sub>Cl<sub>2</sub>O<sub>2</sub>)</li> <li>67.0189 (C<sub>4</sub>H<sub>3</sub>O)</li> </ul> </li> </ul>
228.9465	C <sub>9</sub> H <sub>3</sub> Cl <sub>2</sub> O <sub>3</sub>	7.5	0.119	19.3	√	√√	√	√	 <p>3-(2-chloro-2-oxoacetyl)benzoyl chloride (CL 3)</p>	<ul style="list-style-type: none"> <li>- The highest score in MetFrag</li> <li>- Isotopic pattern of Cl<sub>2</sub></li> <li>- Characteristic fragments: <ul style="list-style-type: none"> <li>228.9465 (C<sub>9</sub>H<sub>2</sub>Cl<sub>2</sub>O<sub>3</sub>)</li> <li>193.9778 (C<sub>9</sub>H<sub>3</sub>ClO<sub>3</sub>)</li> <li>165.9829 (C<sub>8</sub>H<sub>3</sub>ClO<sub>2</sub>)</li> </ul> </li> </ul>
231.0066	C <sub>9</sub> H <sub>9</sub> ClO <sub>5</sub>	5.5	-0.235	10.2	T	√√	√	T	 <p>3,4-dihydroxy-5-(2-hydroxyethoxy)benzoyl chloride (CL 3)</p>	<ul style="list-style-type: none"> <li>- The highest score in MetFrag</li> <li>- Isotopic pattern of Cl</li> <li>- Characteristic fragments: <ul style="list-style-type: none"> <li>231.0065 (C<sub>9</sub>H<sub>8</sub>ClO<sub>5</sub>)</li> <li>198.9804 (C<sub>8</sub>H<sub>4</sub>ClO<sub>4</sub>)</li> <li>187.0166 (C<sub>8</sub>H<sub>8</sub>ClO<sub>3</sub>)</li> <li>170.9855 (C<sub>7</sub>H<sub>4</sub>ClO<sub>3</sub>)</li> <li>154.9906 (C<sub>7</sub>H<sub>4</sub>ClO<sub>2</sub>)</li> <li>67.0187 (C<sub>4</sub>H<sub>3</sub>O)</li> </ul> </li> </ul>
231.0066	C <sub>9</sub> H <sub>9</sub> ClO <sub>5</sub>	5.5	0.068	14.0	T	√√	x	x	 <p>2-(2-chloro-3,4-dihydroxy-6-methylphenyl)-2-hydroxyacetic acid (CL 3)</p>	<ul style="list-style-type: none"> <li>- The highest score in MetFrag</li> <li>- Isotopic pattern of Cl</li> <li>- Characteristic fragments: <ul style="list-style-type: none"> <li>231.0065 (C<sub>9</sub>H<sub>8</sub>ClO<sub>5</sub>)</li> <li>187.0166 (C<sub>8</sub>H<sub>8</sub>ClO<sub>3</sub>)</li> <li>170.9855 (C<sub>7</sub>H<sub>4</sub>ClO<sub>3</sub>)</li> <li>154.9908 (C<sub>7</sub>H<sub>4</sub>ClO<sub>2</sub>)</li> <li>121.0298 (C<sub>7</sub>H<sub>5</sub>O<sub>2</sub>)</li> <li>79.0190 (C<sub>5</sub>H<sub>3</sub>O)</li> </ul> </li> </ul>

236.8959	C <sub>6</sub> H <sub>4</sub> BrClO <sub>3</sub>	4.5	0.939	11.7	√√	√√	√	√√		- The highest score in MetFrag
									 <p><i>2-bromo-4-chloro-benzen-1,2,5-triol (CL 3)</i></p>	<ul style="list-style-type: none"> <li>- Isotopic pattern of BrCl</li> <li>- Characteristic fragments: <ul style="list-style-type: none"> <li>236.8960 (C<sub>6</sub>H<sub>3</sub>BrClO<sub>3</sub>)</li> <li>200.9194 (C<sub>6</sub>H<sub>2</sub>BrO<sub>3</sub>)</li> <li>156.9701 (C<sub>6</sub>H<sub>2</sub>ClO<sub>3</sub>)</li> <li>78.9189 (Br)</li> </ul> </li> </ul>
236.8959	C <sub>6</sub> H <sub>4</sub> BrClO <sub>3</sub>	4.5	0.939	11.9	√√	√√	√	√√		- The highest score in MetFrag
									 <p><i>2-bromo-6(chloromethyl)-3hydroxy-pyran-4-one (CL 3)</i></p>	<ul style="list-style-type: none"> <li>- Isotopic pattern of BrCl</li> <li>- Characteristic fragments: <ul style="list-style-type: none"> <li>156.9701 (C<sub>6</sub>H<sub>2</sub>ClO<sub>3</sub>)</li> <li>78.9189 (Br)</li> </ul> </li> <li>- The highest score in MetFrag</li> </ul>
243.0063	C <sub>10</sub> H <sub>9</sub> ClO <sub>5</sub>	6.5	-1.047	12.4/ 10.7	x	√√	x	√	n/a (CL 4)	<ul style="list-style-type: none"> <li>- Isotopic pattern of Cl</li> <li>- No MS2 available</li> </ul>
245.0217	C <sub>10</sub> H <sub>11</sub> ClO <sub>5</sub>	5.5	-1.242	12.7	x	√√	x	x	n/a (CL 4)	<ul style="list-style-type: none"> <li>- Isotopic pattern of Cl</li> <li>- No MS2 available</li> </ul>
247.0014	C <sub>9</sub> H <sub>9</sub> ClO <sub>6</sub>	5.5	0.409	9.9	x	√√	x	√	n/a (CL 4)	<ul style="list-style-type: none"> <li>- Isotopic pattern of Cl</li> <li>- No MS2 available</li> </ul>
248.8960	C <sub>7</sub> H <sub>4</sub> BrClO <sub>3</sub>	5.5	0.211	20.9	√√	x	x	√√		- The highest score in MetFrag
									 <p><i>2-bromo-3-chloro-6-hydroxy-benzoic acid (CL 3)</i></p>	<ul style="list-style-type: none"> <li>- Isotopic pattern of BrCl</li> <li>- Characteristic fragments: <ul style="list-style-type: none"> <li>248.8960 (C<sub>7</sub>H<sub>3</sub>BrClO<sub>3</sub>)</li> <li>204.9062 (C<sub>6</sub>H<sub>3</sub>BrClO)</li> <li>168.9298 (C<sub>6</sub>H<sub>2</sub>BrO)</li> <li>124.9802 (C<sub>6</sub>H<sub>2</sub>ClO)</li> <li>78.9189 (Br)</li> </ul> </li> <li>- The highest score in MetFrag</li> </ul>

255.0431	C <sub>12</sub> H <sub>13</sub> ClO <sub>4</sub>	6.5	0.471	14.2	x	√√	x	X	 <p><i>methyl 2-(2-chlorocarbonyl-5-methoxy-phenyl)propanoate</i> (CL 3)</p>	<ul style="list-style-type: none"> <li>- Isotopic pattern of Cl</li> <li>- Characteristic fragments: <ul style="list-style-type: none"> <li>255.0428 (C<sub>12</sub>H<sub>12</sub>ClO<sub>4</sub>)</li> <li>211.0974 (C<sub>11</sub>H<sub>15</sub>O<sub>4</sub>)</li> <li>193.08707 (C<sub>4</sub>Cl<sub>2</sub>O<sub>4</sub>)</li> <li>167.1078 (C<sub>10</sub>H<sub>15</sub>O<sub>2</sub>)</li> <li>149.0971 (C<sub>10</sub>Cl<sub>13</sub>O)</li> <li>109.0659 (C<sub>7</sub>H<sub>9</sub>O)</li> <li>58.9692 (C<sub>2</sub>Cl)</li> <li>59.0135 (C<sub>2</sub>H<sub>3</sub>O<sub>2</sub>)</li> </ul> </li> </ul>
256.8413	C <sub>5</sub> HBrCl <sub>2</sub> O <sub>3</sub>	4.5	1.130	13.6	√√√	√√√	X	√√√	 <p><i>3-bromo-5,6-dichloro-4-hydroxy-pyran-2-one</i> (CL 3)</p>	<ul style="list-style-type: none"> <li>- The highest score in MetFrag</li> <li>- Isotopic pattern of BrCl<sub>2</sub></li> <li>- Characteristic fragments: <ul style="list-style-type: none"> <li>256.8414 (C<sub>5</sub>BrCl<sub>2</sub>O<sub>3</sub>)</li> <li>181.9181 (C<sub>4</sub>Cl<sub>2</sub>O<sub>4</sub>)</li> <li>177.9231 (C<sub>5</sub>Cl<sub>2</sub>O<sub>3</sub>)</li> <li>149.9282 (C<sub>4</sub>Cl<sub>2</sub>O<sub>2</sub>)</li> <li>98.9645 (C<sub>4</sub>ClO)</li> <li>78.9189 (Br)</li> <li>58.9692 (C<sub>2</sub>Cl)</li> </ul> </li> </ul>
259.0015	C <sub>10</sub> H <sub>9</sub> ClO <sub>6</sub>	6.5	-0.845	9.7/ 9.1	X	√√	X	X	 <p><i>2-[4-(carboxymethoxy)phenoxy]-2-chloro-acetic acid</i> (CL 3)</p>	<ul style="list-style-type: none"> <li>- The highest score in MetFrag</li> <li>- Isotopic pattern of Cl</li> <li>- Characteristic fragments: <ul style="list-style-type: none"> <li>259.0012 (C<sub>10</sub>H<sub>8</sub>ClO<sub>6</sub>)</li> <li>215.0120 (C<sub>9</sub>H<sub>8</sub>ClO<sub>4</sub>)</li> <li>187.9877 (C<sub>7</sub>H<sub>5</sub>ClO<sub>4</sub>)</li> <li>171.0220 (C<sub>7</sub>H<sub>5</sub>ClO<sub>2</sub>)</li> <li>155.9983 (C<sub>8</sub>H<sub>9</sub>O<sub>3</sub>)</li> <li>135.0451 (C<sub>8</sub>H<sub>7</sub>O<sub>2</sub>)</li> <li>107.0505 (C<sub>7</sub>H<sub>7</sub>O)</li> <li>93.0348 (C<sub>6</sub>H<sub>5</sub>O)</li> </ul> </li> <li>- The highest score in MetFrag</li> </ul>

259.9520	C <sub>9</sub> H <sub>5</sub> Cl <sub>2</sub> O <sub>4</sub> N	7.5	-2.063	19.5	√√	x	x	√√	 <p>6,7-dichloro-3-oxo-4H-1,4-benzoxazine-8-carboxylic acid (CL 3)</p>	<ul style="list-style-type: none"> <li>- Isotopic pattern of Cl<sub>2</sub></li> <li>- Characteristic fragments:               <ul style="list-style-type: none"> <li>259.9517 (C<sub>9</sub>H<sub>4</sub>Cl<sub>2</sub>O<sub>4</sub>N)</li> <li>215.9624 (C<sub>8</sub>H<sub>4</sub>Cl<sub>2</sub>O<sub>2</sub>N)</li> <li>171.9728 (C<sub>7</sub>H<sub>4</sub>Cl<sub>2</sub>N)</li> <li>135.9961 (C<sub>7</sub>H<sub>3</sub>ClN)</li> <li>100.0195 (C<sub>7</sub>H<sub>2</sub>N)</li> </ul> </li> <li>- The highest score in MetFrag</li> </ul>
260.9406	C <sub>8</sub> H <sub>7</sub> BrO <sub>5</sub>	5.5	-0.687	9.88	√	√√	T	x	 <p>2-(3-bromo-4,5-dihydroxyphenyl)-2-hydroxyacetic acid (CL 3)</p>	<ul style="list-style-type: none"> <li>- Isotopic pattern of Br</li> <li>- Characteristic fragments:               <ul style="list-style-type: none"> <li>260.9406 (C<sub>8</sub>H<sub>6</sub>BrO<sub>5</sub>)</li> <li>216.9506 (C<sub>7</sub>H<sub>6</sub>BrO<sub>3</sub>)</li> <li>181.0508 (C<sub>9</sub>H<sub>9</sub>O<sub>4</sub>)</li> <li>109.0297 (C<sub>6</sub>H<sub>5</sub>O<sub>2</sub>)</li> <li>137.0246 (C<sub>7</sub>H<sub>5</sub>O<sub>3</sub>)</li> <li>78.9189 (Br)</li> </ul> </li> <li>- The highest score in MetFrag</li> </ul>
266.8296	C <sub>5</sub> H <sub>2</sub> Br <sub>2</sub> O <sub>3</sub>	4.5	-0.646	10.6	√√	√√	T	X	 <p>bromo-3-bromofuran-2-carboxylate (CL 3)</p>	<ul style="list-style-type: none"> <li>- Isotopic pattern of Br<sub>2</sub></li> <li>- Characteristic fragments:               <ul style="list-style-type: none"> <li>266.8297 (C<sub>5</sub>HBr<sub>2</sub>O<sub>3</sub>)</li> <li>187.9119 (C<sub>5</sub>HBrO<sub>3</sub>)</li> <li>142.9138 (C<sub>4</sub>BrO)</li> <li>78.9190 (Br)</li> </ul> </li> <li>- The highest score in MetFrag</li> </ul>
276.8505	C <sub>7</sub> H <sub>4</sub> Br <sub>2</sub> O <sub>2</sub>	5.5	1.669	19.2	√	X	X	X	 <p>2,3-dibromo-4-hydroxybenzaldehyde (CL 3)</p>	<ul style="list-style-type: none"> <li>- Isotopic pattern of Br<sub>2</sub></li> <li>- Characteristic fragments:               <ul style="list-style-type: none"> <li>276.8505 (C<sub>7</sub>H<sub>3</sub>Br<sub>2</sub>O<sub>2</sub>)</li> <li>78.9190 (Br)</li> </ul> </li> <li>- The highest score in MetFrag</li> </ul>

280.8454	C <sub>6</sub> H <sub>4</sub> Br <sub>2</sub> O <sub>3</sub>	4.5	-0.436	12.5	√√	√√	√	X	 <p><i>2,4-dibromobenzene-1,3,5-triol</i> (CL 3)</p>	<ul style="list-style-type: none"> <li>- Isotopic pattern of Br<sub>2</sub></li> <li>- Characteristic fragments: 280.8455 (C<sub>6</sub>H<sub>3</sub>Br<sub>2</sub>O<sub>3</sub>) 200.9194 (C<sub>6</sub>H<sub>2</sub>BrO<sub>3</sub>) 113.0247 (C<sub>5</sub>H<sub>5</sub>O<sub>3</sub>) 78.9190 (Br)</li> <li>- The highest score in MetFrag</li> </ul>
286.9196	C <sub>9</sub> H <sub>5</sub> BrO <sub>6</sub>	7.5	1.486	16.0	√√	x	x	√	 <p><i>2-(6-bromo-5-hydroxy-1,3-benzodioxol-4-yl)-2-oxo-acetic acid</i> (CL 3)</p>	<ul style="list-style-type: none"> <li>- Isotopic pattern of Br</li> <li>- Characteristic fragments: 242.9305 (C<sub>8</sub>H<sub>4</sub>BrO<sub>4</sub>) 214.9351 (C<sub>7</sub>H<sub>4</sub>BrO<sub>3</sub>) 170.9453 (C<sub>6</sub>H<sub>4</sub>BrO) 78.9190 (Br) 65.0032 (C<sub>4</sub>HO)</li> <li>- The highest score in MetFrag</li> </ul>
286.9520	C <sub>11</sub> H <sub>6</sub> Cl <sub>2</sub> O <sub>5</sub>	8.5	0.063	18.9	x	√√	√	√	n/a (CL 4)	<ul style="list-style-type: none"> <li>- Isotopic pattern of Cl<sub>2</sub></li> <li>- No MS2 available</li> </ul>
292.8454	C <sub>7</sub> H <sub>4</sub> Br <sub>2</sub> O <sub>3</sub>	5.5	1.187	21.9	√√	x	x	x	 <p><i>3,4-dibromo-2-hydroxybenzoic acid</i> (CL 3)</p>	<ul style="list-style-type: none"> <li>- Isotopic pattern of Br<sub>2</sub></li> <li>- Characteristic fragments: 292.8454 (C<sub>7</sub>H<sub>3</sub>Br<sub>2</sub>O<sub>3</sub>) 248.8556 (C<sub>6</sub>H<sub>3</sub>Br<sub>2</sub>O) 168.9296 (C<sub>6</sub>H<sub>2</sub>BrO) 78.9189 (Br)</li> <li>- The highest score in MetFrag</li> </ul>
300.7908	C <sub>5</sub> HBr <sub>2</sub> ClO <sub>3</sub>	4.5	0.565	14.1	√√√	√√√	x	x	 <p><i>3-chloro-5,6-dibromo-4-</i></p>	<ul style="list-style-type: none"> <li>- Isotopic pattern of Br<sub>2</sub>Cl</li> <li>- Characteristic fragments: 300.7909 (C<sub>5</sub>Br<sub>2</sub>ClO<sub>3</sub>) 225.8674 (C<sub>4</sub>BrClO<sub>4</sub>) 221.8725 (C<sub>5</sub>BrClO<sub>3</sub>) 193.8773 (C<sub>4</sub>BrClO<sub>2</sub>) 98.9645 (C<sub>4</sub>ClO)</li> </ul>

									<i>hydroxy-pyran-2-one</i> (CL 3)	78.9189 (Br)
318.9412	C <sub>11</sub> H <sub>6</sub> Cl <sub>2</sub> O <sub>7</sub>	8.5	2.442	15.0	√√	√√	√	√√	n/a (CL 4)	- Isotopic pattern of Cl <sub>2</sub> - No MS2 available
320.8404	C <sub>8</sub> H <sub>4</sub> Br <sub>2</sub> O <sub>4</sub>	6.5	0.695	19.0	√√	X	X	X	 <i>2,5-dibromo-4-formyloxybenzoic acid</i> (CL 3)	- Isotopic pattern of Br <sub>2</sub> - Characteristic fragments: 276.85054 (C <sub>7</sub> H <sub>3</sub> Br <sub>2</sub> O <sub>2</sub> ) 248.8555 (C <sub>6</sub> H <sub>3</sub> Br <sub>2</sub> O) 168.9295 (C <sub>6</sub> H <sub>2</sub> BrO) 78.9189 (Br) - The highest score in MetFrag
324.8353	C <sub>7</sub> H <sub>4</sub> Br <sub>2</sub> O <sub>5</sub>	5.5	-0.190	12.0	√√	√√	T	X	 <i>2,5-dibromotrihydroxybenzoic acid</i> (CL 3)	- Isotopic pattern of Br <sub>2</sub> - Characteristic fragments: 244.9086 (C <sub>7</sub> H <sub>2</sub> BrO <sub>5</sub> ) 200.9194 (C <sub>6</sub> H <sub>2</sub> BrO <sub>3</sub> ) 78.9189 (Br) - The highest score in MetFrag
344.7403	C <sub>5</sub> HBr <sub>3</sub> O <sub>3</sub>	4.5	1.030	13.8	√√√	√√√	X	X	 <i>3,5,6-tribromo-4-hydroxypyran-2-one</i> (CL 3)	- Isotopic pattern of Br <sub>3</sub> - Characteristic fragments: 344.7405 (C <sub>5</sub> Br <sub>3</sub> O <sub>3</sub> ) 269.8173 (C <sub>4</sub> Br <sub>2</sub> O <sub>4</sub> ) 265.8221 (C <sub>5</sub> Br <sub>2</sub> O <sub>3</sub> ) 237.8271 (C <sub>4</sub> Br <sub>2</sub> O <sub>2</sub> ) 186.9039 (C <sub>5</sub> BrO <sub>3</sub> ) 142.9141 (C <sub>4</sub> BrO) 78.9190 (Br)

1036 \*X presence not confirmed, √√√ peak area > 10<sup>8</sup>, √√ peak area > 10<sup>7</sup>, √ peak area > 10<sup>6</sup>, T: Trace amounts.  
1037

1038

1039

1040 **Table 30.** Counts and average neutral mass, elemental proportion, aromaticity, and  
 1041 oxidation degree, weighted by the relative abundance of each DBP identified in  
 1042 disinfected waters as computed from LC-ESI(-)-Orbitrap mass spectra for singly  
 1043 charged ions. Computations are based on formulae in neutral form and are restricted to  
 1044 formulae present in three technical replicates.

	DWTP1	DWTP2	DWPT3	DWPT4
<b># of verified formulae*</b>	48	63	38	50
<b>Neutral mass (Da)</b>	271.1 (94.0-345.7)	225.4 (94.0-345.7)	183.9 (94.0-325.8)	218.9 (94.0-322.9)
<i>Element proportion in formulae</i>				
<b>C [%]</b>	12.9	24.2	30.9	16.6
<b>H [%]</b>	40.7	39.2	39.0	40.4
<b>O [%]</b>	24.6	22.3	21.2	23.7
<b>Cl [%]</b>	10.1	9.3	6.9	17.1
<b>Br [%]</b>	11.8	4.9	2.1	2.2
<b>H/C</b>	0.34 (0.20-2.0)	0.58 (0.20-1.5)	0.83 (0.33-1.5)	0.42 (0.20-2.0)
<b>O/C</b>	0.49 (0.29-3.0)	0.48 (0.29-1.0)	0.57 (0.33-1.0)	0.64 (0.25-3.0)
<b>Cl/C</b>	0.26 (0-2.0)	0.27 (0-1.0)	0.20 (0-1.0)	0.48 (0-2.0)
<b>Br/C</b>	0.32 (0-1.0)	0.016 (0-1.0)	0.08 (0-1.0)	0.07 (0-1.0)
<i>Aromaticity and oxidation degree <sup>a</sup></i>				
<b>DBE</b>	3.9 (0-8)	3.8 (1-8)	3.8 (1-8)	4.0 (0-8)
<b>DBE/C</b>	0.76 (0-0.83)	0.69 (0.43-0.83)	0.65 (0.43-0.83)	0.73 (0-0.83)
<b>AI<sub>mod</sub></b>	1.07 (0.44-1.14)	0.88 (0.36-1.14)	0.72 (0.36-1.0)	1.01 (0.36-1.14)
<b>C<sub>os</sub></b>	1.20 (-0.14-6.0)	0.90 (-0.33-2.0)	0.50 (-0.33-2.0)	1.30 (-0.29-6.0)

1045 <sup>a</sup> DBE/C: double bond equivalent relative to the number of carbon atoms, AI<sub>mod</sub>:  
 1046 modified aromaticity index; C<sub>os</sub>: carbon oxidation state.

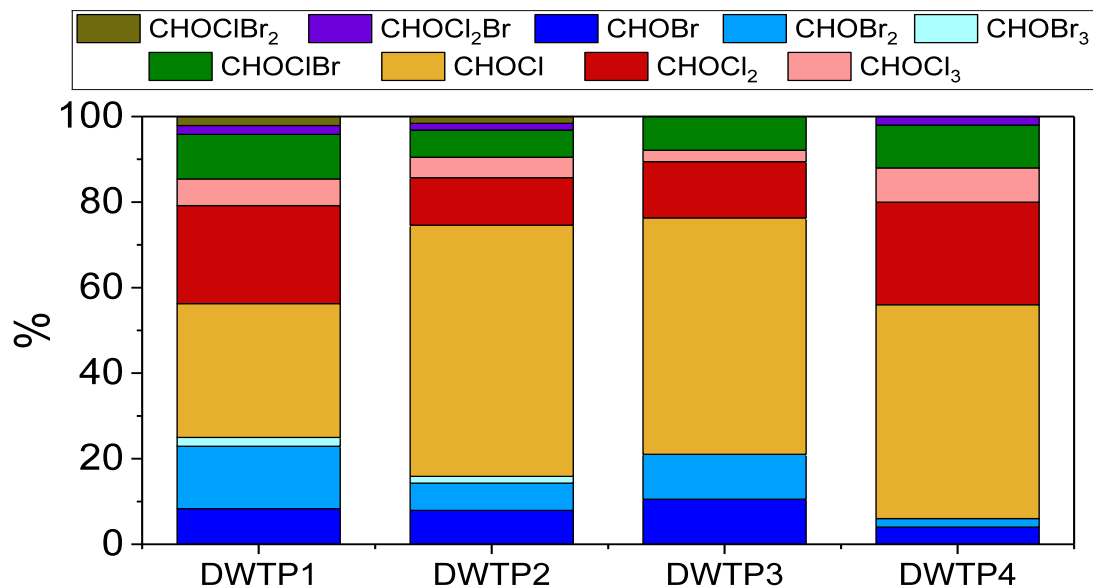
1047 \*Only those halogenated DBPs for which a unique molecular formula could be assigned  
 1048 were considered in the calculations.

1049

1050

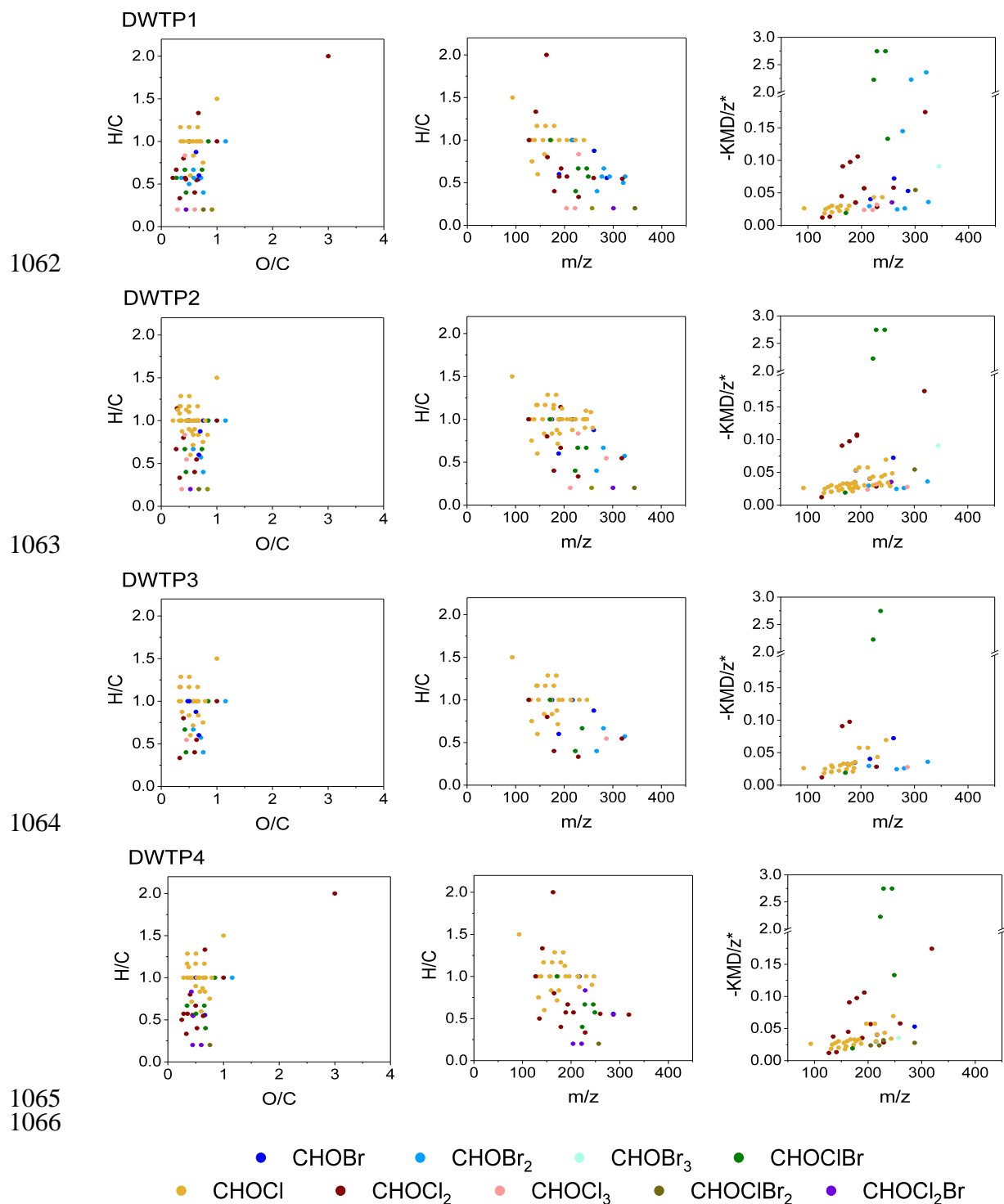


1051  
1052  
1053



1054  
1055  
1056  
1057  
1058  
1059  
1060  
1061

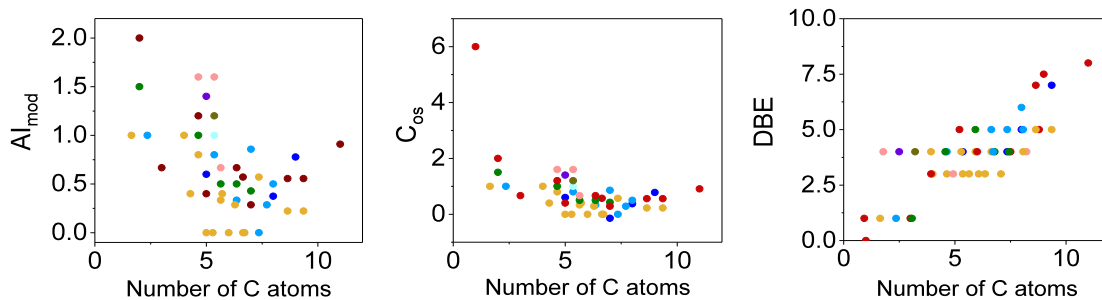
**Figure 19.** Contribution of each group of halogenated compounds to the chemodiversity of the investigated disinfected waters, after LC-ESI(-)-Orbitrap MS analysis. Y-axis shows the percent of confirmed or tentatively identified structures.



1068 **Figure 20.** Molecular composition of the DBPs of each DWTP according to LC-ESI(-)-  
 1069 Orbitrap MS analysis, visualized by van Krevelen diagrams (left panel), mass edited  
 1070 H/C ratios (middle panel), and modified Kendrick mass defect plots (right panel). Only  
 1071 formulae present in all three replicates are shown.

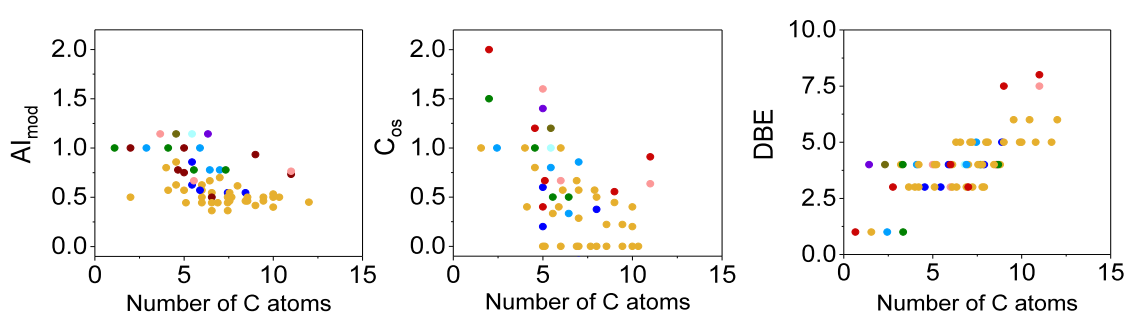
1072

### DWTP1



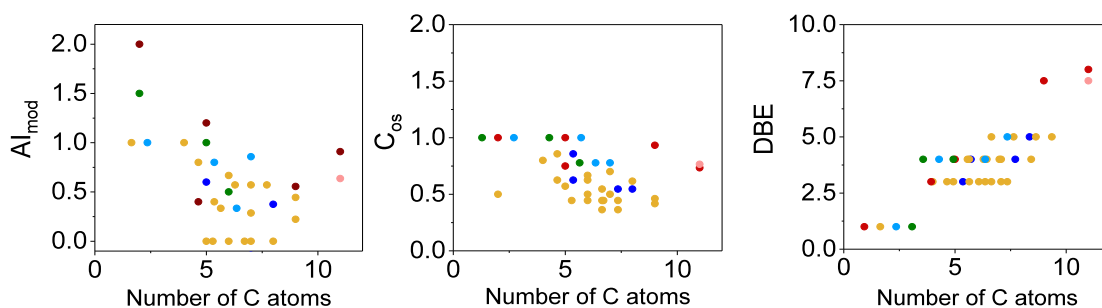
1073

### DWTP2



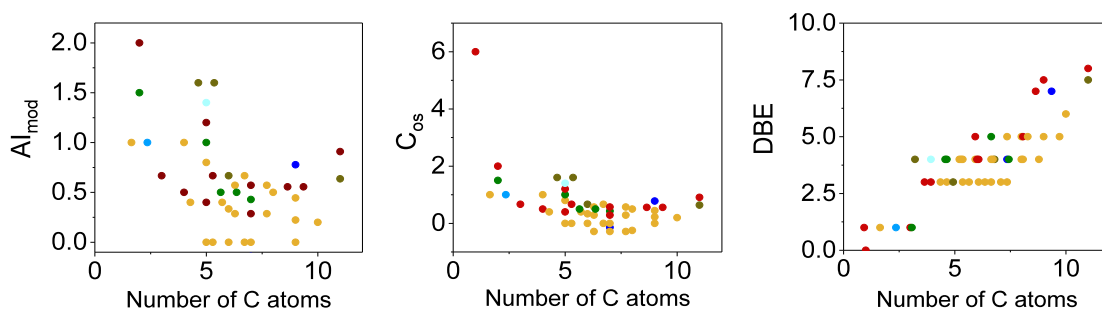
1074

### DWTP3



1075

### DWTP4



1076

1077



1078

1079

**Figure 21.** Plots showing DBE,  $Al_{mod}$ , and  $C_{OS}$  versus the number of carbon of DBPs

1080

( $m/z$  ions only present in disinfected water) according to LC-ESI(-)-Orbitrap MS

1081

analysis.

1082

1083 Cl- and Br- compounds in DBP mixtures

1084 In agreement with ESI(-) FT-ICR MS results, monochlorinated compounds (CHOCI)  
1085 contributed the most to the total DBP mixture (31-59%), followed by dichlorinated  
1086 compounds (CHOCl<sub>2</sub>) (11-24%) (Figure 19). LC-ESI(-)-Orbitrap MS revealed the  
1087 presence of dibrominated (2-15% of total DBPs) and trihalogenated species (3-13% of  
1088 total DBPs) in the mixture. However, the formation of highly substituted (3 halogens)  
1089 was overall minor. As for brominated features, more Br-DBPs were detected with LC-  
1090 Orbitrap MS than with FT-ICR MS. They decreased in the order DWTP1 (40%) >  
1091 DWTP3 (30%) > DWTP2 (25%) > DWTP4 (18%). This finding could be attributed to  
1092 both the bromide content of source waters (DWTP3 > DWTP1 > DWTP2 > DWTP4,  
1093 Table 2), and the disinfection treatment applied, where chlorination (DWTP1) is likely  
1094 to form more Br-DBPs than chloramination (DWTP3).

1095 LC-Orbitrap MS analysis confirmed that substances highly substituted with chlorine  
1096 (dichloro- and trichloro-DBPs) are formed during the chlorination of water with low  
1097 bromide content, as previously published [64, 79] and indicated by target analysis  
1098 (Figure 6 and Table 5) and FT-ICR MS analysis (Figure 13).

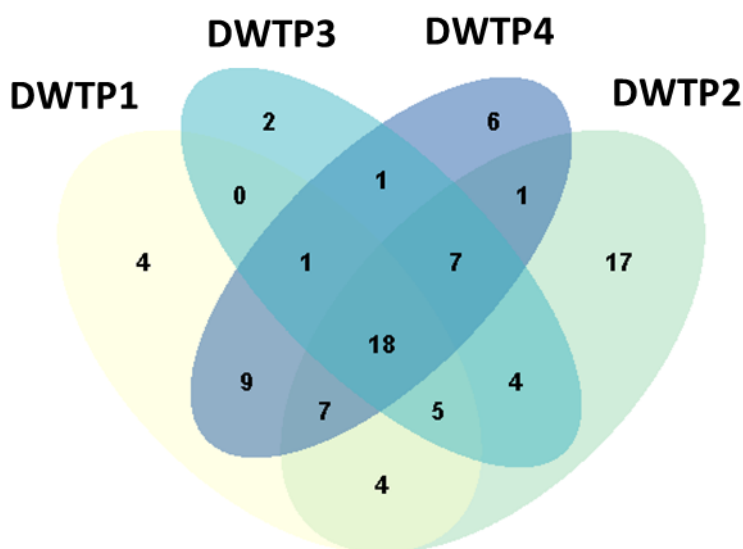
1099 Halogenated DBPs containing one Br and one Cl atom (CHOCIBr) were detected in all  
1100 samples and constituted between 6% and 10% of the total DBPs identified in these  
1101 samples.

1102

1103 Specific molecular composition of DBP mixtures of each water treatment plant

1104 In total, 18 formulae were observed to occur in all disinfected waters; whereas 4, 17, 2,  
1105 and 6 were unique to DWTP1, DWTP2, DWTP3, and DWTP4, respectively (Figure 22  
1106 and Table 29). The molecular composition of the common DBPs and DBPs unique to

1107 each DWTP is summarized in Figures 23-26. Common DBPs included mostly  
 1108 monochlorinated and dichlorinated compounds, but also the confirmed HAAs  
 1109 dibromoacetic acid and bromochloroacetic acid, and 4-bromo-5-methoxy-benzene-1,3-  
 1110 diol (*m/z* 216.0505). Unique DBPs in DWTP1 were mostly dibrominated compounds,  
 1111 whereas exclusive monochlorinated compounds were mainly formed in DWTP2 and  
 1112 DWTP4.



1113 **Figure 22.** Venn diagram showing the chemodiversity of the investigated DBP mixtures  
 1114 according to LC-ESI(-)-Orbitrap MS analysis.  
 1115

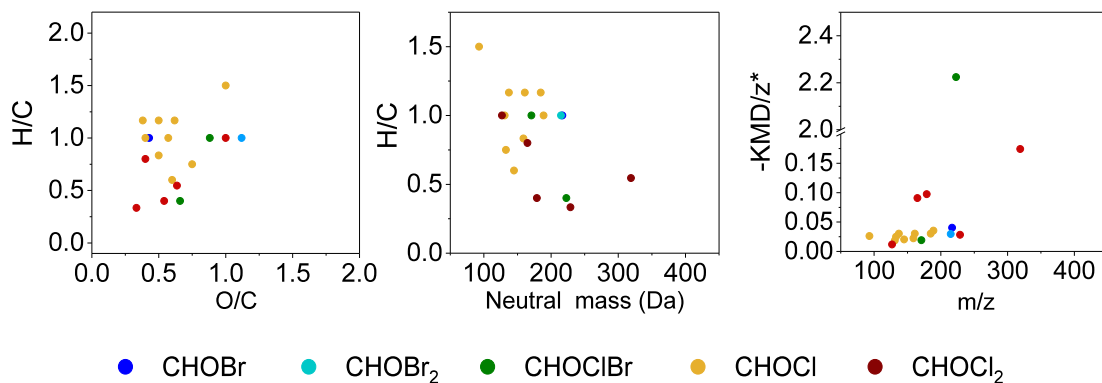
1116

1117 The weighted average molecular mass of DBPs was very similar in all disinfected  
 1118 waters, being all distributed within the mass range of 94 - 346 Da (Table 30) (no  
 1119 statistically significant differences were found). Although the scan range was  
 1120 comparable, the average mass of the DBPs identified with LC-Orbitrap MS was about  
 1121 100 Da lower than that of DBPs characterized using FT-ICR MS. In line with FT-ICR  
 1122 MS analysis, DWTP2 and DWTP4 were the mixtures with the highest heterogeneity of  
 1123 Cl- and Br-DBPs; however, the approach used to process LC-Orbitrap MS data is also

1124 conservative and the analytical technique also affected by matrix effects, which means  
 1125 that the heterogeneity of the other DBP mixtures may be underestimated.

1126

### DBPs common to all DWTPs



1127

1128

1129 **Figure 23.** Molecular composition of the DBPs formed in all DWTPs according to LC-  
 1130 ESI(-)-Orbitrap MS analysis. van Krevelen diagrams (left panel), mass edited H/C ratios  
 1131 (middle panel), and modified Kendrick mass defect plots (right panel) of the compounds  
 1132 present in the disinfected samples. Only formulae present in the three replicates are  
 1133 shown.

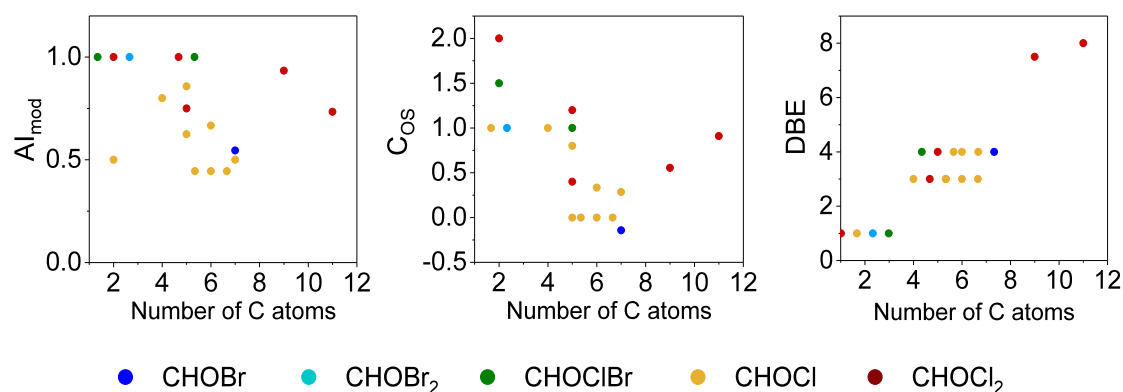
1134

1135

1136

1137

### DBPs common to all DWTPs



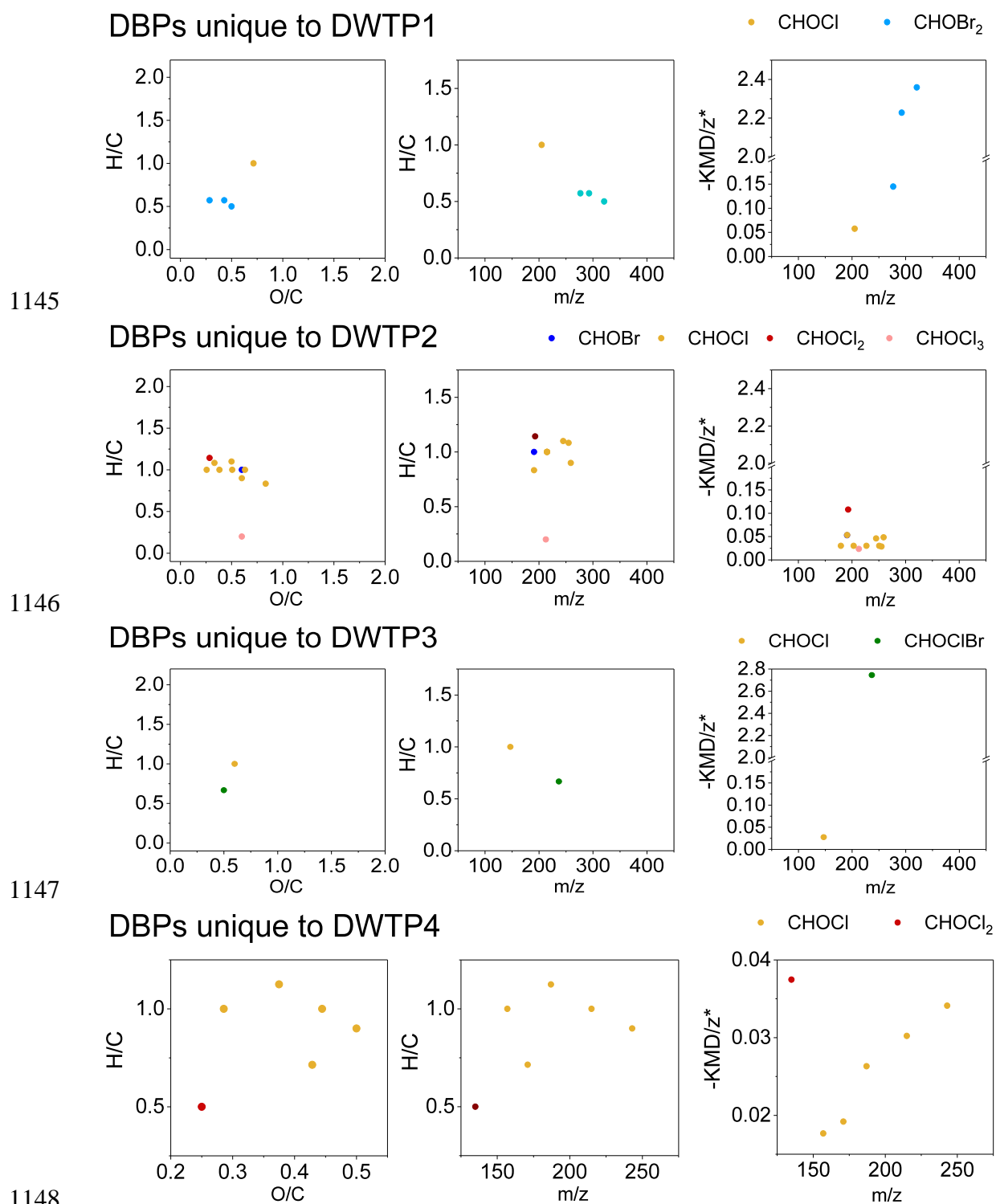
1138

1139

1140

1141 **Figure 24.** Plots showing DBE, AI<sub>mod</sub>, and C<sub>OS</sub> versus the number of carbon for verified  
 1142 DBPs (*m/z* ions only present in disinfected water) common to all DWTPs according to  
 1143 LC-ESI(-)-Orbitrap MS analysis.

1144



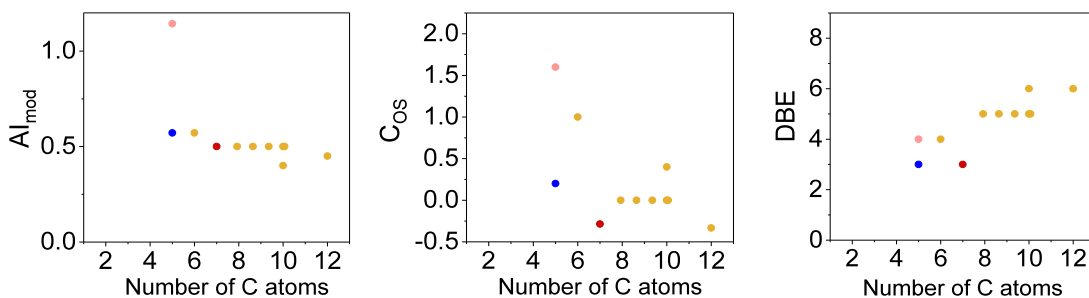
1150 **Figure 25.** Molecular composition of unique DBPs according to LC-ESI(-)-Orbitrap  
 1151 MS analysis. van Krevelen diagrams (left panel), mass edited H/C ratios (middle panel),  
 1152 and modified Kendrick mass defect plots(right panel) of the compounds present in the  
 1153 disinfected samples. Only formulas present in the three replicates are shown.

1154  
 1155

1156  
1157

### DBPs unique to DWTP2

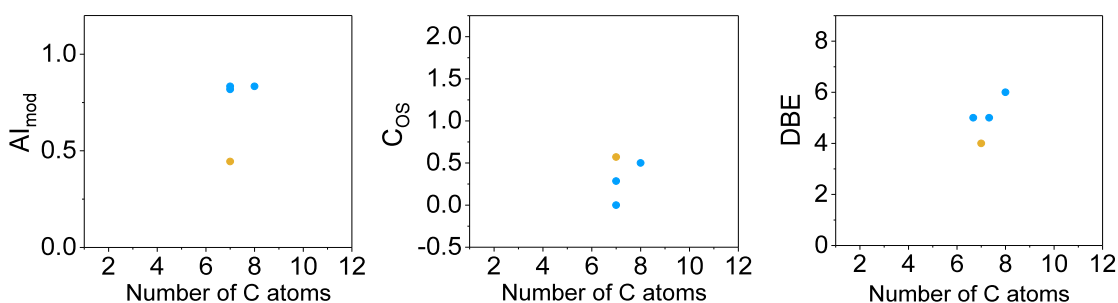
• CHOBr • CHOCI • CHOCl<sub>2</sub> • CHOCl<sub>3</sub>



1158

### DBPs unique to DWTP1

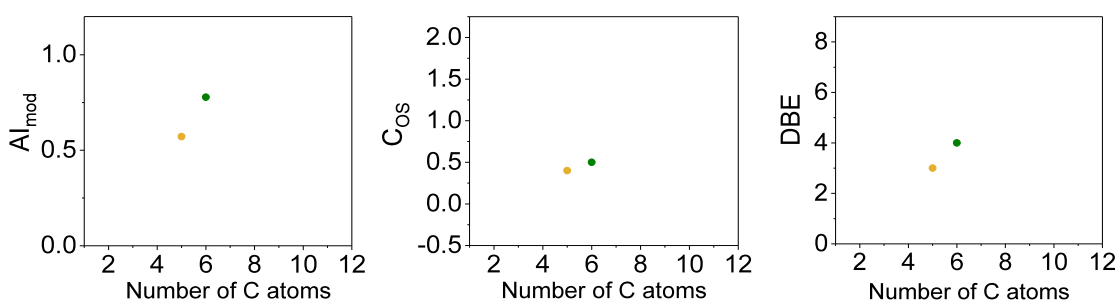
• CHOCI • CHOBr<sub>2</sub>



1159  
1160

### DBPs unique to DWTP3

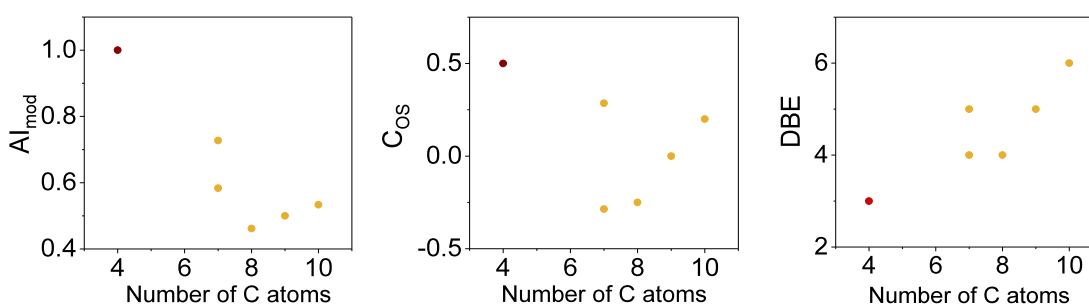
• CHOCI • CHOClBr



1161  
1162

### DBPs unique to DWTP4

• CHOCI • CHOCl<sub>2</sub>



1163  
1164

1165 **Figure 26.** Plots showing DBE, AI<sub>mod</sub>, and C<sub>OS</sub> versus the number of carbon for verified  
1166 DBPs (*m/z* ions only present in disinfected water) in unique DBPs according to LC-  
1167 ESI(-)-Orbitrap MS analysis.



1168 The weighted average O/C ratio and  $C_{OS}$  of the formulae identified in chloraminated  
1169 mixtures (DWTP2 and DWTP3) were lower than that in chlorinated mixtures (although  
1170 differences were not statistically significant). This could be partially attributed to the  
1171 use of chloramine for disinfection that has a lower oxidation potential than chlorine.

1172 Similarly as in FT-ICR MS results, the  $-KMD/z^*$  diagrams revealed two groups of  
1173 DBPs in each DBP mixture (Figure 20). One group, containing most of the features, is  
1174 characterized by less unsaturated compounds ( $-KMD/z^* < 0.12$ ), and the other group,  
1175 containing only a few features, is mainly formed by highly oxygenated and thus, highly  
1176 unsaturated compounds ( $-KMD/z^* > 0.12$ ).

1177 The average Cl/C ratio of the verified formulae decreased in the order  
1178 DWTP4>DWTP2>DWTP1>DWTP3, while the average Br/C ratio decreased as follows  
1179 DWTP1>DWTP2>DWTP3>DWTP4 (Table 30). Thus, this finding confirms that the  
1180 disinfection of low bromide containing waters results in formulae with high chlorine  
1181 incorporation ratios, whereas the chlorination of high bromide containing waters favors  
1182 bromide incorporation into NOM.

1183

1184 Comparing the characteristics of the DBPs verified/identified with the two non-target  
1185 approaches employed in this study (Tables 6 and 30), it can be concluded that different  
1186 DBP groups in the mixture were captured with each approach, despite the use of the  
1187 same ionization source. Overall, halogenated DBPs identified with LC-Orbitrap MS  
1188 presented on average a higher bromine incorporation factor, a higher DBE per number  
1189 of carbon atoms, a higher carbon  $C_{OS}$ , and  $AI_{mod}$  than those detected with FT-ICR MS.  
1190 Furthermore, a very small overlap was obtained among the DBPs identified with the  
1191 different approaches used (4 HAAs between the target GC-MS screening and LC-  
1192 Orbitrap MS and 8 compounds between LC-Orbitrap MS and FT-ICR MS). Thus, this

1193 study demonstrates the relevance of employing different analytical techniques to  
1194 unravel the chemodiversity of DBP mixtures.

1195

## 1196 **CONCLUSIONS**

1197 Target screening of DBPs at four Swedish DWTPs accounted partially for the  
1198 halogenated material formed during disinfection processes. The non-target analysis  
1199 evidenced a wide diversity of the halogenated DBP mixtures formed. The large  
1200 differences observed in the DBP mixture composition among the investigated DWTPs  
1201 indicate that DBP formation is highly dependent on local conditions (disinfection  
1202 treatment and water source characteristics). This makes the development of models to  
1203 predict DBP formation extremely complicated. Furthermore, the regulated volatile  
1204 DBPs routinely monitored (THMs) may not adequately reflect the local DBP  
1205 composition, and efforts to monitor an extended set of DBPs such as in this study  
1206 should be applied at each particular case. For the evaluation of the DBP mixture  
1207 chemodiversity, the use of complementary analytical tools is recommended, as  
1208 evidenced in this work.

1209 Although only a few of the DBPs detected using HRMS analyses were confirmed with  
1210 pure analytical standards, tentative identified DBPs indicate that they are highly  
1211 polyunsaturated and polyphenolic compounds. These 86 DBPs identified can be used to  
1212 design suspect lists that improve the characterization of halogenated compounds in  
1213 waters disinfected with chlorine-based agents. Efforts should be made in the future to  
1214 confirm the identity of these DBPs as well as to assess the relevance of their  
1215 concentrations.

1216 One of the main limitations of non-targeted approaches for exploring DBP mixtures is  
1217 the impossibility of extracting all DBPs formed and capturing all with a single  
1218 analytical technique, due to the different nature of these compounds. While purging and  
1219 trapping procedures aimed at extracting volatile DBPs (e.g., THMs), the use of solid-  
1220 phase extraction techniques is directed for retaining a wide range of hydrophobic to  
1221 hydrophilic compounds. Like in this study, generic-purpose sorbents are commonly  
1222 employed for non-target screening of DBPs. However, the characterization of the most  
1223 polar fraction of the DBP mixture could be also possible with the use of ion-exchange  
1224 cartridges. For this, hydrophilic interaction liquid chromatography (HILIC) coupled to  
1225 HRMS may play a relevant role.

1226 Based on this, the non-target screening approach used in this study covered only  
1227 medium to low polar compounds amenable to ESI(-). Thus, highly polar compounds  
1228 and volatile compounds were excluded. Because of the ionization technique used, the  
1229 identification is limited mainly to compounds containing carboxylic, carbonyl, and  
1230 alcohol moieties, and ion suppression further drastically favors carboxylic acids over  
1231 carbonyl and alcohols. The use of different ionization methods (e.g., positive ESI,  
1232 photoionization), and the development of highly sensitive and specific data processing  
1233 workflows that allow capturing DBPs present at low concentrations could contribute to  
1234 unveil the remaining unknown fraction of AOX.

1235 The AOX fraction not (un)covered in our approach may include halogenated  
1236 polyunsaturated and polyphenolic compounds (like the ones found in this study but  
1237 present at levels below the method detection limit), nitrogen-containing DBPs with  
1238 different heteroatoms (amines or amides, not hydrolyzed under the acidic conditions of  
1239 the extraction procedure and thus, amenable to positive ESI), and high molecular weight  
1240 halogenated fulvic acid molecules little fragmented, as suggested elsewhere [85]. Thus,

1241 efforts should be conducted in the future to characterize this unknown fraction and  
1242 evaluate its bioactivity.

1243

#### 1244 **ACKNOWLEDGMENTS**

1245 CP acknowledges support from the Swedish University of Agricultural Sciences  
1246 through the August T Larsson Guest Researcher Programme and the Fundación General  
1247 del Consejo Superior de Investigaciones Científicas (FGCSIC) through the 2<sup>nd</sup> edition  
1248 of the ComFuturo Programme. This work was supported by the Government of  
1249 Catalonia (Consolidated Research Groups 2017 SGR 01404), the Spanish Ministry of  
1250 Science and Innovation (Project CEX2018-000794-S), and the Swedish Research  
1251 Council FORMAS (grant 2013-01077). Biotage is acknowledged for the gift of  
1252 ISOLUTE® Na<sub>2</sub>SO<sub>4</sub> drying cartridges.

1253

#### 1254 **REFERENCES**

- 1255 [1] A.D. Russell, Similarities and differences in the responses of microorganisms to  
1256 biocides, *Journal of Antimicrobial Chemotherapy*, 52 (2003) 750-763.
- 1257 [2] S.D. Richardson, Disinfection By-Products: Formation and Occurrence in Drinking  
1258 Water, in: J.O. Nriagu (Ed.) *Encyclopedia of Environmental Health*, Elsevier,  
1259 Burlington, 2011, pp. 110-136.
- 1260 [3] T. Bellar, J. Lichtenberg, R. Kroner, The occurrence of organohalides in finished  
1261 drinking waters, *Journal of American Water Works Association*, 66 (1974) 703-706.
- 1262 [4] J.J. Rook, Formation of haloforms during chlorination of natural waters, *Water*  
1263 *Treatment Examination*, 23 (1974) 234-243.

1264 [5] E.D. Wagner, M.J. Plewa, CHO cell cytotoxicity and genotoxicity analyses of  
1265 disinfection by-products: An updated review, *Journal of Environmental Sciences*, 58  
1266 (2017) 64-76.

1267 [6] S.D. Richardson, M.J. Plewa, E.D. Wagner, R. Schoeny, D.M. DeMarini,  
1268 Occurrence, genotoxicity, and carcinogenicity of regulated and emerging disinfection  
1269 by-products in drinking water: A review and roadmap for research, *Mutation  
1270 Research/Reviews in Mutation Research*, 636 (2007) 178-242.

1271 [7] C.M. Villanueva, S. Cordier, L. Font-Ribera, L.A. Salas, P. Levallois, Overview of  
1272 Disinfection By-products and Associated Health Effects, *Current Environmental Health  
1273 Reports*, 2 (2015) 107-115.

1274 [8] R.G. Tardiff, M.L. Carson, M.E. Ginevan, Updated weight of evidence for an  
1275 association between adverse reproductive and developmental effects and exposure to  
1276 disinfection by-products, *Regulatory Toxicology and Pharmacology*, 45 (2006) 185-  
1277 205.

1278 [9] M.J. Plewa, E.D. Wagner, M.G. Muellner, K.-M. Hsu, S.D. Richardson,  
1279 Comparative Mammalian Cell Toxicity of N-DBPs and C-DBPs, in: *Disinfection By-  
1280 Products in Drinking Water*, American Chemical Society, 2008, pp. 36-50.

1281 [10] J. Liu, X. Zhang, Comparative toxicity of new halophenolic DBPs in chlorinated  
1282 smsaline wastewater effluents against a marine alga: Halophenolic DBPs are generally  
1283 more toxic than haloaliphatic ones, *Water Research*, 65 (2014) 64-72.

1284 [11] S.W. Krasner, The formation and control of emerging disinfection by-products of  
1285 health concern, *Philosophical Transactions of the Royal Society A: Mathematical,  
1286 Physical and Engineering Sciences*, 367 (2009) 4077-4095.

1287 [12] K. Doederer, W. Gernjak, H.S. Weinberg, M.J. Farré, Factors affecting the  
1288 formation of disinfection by-products during chlorination and chloramination of

1289 secondary effluent for the production of high quality recycled water, *Water Research*,  
1290 48 (2014) 218-228.

1291 [13] C. Postigo, B. Zonja, Iodinated disinfection byproducts: Formation and concerns,  
1292 *Current opinion in environmental science & health*, v. 7 (2019) pp. 19-25-2019 v.2017.

1293 [14] G. Hua, D.A. Reckhow, DBP formation during chlorination and chloramination:  
1294 Effect of reaction time, pH, dosage, and temperature, *Journal - AWWA*, 100 (2008) 82-  
1295 95.

1296 [15] N. Cortés-Francisco, M. Harir, M. Lucio, G. Ribera, X. Martínez-Lladó, M.  
1297 Rovira, P. Schmitt-Kopplin, N. Hertkorn, J. Caixach, High-field FT-ICR mass  
1298 spectrometry and NMR spectroscopy to characterize DOM removal through a  
1299 nanofiltration pilot plant, *Water Research*, 67 (2014) 154-165.

1300 [16] A. Andersson, E. Lavonen, M. Harir, M. Gonsior, N. Hertkorn, P. Schmitt-  
1301 Kopplin, H. Kylin, D. Bastviken, Selective removal of natural organic matter during  
1302 drinking water production changes the composition of disinfection by-products,  
1303 *Environmental Science: Water Research & Technology*, 6 (2020) 779-794.

1304 [17] Y. Pan, H. Li, X. Zhang, A. Li, Characterization of natural organic matter in  
1305 drinking water: Sample preparation and analytical approaches, *Trends in Environmental*  
1306 *Analytical Chemistry*, 12 (2016) 23-30.

1307 [18] X.-F. Li, W.A. Mitch, Drinking Water Disinfection Byproducts (DBPs) and  
1308 Human Health Effects: Multidisciplinary Challenges and Opportunities, *Environmental*  
1309 *Science & Technology*, 52 (2018) 1681-1689.

1310 [19] S.D. Richardson, C. Postigo, Chapter Ten - Liquid Chromatography–Mass  
1311 Spectrometry of Emerging Disinfection By-products, in: A. Cappiello, P. Palma (Eds.)  
1312 *Comprehensive Analytical Chemistry*, Elsevier, 2018, pp. 267-295.

1313 [20] M. Yang, H.K. Liberatore, X. Zhang, Current methods for analyzing drinking  
1314 water disinfection byproducts, *Current Opinion in Environmental Science & Health*, 7  
1315 (2019) 98-107.

1316 [21] D. Stalter, L.I. Peters, E. O'Malley, J.Y.-M. Tang, M. Revalor, M.J. Farré, K.  
1317 Watson, U. von Gunten, B.I. Escher, Sample Enrichment for Bioanalytical Assessment  
1318 of Disinfected Drinking Water: Concentrating the Polar, the Volatiles, and the  
1319 Unknowns, *Environmental Science & Technology*, 50 (2016) 6495-6505.

1320 [22] M. Yang, X. Zhang, Q. Liang, B. Yang, Application of (LC/)MS/MS precursor ion  
1321 scan for evaluating the occurrence, formation and control of polar halogenated DBPs in  
1322 disinfected waters: A review, *Water Research*, 158 (2019) 322-337.

1323 [23] S.Y. Kimura, A.A. Cuthbertson, J.D. Byer, S.D. Richardson, The DBP exposome:  
1324 Development of a new method to simultaneously quantify priority disinfection by-  
1325 products and comprehensively identify unknowns, *Water Research*, 148 (2019) 324-  
1326 333.

1327 [24] L. Powers, M. Gonsior, Non-targeted screening of disinfection by-products in  
1328 desalination plants using mass spectrometry: A review, *Current Opinion in*  
1329 *Environmental Science & Health*, 7 (2019) 52-60.

1330 [25] C. Postigo, C.I. Cojocariu, S.D. Richardson, P.J. Silcock, D. Barcelo,  
1331 Characterization of iodinated disinfection by-products in chlorinated and chloraminated  
1332 waters using Orbitrap based gas chromatography-mass spectrometry, *Analytical and*  
1333 *Bioanalytical Chemistry*, 408 (2016) 3401-3411.

1334 [26] A. Andersson, M. Harir, M. Gonsior, N. Hertkorn, P. Schmitt-Kopplin, H. Kylin,  
1335 S. Karlsson, M.J. Ashiq, E. Lavonen, K. Nilsson, Ä. Pettersson, H. Stavklint, D.  
1336 Bastviken, Waterworks-specific composition of drinking water disinfection by-  
1337 products, *Environmental Science: Water Research and Technology*, 5 (2019) 861-872.

1338 [27] M. Gonsior, Chapter 13 - FT-ICR MS and Orbitrap mass spectrometry approaches  
1339 in environmental chemistry, in: B. Kanawati, P. Schmitt-Kopplin (Eds.) Fundamentals  
1340 and Applications of Fourier Transform Mass Spectrometry, Elsevier, 2019, pp. 407-423.

1341 [28] M. Gonsior, C. Mitchelmore, A. Heyes, M. Harir, S.D. Richardson, W.T. Petty,  
1342 D.A. Wright, P. Schmitt-Kopplin, Bromination of Marine Dissolved Organic Matter  
1343 following Full Scale Electrochemical Ballast Water Disinfection, Environmental  
1344 Science & Technology, 49 (2015) 9048-9055.

1345 [29] E.E. Lavonen, M. Gonsior, L.J. Tranvik, P. Schmitt-Kopplin, S.J. Köhler, Selective  
1346 Chlorination of Natural Organic Matter: Identification of Previously Unknown  
1347 Disinfection Byproducts, Environmental Science & Technology, 47 (2013) 2264-2271.

1348 [30] H. Zhang, Y. Zhang, Q. Shi, S. Ren, J. Yu, F. Ji, W. Luo, M. Yang,  
1349 Characterization of low molecular weight dissolved natural organic matter along the  
1350 treatment trait of a waterworks using Fourier transform ion cyclotron resonance mass  
1351 spectrometry, Water Research, 46 (2012) 5197-5204.

1352 [31] H. Zhang, Y. Zhang, Q. Shi, H. Zheng, M. Yang, Characterization of Unknown  
1353 Brominated Disinfection Byproducts during Chlorination Using Ultrahigh Resolution  
1354 Mass Spectrometry, Environmental Science & Technology, 48 (2014) 3112-3119.

1355 [32] G. Ziegler, M. Gonsior, D.J. Fisher, P. Schmitt-Kopplin, M.N. Tamburri,  
1356 Formation of Brominated Organic Compounds and Molecular Transformations in  
1357 Dissolved Organic Matter (DOM) after Ballast Water Treatment with Sodium  
1358 Dichloroisocyanurate Dihydrate (DICD), Environmental Science & Technology, 53  
1359 (2019) 8006-8016.

1360 [33] M. Gonsior, L.C. Powers, E. Williams, A. Place, F. Chen, A. Ruf, N. Hertkorn, P.  
1361 Schmitt-Kopplin, The chemodiversity of algal dissolved organic matter from lysed



1362 Microcystis aeruginosa cells and its ability to form disinfection by-products during  
1363 chlorination, *Water Research*, 155 (2019) 300-309.

1364 [34] M. Gonsior, P. Schmitt-Kopplin, H. Stavkint, S.D. Richardson, N. Hertkorn, D.  
1365 Bastviken, Changes in dissolved organic matter during the treatment processes of a  
1366 drinking water plant in sweden and formation of previously unknown disinfection  
1367 byproducts, *Environmental Science and Technology*, 48 (2014) 12714-12722.

1368 [35] J.E. Schollée, M. Bourgin, U. von Gunten, C.S. McArdell, J. Hollender, Non-target  
1369 screening to trace ozonation transformation products in a wastewater treatment train  
1370 including different post-treatments, *Water Research*, 142 (2018) 267-278.

1371 [36] A. Rubirola, M.R. Boleda, M.T. Galceran, E. Moyano, Formation of new  
1372 disinfection by-products of priority substances (Directive 2013/39/UE and Watch List)  
1373 in drinking water treatment, *Environmental Science and Pollution Research*, 26 (2019)  
1374 28270-28283.

1375 [37] X. Zhang, Y. Yang, J. Zhang, Y. Yang, F. Shen, J. Shen, B. Shao, Determination of  
1376 emerging chlorinated byproducts of diazepam in drinking water, *Chemosphere*, 218  
1377 (2019) 223-231.

1378 [38] A.J. Li, P. Wu, J.C.-F. Law, C.-H. Chow, C. Postigo, Y. Guo, K.S.-Y. Leung,  
1379 Transformation of acesulfame in chlorination: Kinetics study, identification of  
1380 byproducts, and toxicity assessment, *Water Research*, 117 (2017) 157-166.

1381 [39] I. González-Mariño, I. Rodríguez, J.B. Quintana, R. Cela, Investigation of the  
1382 transformation of 11-nor-9-carboxy- $\Delta^9$ -tetrahydrocannabinol during water chlorination  
1383 by liquid chromatography–quadrupole-time-of-flight-mass spectrometry, *Journal of*  
1384 *Hazardous Materials*, 261 (2013) 628-636.

1385 [40] Y. Wang, C. Luo, M. Yang, J. Ren, W. Wang, L. Yong, G. Gao, L. Ren, Z. Xiaoli,  
1386 Target quantification and semi-target screening of halogenated carboxylic acids in

1387 drinking water using ultra-high performance liquid chromatography-quadrupole orbitrap  
1388 high-resolution mass spectrometry, *Journal of Chromatography A*, 1614 (2020) 460710.  
1389 [41] Z. Liu, C.B. Craven, G. Huang, P. Jiang, D. Wu, X.-F. Li, Stable Isotopic Labeling  
1390 and Nontarget Identification of Nanogram/Liter Amino Contaminants in Water,  
1391 *Analytical Chemistry*, 91 (2019) 13213-13221.  
1392 [42] Y. Tang, Y. Xu, F. Li, L. Jmaiff, S.E. Hrudey, X.-F. Li, Nontargeted identification  
1393 of peptides and disinfection byproducts in water, *Journal of Environmental Sciences*, 42  
1394 (2016) 259-266.  
1395 [43] M.J. Farré, A. Jaén-Gil, J. Hawkes, M. Petrovic, N. Catalán, Orbitrap molecular  
1396 fingerprint of dissolved organic matter in natural waters and its relationship with  
1397 NDMA formation potential, *Science of The Total Environment*, 670 (2019) 1019-1027.  
1398 [44] J. Sanchís, A. Jaén-Gil, P. Gago-Ferrero, E. Munthali, M.J. Farré, Characterization  
1399 of organic matter by HRMS in surface waters: Effects of chlorination on molecular  
1400 fingerprints and correlation with DBP formation potential, *Water Research*, (2020)  
1401 115743.  
1402 [45] X. Zhang, R.A. Minear, S.E. Barrett, Characterization of High Molecular Weight  
1403 Disinfection Byproducts from Chlorination of Humic Substances with/without  
1404 Coagulation Pretreatment Using UF–SEC–ESI-MS/MS, *Environmental Science &  
1405 Technology*, 39 (2005) 963-972.  
1406 [46] X. Zhang, J.W. Talley, B. Boggess, G. Ding, D. Birdsell, Fast Selective Detection  
1407 of Polar Brominated Disinfection Byproducts in Drinking Water Using Precursor Ion  
1408 Scans, *Environmental Science & Technology*, 42 (2008) 6598-6603.  
1409 [47] G. Ding, X. Zhang, A Picture of Polar Iodinated Disinfection Byproducts in  
1410 Drinking Water by (UPLC/ESI-tq)MS, *Environmental Science & Technology*, 43  
1411 (2009) 9287-9293.

1412 [48] R.Y.L. Yeh, M.J. Farré, D. Stalter, J.Y.M. Tang, J. Molendijk, B.I. Escher,  
1413 Bioanalytical and chemical evaluation of disinfection by-products in swimming pool  
1414 water, *Water Research*, 59 (2014) 172-184.

1415 [49] CEN- European Committee for Standardization. 2004. Water quality -  
1416 Determination of adsorbable organically bound halogens (AOX) EN ISO 9562:2004.  
1417 Brussels. Retrieved from: <https://bit.ly/2CRzzGF>.

1418 [50] I. Kristiana, A. Lethorn, C. Joll, A. Heitz, To add or not to add: The use of  
1419 quenching agents for the analysis of disinfection by-products in water samples, *Water*  
1420 *Research*, 59 (2014) 90-98.

1421 [51] T. Dittmar, B. Koch, N. Hertkorn, G. Kattner, A simple and efficient method for  
1422 the solid-phase extraction of dissolved organic matter (SPE-DOM) from seawater,  
1423 *Limnol. Oceanogr.: Methods*, 6 (2008) 230-235.

1424 [52] ISO 10304-1:2007 -Water quality - Determination of dissolved anions by liquid  
1425 chromatography of ions - Part 1: Determination of bromide, chloride, fluoride, nitrate,  
1426 nitrite, phosphate and sulfate

1427 [53] R.L. Seiler, Combined use of  $^{15}\text{N}$  and  $^{18}\text{O}$  of nitrate and  $^{11}\text{B}$  to evaluate nitrate  
1428 contamination in groundwater, *Applied Geochemistry*, 20 (2005) 1626-1636.

1429 [54] Baird R.B., Rice E.W., Posaven S. (eds) Standard method 5310B - Total Organic  
1430 Carbon: High-Temperature Combustion Method. In: *Standard Methods for the*  
1431 *Examination of Water and Wastewater*. 2017 American Water Works Association; 23rd  
1432 edition. pp. 5-26.

1433 [55] Baird R.B., Rice E.W., Posaven S. (eds) Standard method 5910 - UV - absorbing  
1434 organic constituents. In: *Standard Methods for the Examination of Water and*  
1435 *Wastewater*. 2017 American Water Works Association; 23rd edition. pp. 5-26.

1436 [56] S. Kim, R.W. Kramer, P.G. Hatcher, Graphical Method for Analysis of Ultrahigh-  
1437 Resolution Broadband Mass Spectra of Natural Organic Matter, the Van Krevelen  
1438 Diagram, *Analytical Chemistry*, 75 (2003) 5336-5344.

1439 [57] C.A. Hughey, C.L. Hendrickson, R.P. Rodgers, A.G. Marshall, K. Qian, Kendrick  
1440 Mass Defect Spectrum: A Compact Visual Analysis for Ultrahigh-Resolution  
1441 Broadband Mass Spectra, *Analytical Chemistry*, 73 (2001) 4676-4681.

1442 [58] B.P. Koch, T. Dittmar, From mass to structure: an aromaticity index for high-  
1443 resolution mass data of natural organic matter, *Rapid Communications in Mass*  
1444 *Spectrometry*, 20 (2006) 926-932.

1445 [59] C. Ruttkies, E.L. Schymanski, S. Wolf, J. Hollender, S. Neumann, MetFrag  
1446 relaunched: incorporating strategies beyond in silico fragmentation, *Journal of*  
1447 *cheminformatics*, 8 (2016) 3-3.

1448 [60] M.J. Farré, K. Doederer, W. Gernjak, Y. Poussade, H. Weinberg, Disinfection by-  
1449 products management in high quality recycled water, *Water Supply*, 12 (2012) 573-579.

1450 [61] C.M.M. Bougeard, E.H. Goslan, B. Jefferson, S.A. Parsons, Comparison of the  
1451 disinfection by-product formation potential of treated waters exposed to chlorine and  
1452 monochloramine, *Water Research*, 44 (2010) 729-740.

1453 [62] H. Sakai, S. Tokuhara, M. Murakami, K. Kosaka, K. Oguma, S. Takizawa,  
1454 Comparison of chlorination and chloramination in carbonaceous and nitrogenous  
1455 disinfection byproduct formation potentials with prolonged contact time, *Water*  
1456 *Research*, 88 (2016) 661-670.

1457 [63] G. Hua, D.A. Reckhow, J. Kim, Effect of Bromide and Iodide Ions on the  
1458 Formation and Speciation of Disinfection Byproducts during Chlorination,  
1459 *Environmental Science & Technology*, 40 (2006) 3050-3056.

1460 [64] C. Postigo, P. Emiliano, D. Barceló, F. Valero, Chemical characterization and  
1461 relative toxicity assessment of disinfection byproduct mixtures in a large drinking water  
1462 supply network, *Journal of Hazardous Materials*, 359 (2018) 166-173.

1463 [65] G.A. Cowman, P.C. Singer, Effect of Bromide Ion on Haloacetic Acid Speciation  
1464 Resulting from Chlorination and Chloramination of Aquatic Humic Substances,  
1465 *Environmental Science & Technology*, 30 (1996) 16-24.

1466 [66] G. Hua, D.A. Reckhow, Comparison of disinfection byproduct formation from  
1467 chlorine and alternative disinfectants, *Water Research*, 41 (2007) 1667-1678.

1468 [67] E.H. Goslan, S.W. Krasner, M. Bower, S.A. Rocks, P. Holmes, L.S. Levy, S.A.  
1469 Parsons, A comparison of disinfection by-products found in chlorinated and  
1470 chloraminated drinking waters in Scotland, *Water Research*, 43 (2009) 4698-4706.

1471 [68] X. Zhu, X. Zhang, Modeling the formation of TOCl, TOBr and TOI during  
1472 chlor(am)ination of drinking water, *Water Research*, 96 (2016) 166-176.

1473 [69] P.J. Vikesland, K. Ozekin, R.L. Valentine, Monochloramine Decay in Model and  
1474 Distribution System Waters, *Water Research*, 35 (2001) 1766-1776.

1475 [70] A.C. Diehl, G.E. Speitel Jr., J.M. Symons, S.W. Krasner, C.J. Hwang, S.E. Barrett,  
1476 DBP formation during chloramination, *Journal AWWA*, 92 (2000) 76-90.

1477 [71] J. Luh, B.J. Mariñas, Kinetics of Bromochloramine Formation and Decomposition,  
1478 *Environmental Science & Technology*, 48 (2014) 2843-2852.

1479 [72] S. Y. Kimura, W. Zheng, T. N. Hipp, J. M. Allen, S. D. Richardson, Total organic  
1480 halogen (TOX) in human urine: A halogen-specific method for human exposure studies,  
1481 *Journal of Environmental Sciences*, 58 (2017) 285-295.

1482 [73] I. Kristiana, S. McDonald, J. Tan, C. Joll, A. Heitz, Analysis of halogen-specific  
1483 TOX revisited: Method improvement and application, *Talanta*, 139 (2015) 104-110.

1484 [74] I. Kristiana, H. Gallard, C. Joll, J.-P. Croué, The formation of halogen-specific  
1485 TOX from chlorination and chloramination of natural organic matter isolates, *Water*  
1486 *Research*, 43 (2009) 4177-4186.

1487 [75] Singer PC, Obolensky A, Greiner T. 1996 Disinfection by-products in selected  
1488 North Carolina drinking waters. Report of Project No.50168. Water Resources Research  
1489 Institute of The  
1490 University of North Carolina. Retrieved from: <https://p2infohouse.org/ref/43/42458.pdf>.

1491 [76] S.W. Krasner, H.S. Weinberg, S.D. Richardson, S.J. Pastor, R. Chinn, M.J.  
1492 Scilimenti, G.D. Onstad, A.D. Thruston, Occurrence of a New Generation of  
1493 Disinfection Byproducts, *Environmental Science & Technology*, 40 (2006) 7175-7185.

1494 [77] M. José Farré, B. Lyon, A. de Vera Glen, D. Stalter, W. Gernjak, Assessing  
1495 Adsorbable Organic Halogen Formation and Precursor Removal during Drinking Water  
1496 Production, *Journal of Environmental Engineering*, 142 (2016) 04015087.

1497 [78] W.W. Wu, P.A. Chadik, J.J. Delfino, The relationship between disinfection by-  
1498 product formation and structural characteristics of humic substances in chloramination,  
1499 *Environmental Toxicology and Chemistry*, 22 (2003) 2845-2852.

1500 [79] Y. Yang, Y. Komaki, S.Y. Kimura, H.-Y. Hu, E.D. Wagner, B.J. Mariñas, M.J.  
1501 Plewa, Toxic Impact of Bromide and Iodide on Drinking Water Disinfected with  
1502 Chlorine or Chloramines, *Environmental Science & Technology*, 48 (2014) 12362-  
1503 12369.

1504 [80] B.D. Harris, T.A. Brown, J.L. McGehee, D. Houserova, B.A. Jackson, B.C.  
1505 Buchel, L.C. Krajewski, A.J. Whelton, A.C. Stenson, Characterization of Disinfection  
1506 By-Products from Chromatographically Isolated NOM through High-Resolution Mass  
1507 Spectrometry, *Environmental Science and Technology*, 49 (2015) 14239-14248.

1508 [81] L.L. Hohrenk, F. Itzel, N. Baetz, J. Tuerk, M. Vosough, T.C. Schmidt, Comparison  
1509 of Software Tools for Liquid Chromatography–High-Resolution Mass Spectrometry  
1510 Data Processing in Nontarget Screening of Environmental Samples, *Analytical*  
1511 *Chemistry*, 92 (2020) 1898-1907.

1512 [82] Y. Li, J.S. Whitaker, C.L. McCarty, Analysis of iodinated haloacetic acids in  
1513 drinking water by reversed-phase liquid chromatography/electrospray ionization/tandem  
1514 mass spectrometry with large volume direct aqueous injection, *Journal of*  
1515 *Chromatography A*, 1245 (2012) 75-82.

1516 [83] T. Gong, Y. Tao, X. Zhang, S. Hu, J. Yin, Q. Xian, J. Ma, B. Xu, Transformation  
1517 among Aromatic Iodinated Disinfection Byproducts in the Presence of  
1518 Monochloramine: From Monoiodophenol to Triiodophenol and Diiodonitrophenol,  
1519 *Environmental Science & Technology*, 51 (2017) 10562-10571.

1520 [84] E.L. Schymanski, J. Jeon, R. Gulde, K. Fenner, M. Ruff, H.P. Singer, J. Hollender,  
1521 Identifying Small Molecules via High Resolution Mass Spectrometry: Communicating  
1522 Confidence, *Environmental Science & Technology*, 48 (2014) 2097-2098.

1523 [85] Reckhow, David A., Hua, Guanghui, Kim, Junsung, Hatcher, Patrick G.,  
1524 Caccamise, Sarah A. L., and Sachdeva, Rakesh. Characterization of TOX Produced  
1525 During Disinfection Processes. 2007. Denver, CO, American Water Works Association  
1526 Research Foundation.

1527

1528

1529

1530